Tevatron Lattice Function Fits based on Comparisons of Flying Wire and Synchrotron Light Detector Normalized Transverse Emittance Measurements at 150 and 980GeV Beams Division Doc # 888-v3

November 26, 2003

Krzysztof Genser

Computing Division, Fermilab

Abstract

This note presents plots related to Tevatron Normalized Transverse Emittance measurement comparisons done using Flying Wire and Synchrotron Light detectors for stores in the 2650-3000 range. Results of fits of the lattice functions based on those plots are also shown.

Data Selection

The stores for the plots were selected from June-September 2003 running period after insertion of the attenuators in the antiproton Flying Wire detector system (stores 2650 to 3000).

The Tevatron Case chosen for analysis were "Before Ramp" (with the beam energy of 150GeV) and "Remove Halo" (with the beam energy of 980GeV) the latter is one of the cases where both FW and SL systems are activated. The requirements imposed on the data were:

1. The FW freshness number (ACcelerator NETwork (ACNET) variable T:FWFRSH) in case "Before Ramp" had to be incremented by at least one with respect to the case " Inject Pbars" and "Remove Halo" had to be incremented by at least one with respect to the case "Initiate Collisions".
2. The Transverse Emittance as measured by the FW E11 (combined with SBD in the Horizontal cases) had to be between 0 and 40 ($\pi \cdot mm \cdot mrad$) (to avoid both nonphysical or difficult to measure cases).
3. The antiprotons intensity had to be greater than 15E9 and the protons intensity had to be greater than 215E9 (to avoid difficult to measure cases)

In addition to the above cuts the following stores were removed from the sample at 150 GeV: 2830, 2839, 2847, 2857, 2868, 2879, 2883, 2971, 2973, 2979 due to either detector or operational reasons. Similarly at 980 GeV the following store were rejected: 2768, 2770, 2791, 2792, 2795, 2805, 2810, 2813, 2815, 2817, 2826, 2828 ,2830, 2839, 2847, 2857, 2868, 2879, 2883, 2908, 2910, 2912, 2916 ,2952, 2971, 2973, 2979, 2988.

1 Emittance calculations

The following formulas were used to calculate the Horizontal and Vertical (Normalized) Emittances:

$$\varepsilon_h = 6\left(\sigma^2 - (\frac{\delta p}{p})^2 D^2\right)\frac{\gamma_L}{\beta} \qquad \varepsilon_v = 6\sigma^2\frac{\gamma_L}{\beta}$$

where

$$\delta p = \delta t * (32.657 + \delta t * (-3.5269 + \delta t * 0.13114))$$

at 150 GeV and

$$\delta p = \delta t * (83.293 + \delta t * (-10.562 + \delta t * 0.8023))$$

at 980 GeV low Beta See ref [1]), δt is the T:SBD[A,P]WS ACNET variable (longitudinal beam bunch spread in ns), p is the beam momentum in GeV, γ_L is the Lorentz gamma, σ are bunch width as measured by each of the detectors (ACNET variables T:SL[A,P]S[H,V], T:FW[H,V,E][A,P]SG). In the FW case the width is the arithmetic average of the two measurements (for both of the wire passes trough the beam). In the so called modified calculations (see figures 29, 32) 42, 44) 54, 56) to calculate the vertical emittance the formula with the dispersion term similar to the horizontal one was used. The dispersion (D) and β lattice functions at E11, E17, C11 (location of the SL detector) are shown in Table 1.

2 Lattice Function Fits and related Plots

Relationships between lattice functions were fitted using the following formula

$$\sigma_2{}^2 = \frac{\beta_2}{\beta_{11}}\sigma_{11}{}^2 + \left(\frac{\delta p}{p}\right)^2 \left(D_2{}^2 - \frac{\beta_2}{\beta_{11}} D_{11}{}^2\right)$$

where subscript 2 refers to either Synchrotron Light (C11) or Flying Wire E17 detectors, see figures: 2, 5, 7, 9, 11, 13, 19, 25, 28, 31. 35, 39, 41, 43. 47, 51, 53, 55. The fit procedure returned values of $\frac{\beta_2}{\beta_{11}}$ and $D_2{}^2 - \frac{\beta_2}{\beta_{11}} D_{11}{}^2$ which were subsequently used to derive Synchrotron Light (C11) or Flying Wire E17 lattice functions given the nominal Flying Wire E11 values, see figures: 3, 6, 8, 10, 12, 14, 20, 26, 29, 32. 36, 40, 42, 44. 48, 52, 54, 56. In the vertical cases in addition to the above procedure the plot of Synchrotron Light (C11) versus Flying Wire E11 emittance was used to fit straight line with no offset to determine the multiplicative correction factor for Synchrotron Light (C11) beta lattice functions assuming the nominal Flying Wire E11 values, see figures: 28, 31, 41, 43, 53, 55. In addition to the fits plots of $\sigma_{17}{}^2$ versus $\sigma_{11}{}^2$ and the following quantities were made:

$$\sigma_{17}{}^2 - \frac{\beta_{17}}{\beta_{11}}\sigma_{11}{}^2 = \left(\frac{\delta p}{p}\right)^2 \left(D_{17}{}^2 - \frac{\beta_{17}}{\beta_{11}} D_{11}{}^2\right) \qquad \text{and} \qquad \left(\sigma_{17}{}^2 - \frac{\beta_{17}}{\beta_{11}}\sigma_{11}{}^2\right) / \left(\frac{\delta p}{p}\right)^2 = D_{17}{}^2 - \frac{\beta_{17}}{\beta_{11}} D_{11}{}^2$$

the former should be a linear function of $\delta p/p$ (see figures: 68,69, 70,71, 72,73, 74,75) and the latter should be constant if the accelerator parameters were not changing (see figures: 69, 71, 73, 75). Table 1 shows the results of the lattice function fits compared to their nominal values.

Summary, Conclusions

1. Tevatron Lattice Function Fits based on Transverse Normalized Emittance measurement comparisons using Flying Wire and Synchrotron Light detectors for stores in the 2650-3000 range at 150 and 980 GeV were performed.

2. Comparisons of the emittance measurements using nominal lattice functions show significant disagreements.

3. using SBD[A,P]WS or SBD[A,P]SS variables to calculate longitudinal momentum spread makes significant numerical difference in emittance calculations.

4. Comparisons of the emittance measurements show significant store to store variations of the emittance ratios which probably indicates changing lattice functions for both certain store ranges and individual stores. The variations at the "Before Ramp" case seem to be independent from variations at the "Remove Halo" case. (see e.g. figures 1, 4 18, 24 and 69, 71, 73, 75. The largest step in the mentioned plots at 150GeV beam energy can also be correlated with significant changes in the so called S6 sextupole circuit which were done before store 2810 [5].

5. Analysis of centroid positions at E11/E17/C11 locations (see figures 57, 58, 59) shows that

   (a) beam position at E11/E17 changes very significantly ($\sim 5-7mm$) between "Before Ramp" and "Remove Halo" cases (note the difference in the E11 vertical shift for protons and antiproton, figure 57)

   (b) beam position at C11 in "Remove Halo" case shows much stronger store to store changes than the position at E11/E17. This may have an effect on the store dependent lattice function changes at both E11/E17 and C11 locations.

   (c) vertical antiproton beam position store dependence pattern at C11 (see figure 59) shows quite some resemblance to the pattern of the store dependence of the ratio of the E17/E11 emittances in the "Before Ramp" case (see e.g. figures 1, 4)

6. By performing fits based on beam transverse and longitudinal spread and adjusting lattice functions one can make the measurements agree better except for

   (a) at the E17 location one would need to separate lattice functions for protons and antiprotons

   (b) there is a dependence on bunch number (or $\delta p/p$) in many cases

   (c) one needs to use different lattice functions for different store ranges

Some of the above results may be affected by the $\approx 10\%$ horizontal proton emittance measurement fluctuations due to still not understood detector effect [4] although we believe that qualitatively the conclusions should remain the same.

Acknowledgments

We would like to thank Harry Cheung, Andreas Jansson, Paul Lebrun, Alberto Marchionni, Stephen Pordes, Vladimir Shiltsev, Jean Slaughter and Alvin Tollestrup for their suggestions and comments.

References

[1] M. Church, *Study of of Tev FW emittances and formulas for dp/p and longitudinal emittance from the SBD aka A Study of the Emittances of P1 during Proton Injections for Store 2070 and 2155*, talk on January 16th, 2003, Beams Division Document 694-v1

[2] K. Genser, *A Snapshot of Tevatron Flying Wire and Synchrotron Light Detector Transverse Emittance Measurements at 980GeV* dated June 3rd, 2003, Beams Division Document 656-v1

[3] K. Genser, *Update of a Snapshot of Tevatron Flying Wire and Synchrotron Light Detector Transverse Emittance Measurements at 980GeV* dated September 19th, 2003, Beams Division Document 838-v1

[4] K. Genser, *On Transverse Emittance Fluctuations as measured by Tevatron Flying Wire Horizontal Detector at E11 location at 150GeV* September 9th, 2003, Beams Division Doc 699-v3

[5] V. Shiltsev, private communication, and Tevatron electronic log-book entries on July 21, 2003

Store Range Energy/Case Detector	nminl beta Funct [m]	nominal disp Funct [m]	nominal beta ratio	fitted beta ratio	fitted beta Funct [m]	fitted disp Funct [m]	after fit agreemnt with E11	fitted beta ratio	fitted beta Funct [m]	fitted disp Funct [m]	after fit agreemnt with E11
2650-2997				using sigma dt				using rms dt			
150 GeV Before Ramp											
FW E11H p & $\overline{p}$	83.5	2.83	N/A	N/A	N/A	N/A	N/A	N/A	N/A	N/A	N/A
FW E11V p & $\overline{p}$	84.5	0.09	N/A	N/A	N/A	N/A	N/A	N/A	N/A	N/A	N/A
FW E17H p	62.5	4.58	0.7485	1.0032	83.77	4.456	bad?	0.2069	17.27	5.865	v. bad???
FW E17H $\overline{p}$	62.5	4.58	0.7485	1.0715	89.47	4.503	accptble?	0.7407	61.85	4.894	bad
980 GeV Remove Halo											
FW E11H p & $\overline{p}$	80.1	2.030	N/A	N/A	N/A	N/A	N/A	N/A	N/A	N/A	N/A
FW E11V p & $\overline{p}$	80.8	0.039	N/A	N/A	N/A	N/A	N/A	N/A	N/A	N/A	N/A
FW E17H p	68.1	5.278	0.8502	0.7080	56.8	5.653	ok?	1.3515	108.3	5.221	ok?
FW E17H $\overline{p}$	68.1	5.278	0.8502	0.7750	62.1	5.337	ok	1.4025	112.4	4.997	accptble
SL C11H p	50.0	1.517	0.6238	0.5855	46.9	2.934	accptble?	0.6697	53.68	2.957	accptble?
SL C11H $\overline{p}$	34.0	1.182	0.4246	0.9422	75.5	2.500	bad	1.0258	82.23	2.329	accptble?
SL C11V p	107.8	-0.082	1.3348	1.7219	139.1	N/A	accptble?	1.7234	139.2	N/A	ok?
SL C11V $\overline{p}$	101.6	-0.045	1.2579	2.3750	191.9	N/A	accptble?	2.3372	188.8	N/A	bad?
SL C11V p	107.8	-0.082	1.3348	1.6142	130.4	1.370	ok?	1.6404	132.6	1.170	ok?
SL C11V $\overline{p}$	101.6	-0.045	1.2579	1.4654	118.4	3.293	accptble?	1.3184	106.5	3.702	bad?
2810-2997											
150 GeV Before Ramp											
FW E11H p & $\overline{p}$	83.5	2.83	N/A	N/A	N/A	N/A	N/A	N/A	N/A	N/A	N/A
FW E11V p & $\overline{p}$	84.5	0.09	N/A	N/A	N/A	N/A	N/A	N/A	N/A	N/A	N/A
FW E17H p	62.5	4.58	0.7485	1.0783	90.04	4.308	ok	0.6970	58.20	5.114	bad?
FW E17H $\overline{p}$	62.5	4.58	0.7485	1.1439	95.51	4.343	accptble	0.9913	82.77	4.616	accptble?
980 GeV Remove Halo											
FW E11H p & $\overline{p}$	80.1	2.030	N/A	N/A	N/A	N/A	N/A	N/A	N/A	N/A	N/A
FW E11V p & $\overline{p}$	80.8	0.039	N/A	N/A	N/A	N/A	N/A	N/A	N/A	N/A	N/A
FW E17H p	68.1	5.278	0.8502	0.7282	58.3	5.637	accptble	1.2000	96.19	5.497	ok?
FW E17H $\overline{p}$	68.1	5.278	0.8502	1.2463	99.9	4.827	ok	1.6915	135.6	4.535	accptble?
SL C11H p	50.0	1.517	0.6238	0.4759	38.1	3.151	bad	0.6204	49.73	3.077	accptble?
SL C11H $\overline{p}$	34.0	1.182	0.4246	1.0802	86.5	2.385	bad	0.8902	71.36	2.764	accptble?
SL C11V p	107.8	-0.082	1.3348	1.7483	141.2	0.000	bad fit?	1.7849	144.2	0.000	bad fit?
SL C11V $\overline{p}$	101.6	-0.045	1.2579	1.4428	116.5	3.379	bad	1.2321	99.56	4.000	bad?
2676-2805											
150 GeV Before Ramp											
FW E11H p & $\overline{p}$	83.5	2.83	N/A	N/A	N/A	N/A	N/A	N/A	N/A	N/A	N/A
FW E11V p & $\overline{p}$	84.5	0.09	N/A	N/A	N/A	N/A	N/A	N/A	N/A	N/A	N/A
FW E17H p	62.5	4.58	0.7485	1.1263	94.05	4.519	accptble	0.5313	44.37	5.555	accptble?
FW E17H $\overline{p}$	62.5	4.58	0.7485	1.3432	112.2	4.406	accptble?	1.1038	92.16	4.733	ok?
980 GeV Remove Halo											
FW E11H p & $\overline{p}$	80.1	2.030	N/A	N/A	N/A	N/A	N/A	N/A	N/A	N/A	N/A
FW E11V p & $\overline{p}$	80.8	0.039	N/A	N/A	N/A	N/A	N/A	N/A	N/A	N/A	N/A
FW E17H p	68.1	5.278	0.8502	0.6435	51.5	5.712	accptble?	1.6593	133.0	4.775	accptble?
FW E17H $\overline{p}$	68.1	5.278	0.8502	0.7619	61.0	5.370	ok	1.4284	114.5	5.054	accptble?
SL C11H p	50.0	1.517	0.6238	0.8688	69.6	2.321	ok	0.9258	74.21	2.265	ok?
SL C11H $\overline{p}$	34.0	1.182	0.4246	0.8539	68.4	2.614	accptble?	1.0304	82.60	2.283	accptble?
SL C11V p	107.8	-0.082	1.3348	1.4877	120.2	2.225	ok?	1.4698	118.8	2.543	ok?
SL C11V $\overline{p}$	101.6	-0.045	1.2579	1.4796	119.5	3.317	accptble	1.4747	119.2	3.507	accptble?

Table 1: Tevatron nominal and fitted beta and dispersion functions for given store ranges lattice configurations and measurement locations.

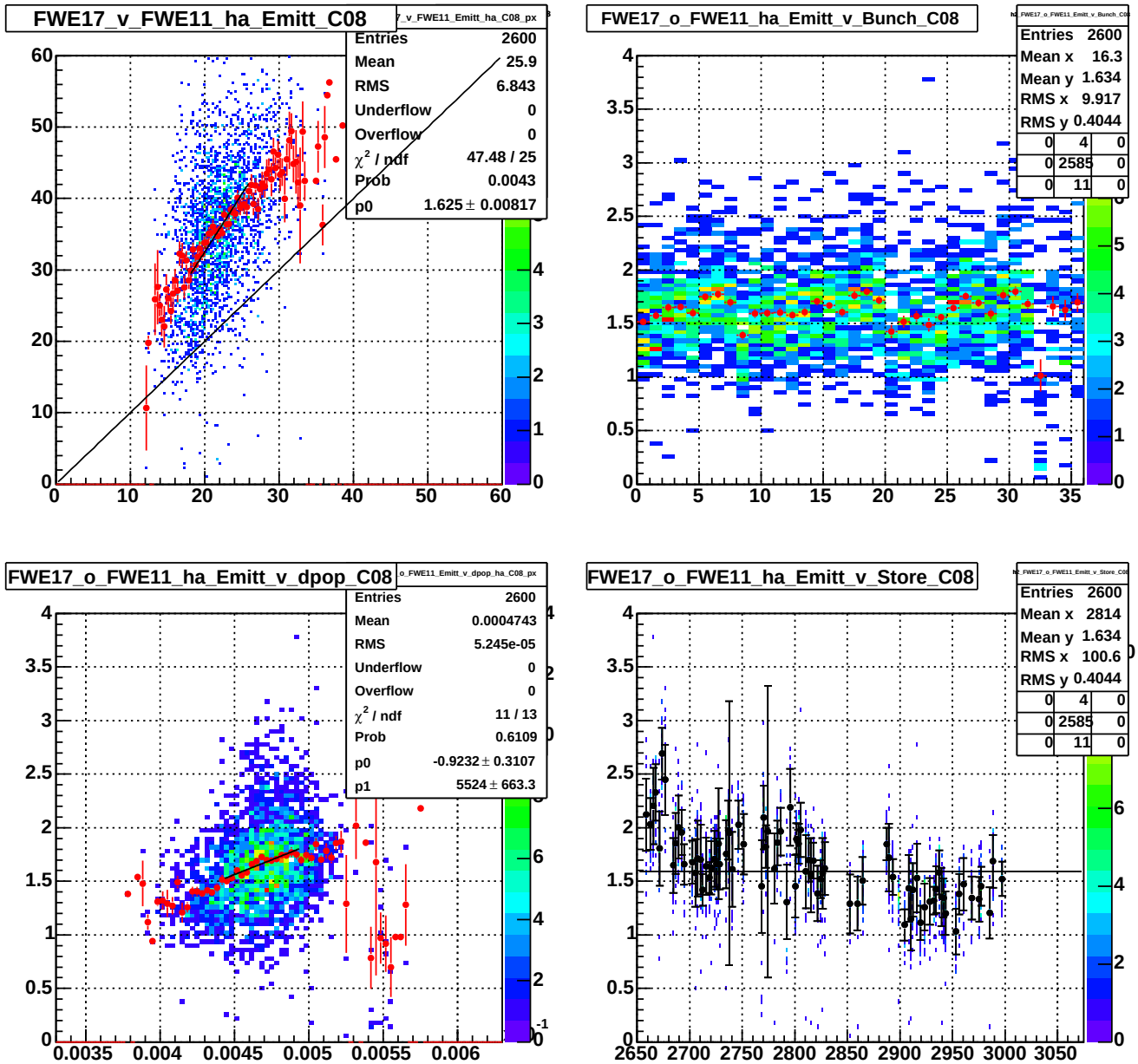

Figure 1: Antiproton beam, horizontal detectors, nominal lattice: Stores 2650-2997, 150 GeV Case Before Ramp: Comparisons of Emittance measurements as done by Flying Wire (FW) Detector at E17 and Flying Wire Detector at E11: Bunch emittance (in $\pi \cdot mm \cdot mrad$) as measured by FW E17 Detector versus bunch emittance as measured by the FW E11 Detector with an overlaid horizontal profile distribution with a straight line fit and the ideal prediction; bunch emittance as measured by FW E17 Detector over bunch emittance as measured by the FW E11 Detector versus bunch number together with an overlaid horizontal profile; bunch emittance as measured by FW E17 Detector over bunch emittance as measured by the FW E11 Detector versus recalculated $\delta p/p$ (based on δt the T:SBD[A,P]WS ACNET variable) with an overlaid horizontal profile with a straight line fit; bunch emittance as measured by FW E17 Detector over bunch emittance as measured by the FW E11 Detector versus store number with overlaid averaged ratios for each store and a horizontal line fit.

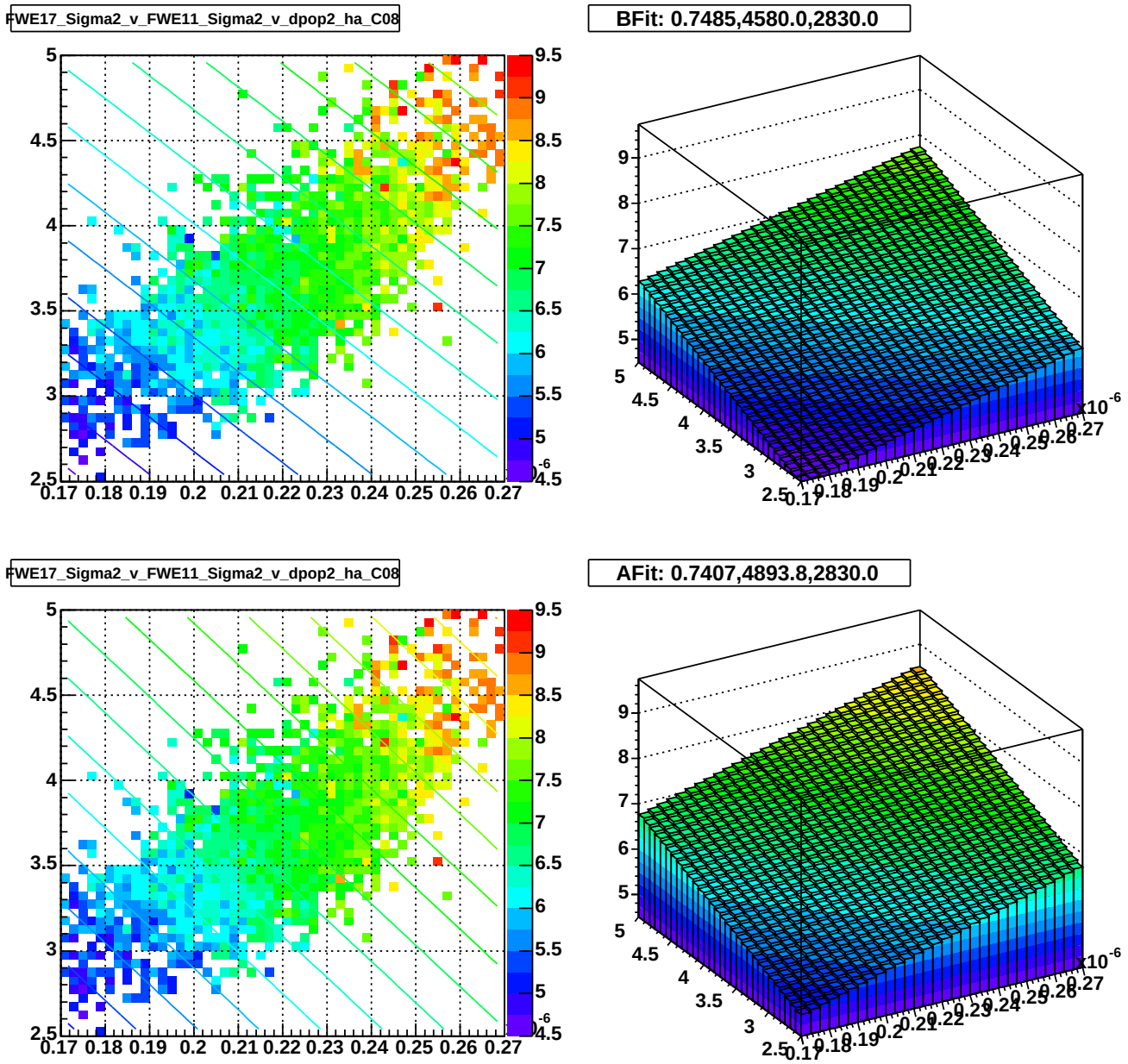

Figure 2: Antiproton beam, horizontal detectors, nominal lattice: Stores 2650-2997, 150 GeV Case Before Ramp: Comparisons of Sigma squared of the bunch width distribution measurements as done by Flying Wire (FW) E17 Detector with predictions based on the FW E11 Detector measurement: Sigma squared of the bunch width distribution (in mm^2) as measured by the FW E17 Detector as a function of sigma squared of the bunch width distribution (in mm^2) as measured by the FW E11 Detector versus recalculated $\delta p/p$ squared (based on δt the T:SBD[A,P]WS ACNET variable) with an overlaid contour of the prediction based on the nominal lattice functions; Prediction of sigma squared of the bunch width distribution (in mm^2) for E17 Detector as a function of sigma squared of the bunch width distribution (in mm^2) as measured by the FW E11 Detector versus recalculated $\delta p/p$ squared based on the nominal lattice functions; two lower plots have the same data points but have contours based on the fitted lattice functions.

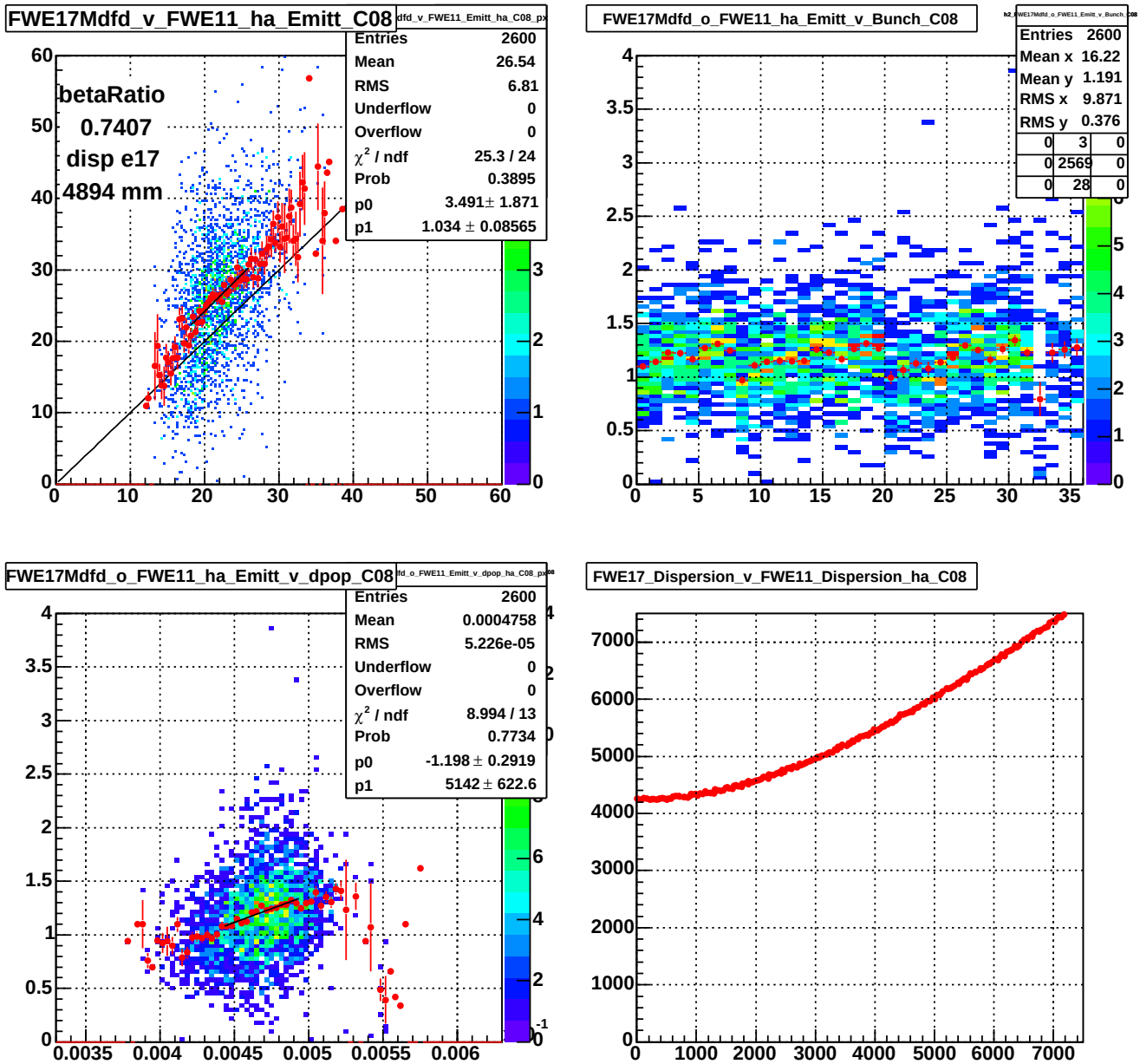

Figure 3: Antiproton beam, horizontal detectors, modified lattice: Stores 2650-2997, 150 GeV Case Before Ramp: Comparisons of Emittance measurements as done by Flying Wire (FW) Detector at E17 and Flying Wire Detector at E11 using fitted lattice parameters: Bunch emittance (in $\pi \cdot mm \cdot mrad$) as measured by FW E17 Detector versus bunch emittance as measured by the FW E11 Detector with an overlaid horizontal profile distribution with a straight line fit and the ideal prediction; bunch emittance as measured by FW E17 Detector over bunch emittance as measured by the FW E11 Detector versus bunch number together with an overlaid horizontal profile; bunch emittance as measured by FW E17 Detector over bunch emittance as measured by the FW E11 Detector versus recalculated $\delta p/p$ (based on δt the T:SBD[A,P]WS ACNET variable) with an overlaid horizontal profile with a straight line fit; fit based E17 dispersion function as a function of the E11 dispersion function.

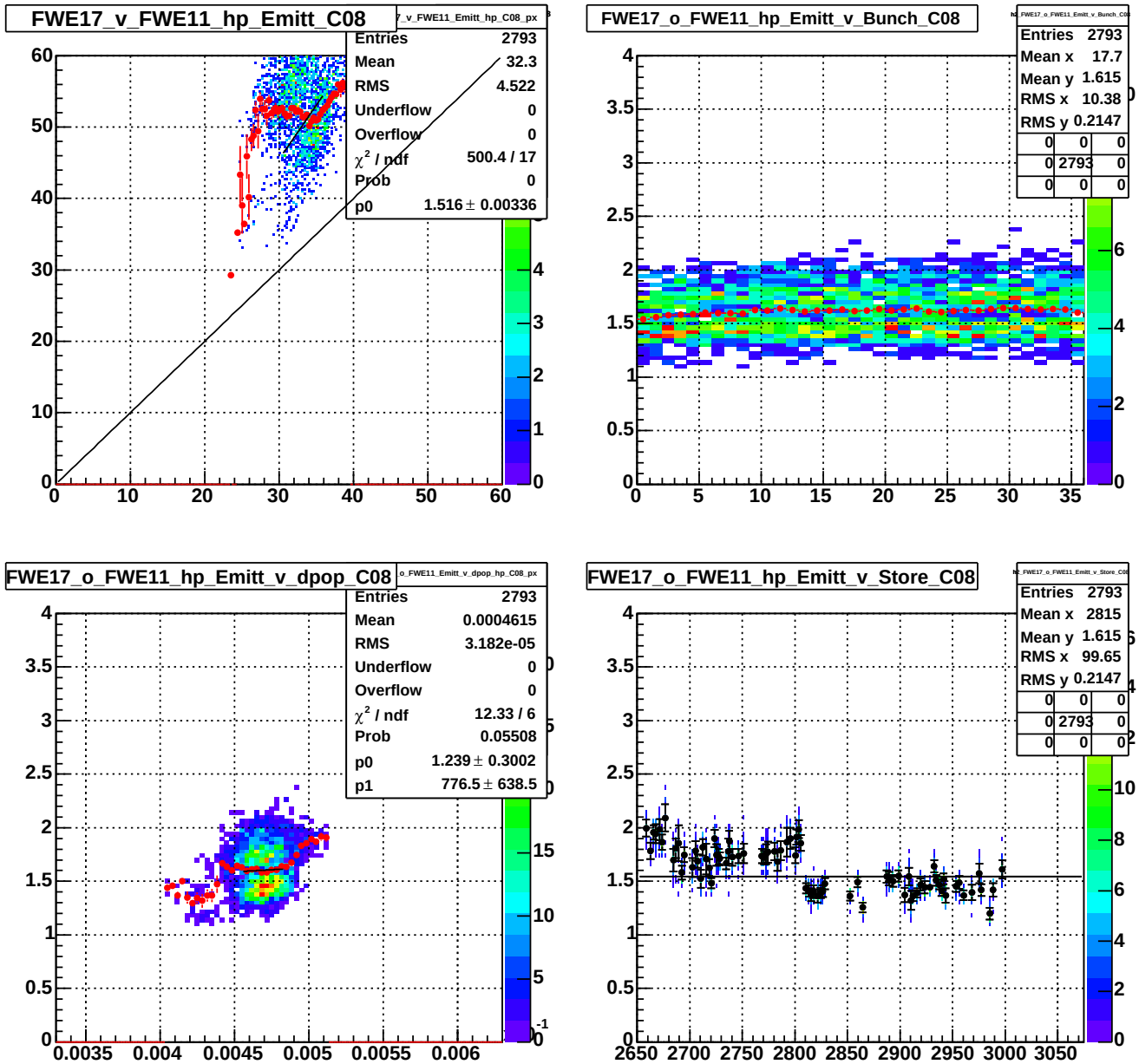

Figure 4: Proton beam, horizontal detectors, nominal lattice: Stores 2650-2997, 150 GeV Case Before Ramp: Comparisons of Emittance measurements as done by Flying Wire (FW) Detector at E17 and Flying Wire Detector at E11: Bunch emittance (in $\pi \cdot mm \cdot mrad$) as measured by FW E17 Detector versus bunch emittance as measured by the FW E11 Detector with an overlaid horizontal profile distribution with a straight line fit and the ideal prediction; bunch emittance as measured by FW E17 Detector over bunch emittance as measured by the FW E11 Detector versus bunch number together with an overlaid horizontal profile; bunch emittance as measured by FW E17 Detector over bunch emittance as measured by the FW E11 Detector versus recalculated $\delta p/p$ (based on δt the T:SBD[A,P]WS ACNET variable) with an overlaid horizontal profile with a straight line fit; bunch emittance as measured by FW E17 Detector over bunch emittance as measured by the FW E11 Detector versus store number with overlaid averaged ratios for each store and a horizontal line fit.

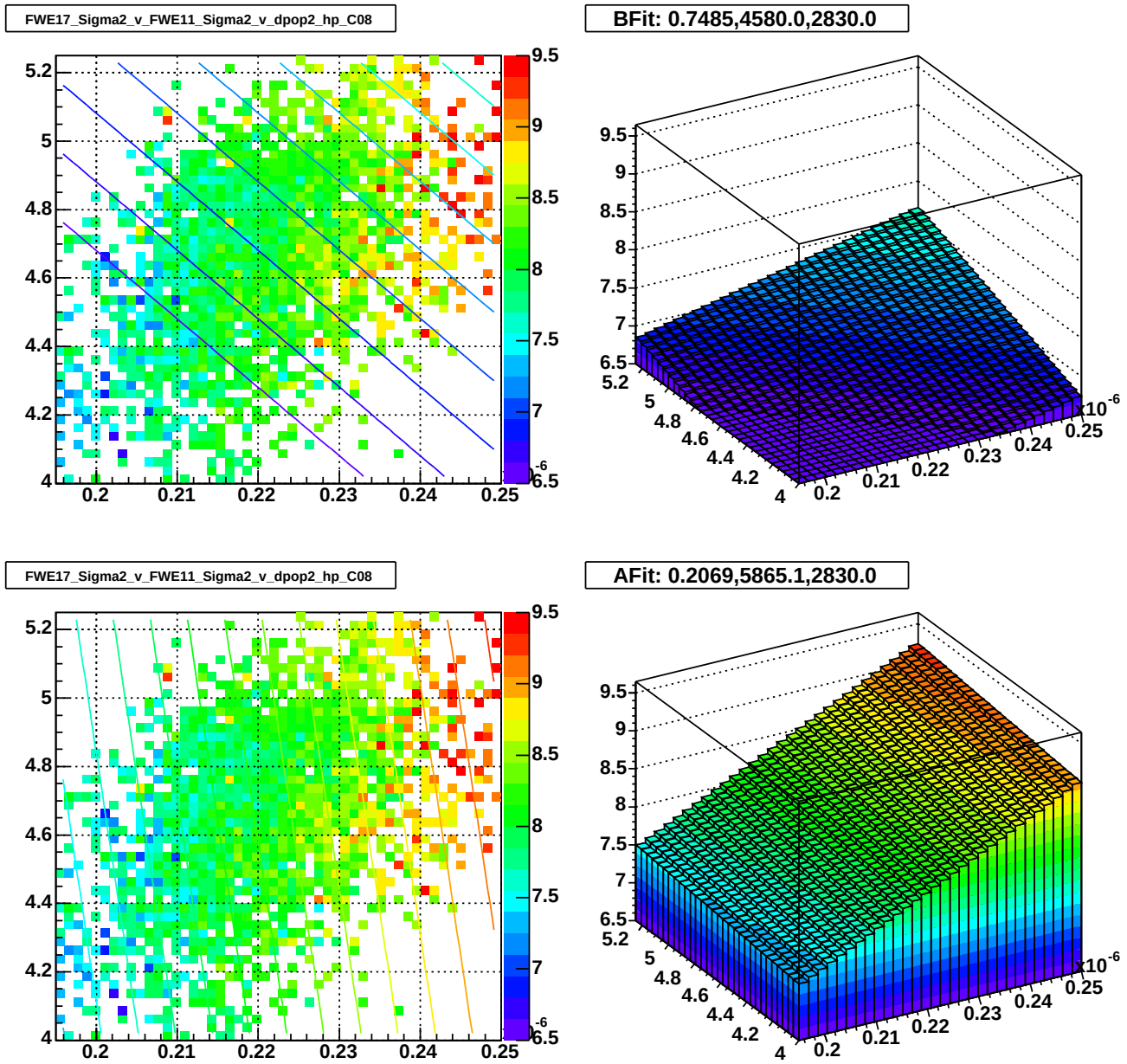

Figure 5: Proton beam, horizontal detectors, nominal lattice: Stores 2650-2997, 150 GeV Case Before Ramp: Comparisons of Sigma squared of the bunch width distribution measurements as done by Flying Wire (FW) E17 Detector with predictions based on the FW E11 Detector measurement: Sigma squared of the bunch width distribution (in mm^2) as measured by the FW E17 Detector as a function of sigma squared of the bunch width distribution (in mm^2) as measured by the FW E11 Detector versus recalculated $\delta p/p$ squared (based on δt the T:SBD[A,P]WS ACNET variable) with an overlaid contour of the prediction based on the nominal lattice functions; Prediction of sigma squared of the bunch width distribution (in mm^2) for E17 Detector as a function of sigma squared of the bunch width distribution (in mm^2) as measured by the FW E11 Detector versus recalculated $\delta p/p$ squared based on the nominal lattice functions; two lower plots have the same data points but have contours based on the fitted lattice functions.

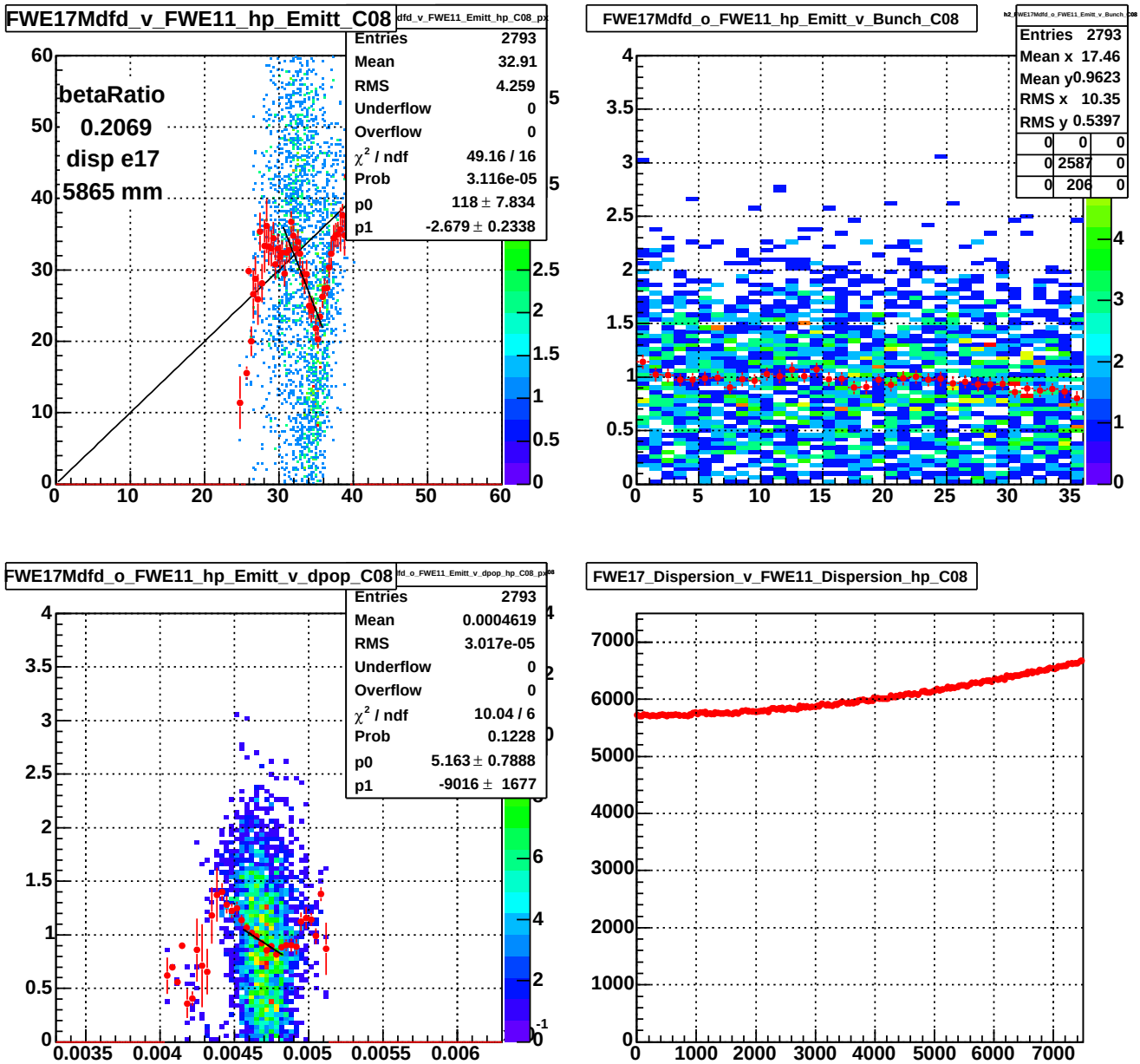

Figure 6: Proton beam, horizontal detectors, modified lattice: Stores 2650-2997, 150 GeV Case Before Ramp: Comparisons of Emittance measurements as done by Flying Wire (FW) Detector at E17 and Flying Wire Detector at E11 using fitted lattice parameters: Bunch emittance (in $\pi \cdot mm \cdot mrad$) as measured by FW E17 Detector versus bunch emittance as measured by the FW E11 Detector with an overlaid horizontal profile distribution with a straight line fit and the ideal prediction; bunch emittance as measured by FW E17 Detector over bunch emittance as measured by the FW E11 Detector versus bunch number together with an overlaid horizontal profile; bunch emittance as measured by FW E17 Detector over bunch emittance as measured by the FW E11 Detector versus recalculated $\delta p/p$ (based on δt the T:SBD[A,P]WS ACNET variable) with an overlaid horizontal profile with a straight line fit; fit based E17 dispersion function as a function of the E11 dispersion function.

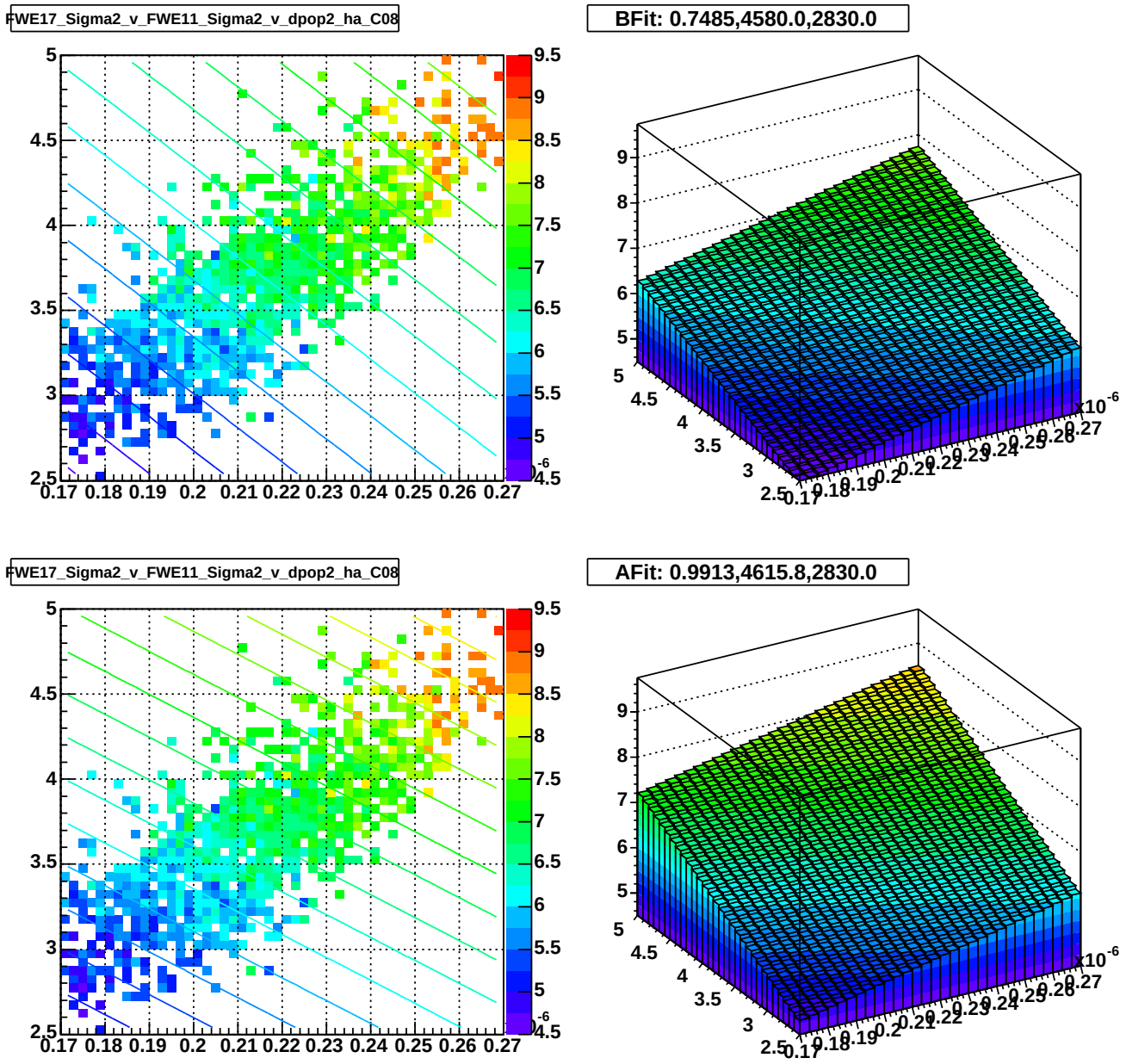

Figure 7: Antiproton beam, horizontal detectors, nominal lattice: Stores 2810-2997, 150 GeV Case Before Ramp: Comparisons of Sigma squared of the bunch width distribution measurements as done by Flying Wire (FW) E17 Detector with predictions based on the FW E11 Detector measurement: Sigma squared of the bunch width distribution (in mm^2) as measured by the FW E17 Detector as a function of sigma squared of the bunch width distribution (in mm^2) as measured by the FW E11 Detector versus recalculated $\delta p/p$ squared (based on δt the T:SBD[A,P]WS ACNET variable) with an overlaid contour of the prediction based on the nominal lattice functions; Prediction of sigma squared of the bunch width distribution (in mm^2) for E17 Detector as a function of sigma squared of the bunch width distribution (in mm^2) as measured by the FW E11 Detector versus recalculated $\delta p/p$ squared based on the nominal lattice functions; two lower plots have the same data points but have contours based on the fitted lattice functions.

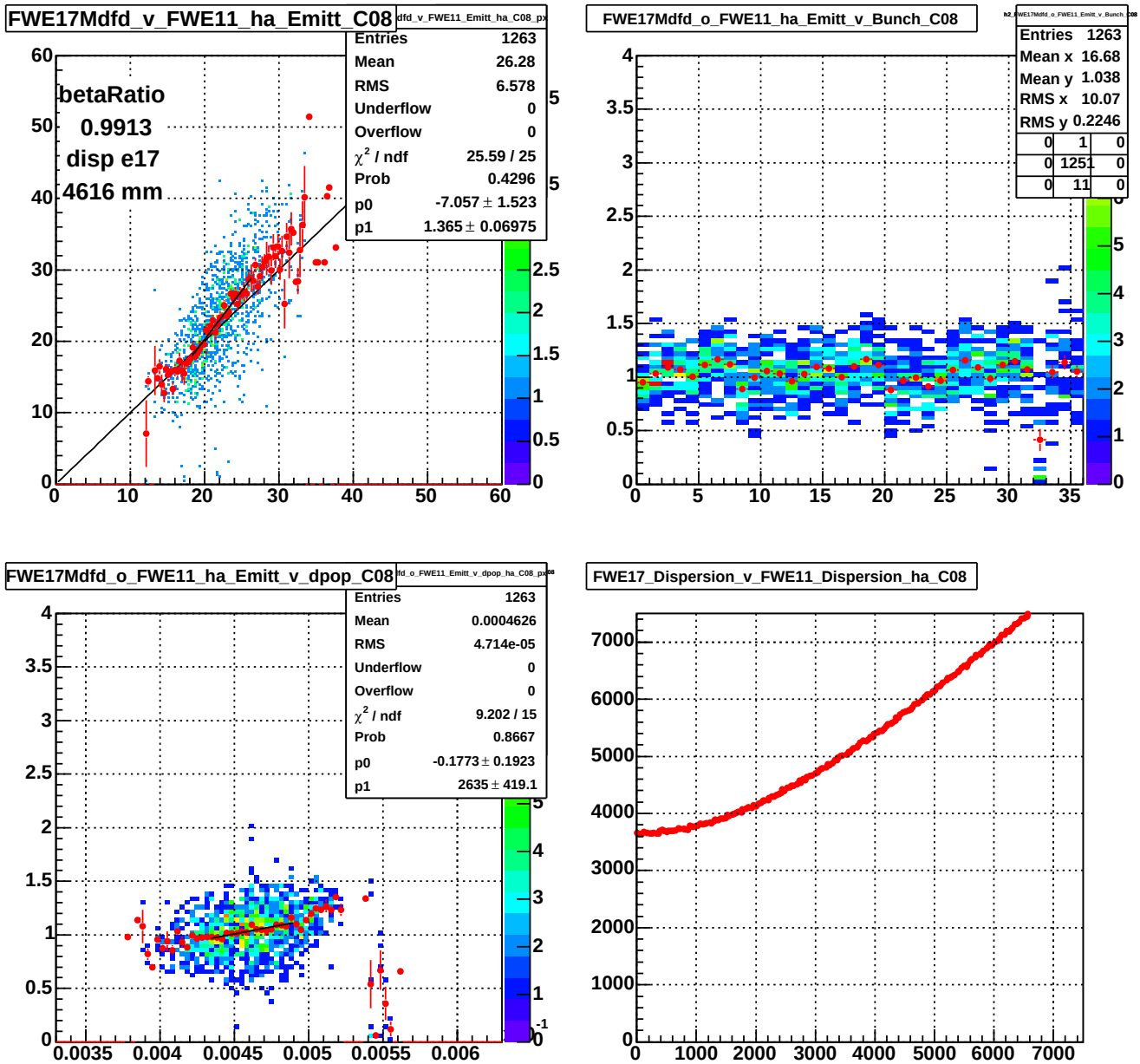

Figure 8: Antiproton beam, horizontal detectors, modified lattice: Stores 2810-2997, 150 GeV Case Before Ramp: Comparisons of Emittance measurements as done by Flying Wire (FW) Detector at E17 and Flying Wire Detector at E11 using fitted lattice parameters: Bunch emittance (in $\pi \cdot mm \cdot mrad$) as measured by FW E17 Detector versus bunch emittance as measured by the FW E11 Detector with an overlaid horizontal profile distribution with a straight line fit and the ideal prediction; bunch emittance as measured by FW E17 Detector over bunch emittance as measured by the FW E11 Detector versus bunch number together with an overlaid horizontal profile; bunch emittance as measured by FW E17 Detector over bunch emittance as measured by the FW E11 Detector versus recalculated $\delta p/p$ (based on δt the T:SBD[A,P]WS ACNET variable) with an overlaid horizontal profile with a straight line fit; fit based E17 dispersion function as a function of the E11 dispersion function.

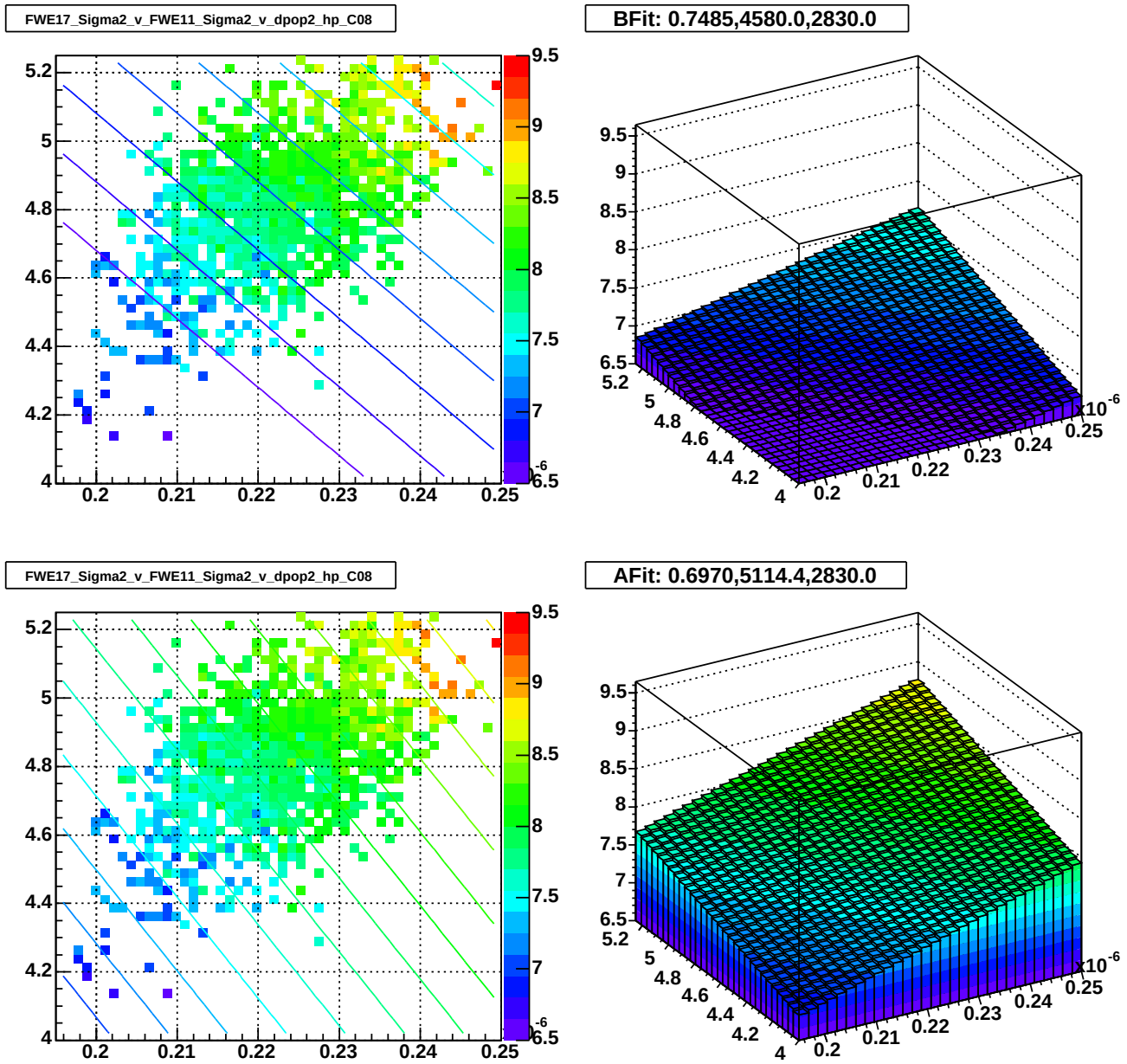

Figure 9: Proton beam, horizontal detectors, nominal lattice: Stores 2810-2997, 150 GeV Case Before Ramp: Comparisons of Sigma squared of the bunch width distribution measurements as done by Flying Wire (FW) E17 Detector with predictions based on the FW E11 Detector measurement: Sigma squared of the bunch width distribution (in mm^2) as measured by the FW E17 Detector as a function of sigma squared of the bunch width distribution (in mm^2) as measured by the FW E11 Detector versus recalculated $\delta p/p$ squared (based on δt the T:SBD[A,P]WS ACNET variable) with an overlaid contour of the prediction based on the nominal lattice functions; Prediction of sigma squared of the bunch width distribution (in mm^2) for E17 Detector as a function of sigma squared of the bunch width distribution (in mm^2) as measured by the FW E11 Detector versus recalculated $\delta p/p$ squared based on the nominal lattice functions; two lower plots have the same data points but have contours based on the fitted lattice functions.

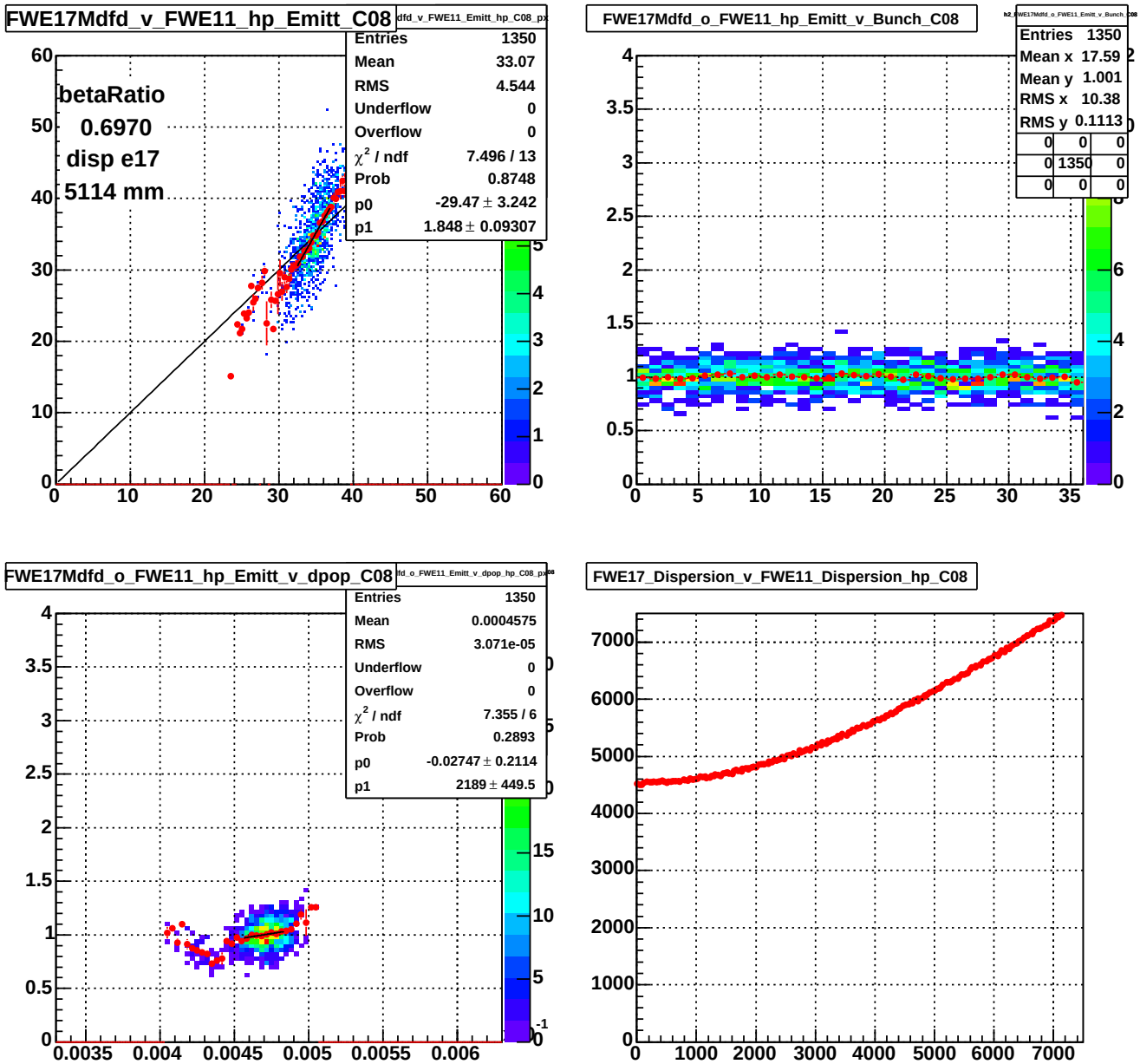

Figure 10: Proton beam, horizontal detectors, modified lattice: Stores 2810-2997, 150 GeV Case Before Ramp: Comparisons of Emittance measurements as done by Flying Wire (FW) Detector at E17 and Flying Wire Detector at E11 using fitted lattice parameters: Bunch emittance (in $\pi \cdot mm \cdot mrad$) as measured by FW E17 Detector versus bunch emittance as measured by the FW E11 Detector with an overlaid horizontal profile distribution with a straight line fit and the ideal prediction; bunch emittance as measured by FW E17 Detector over bunch emittance as measured by the FW E11 Detector versus bunch number together with an overlaid horizontal profile; bunch emittance as measured by FW E17 Detector over bunch emittance as measured by the FW E11 Detector versus recalculated $\delta p/p$ (based on δt the T:SBD[A,P]WS ACNET variable) with an overlaid horizontal profile with a straight line fit; fit based E17 dispersion function as a function of the E11 dispersion function.

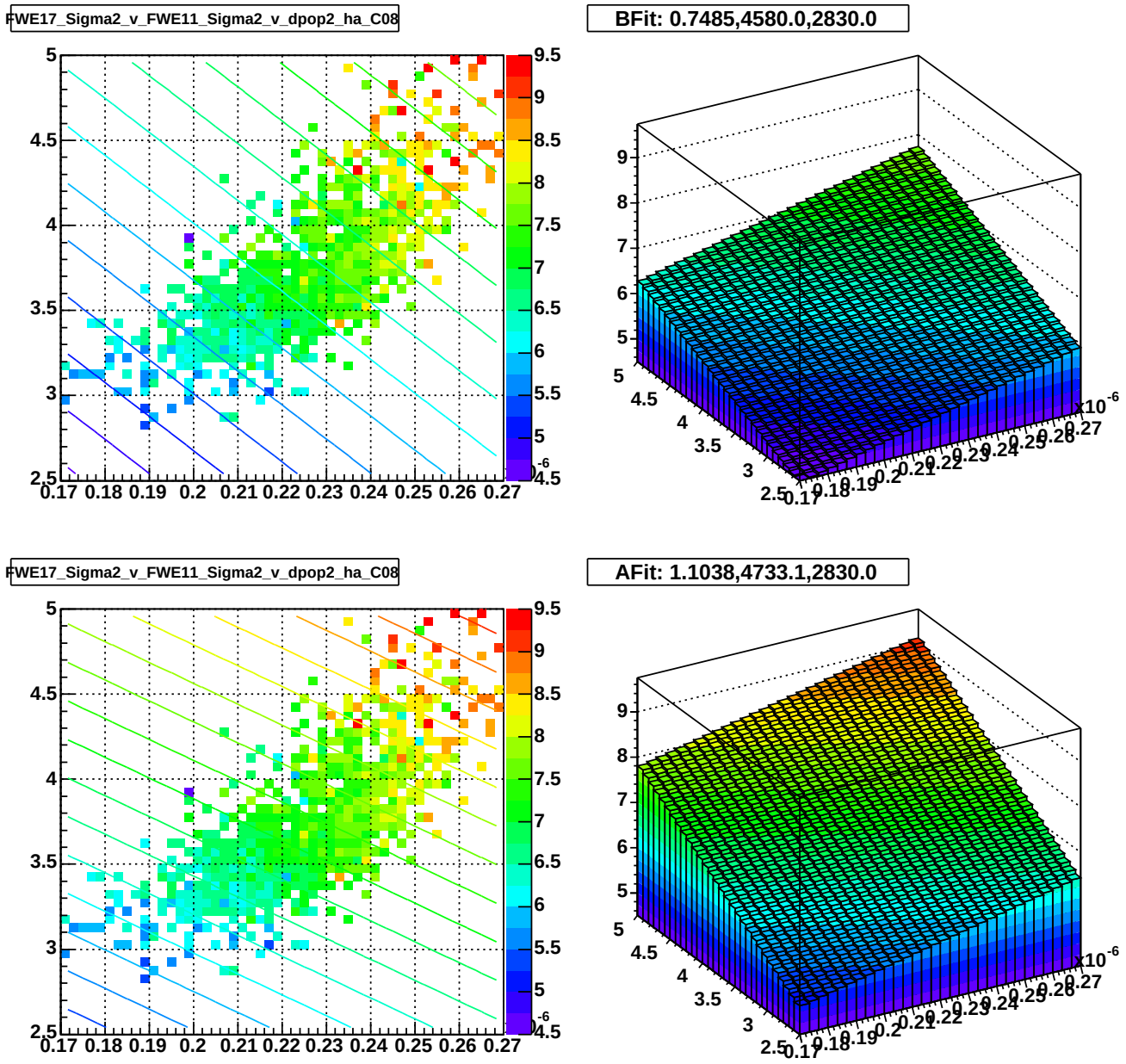

Figure 11: Antiproton beam, horizontal detectors, nominal lattice: Stores 2676-2805, 150 GeV Case Before Ramp: Comparisons of Sigma squared of the bunch width distribution measurements as done by Flying Wire (FW) E17 Detector with predictions based on the FW E11 Detector measurement: Sigma squared of the bunch width distribution (in mm^2) as measured by the FW E17 Detector as a function of sigma squared of the bunch width distribution (in mm^2) as measured by the FW E11 Detector versus recalculated $\delta p/p$ squared (based on δt the T:SBD[A,P]WS ACNET variable) with an overlaid contour of the prediction based on the nominal lattice functions; Prediction of sigma squared of the bunch width distribution (in mm^2) for E17 Detector as a function of sigma squared of the bunch width distribution (in mm^2) as measured by the FW E11 Detector versus recalculated $\delta p/p$ squared based on the nominal lattice functions; two lower plots have the same data points but have contours based on the fitted lattice functions.

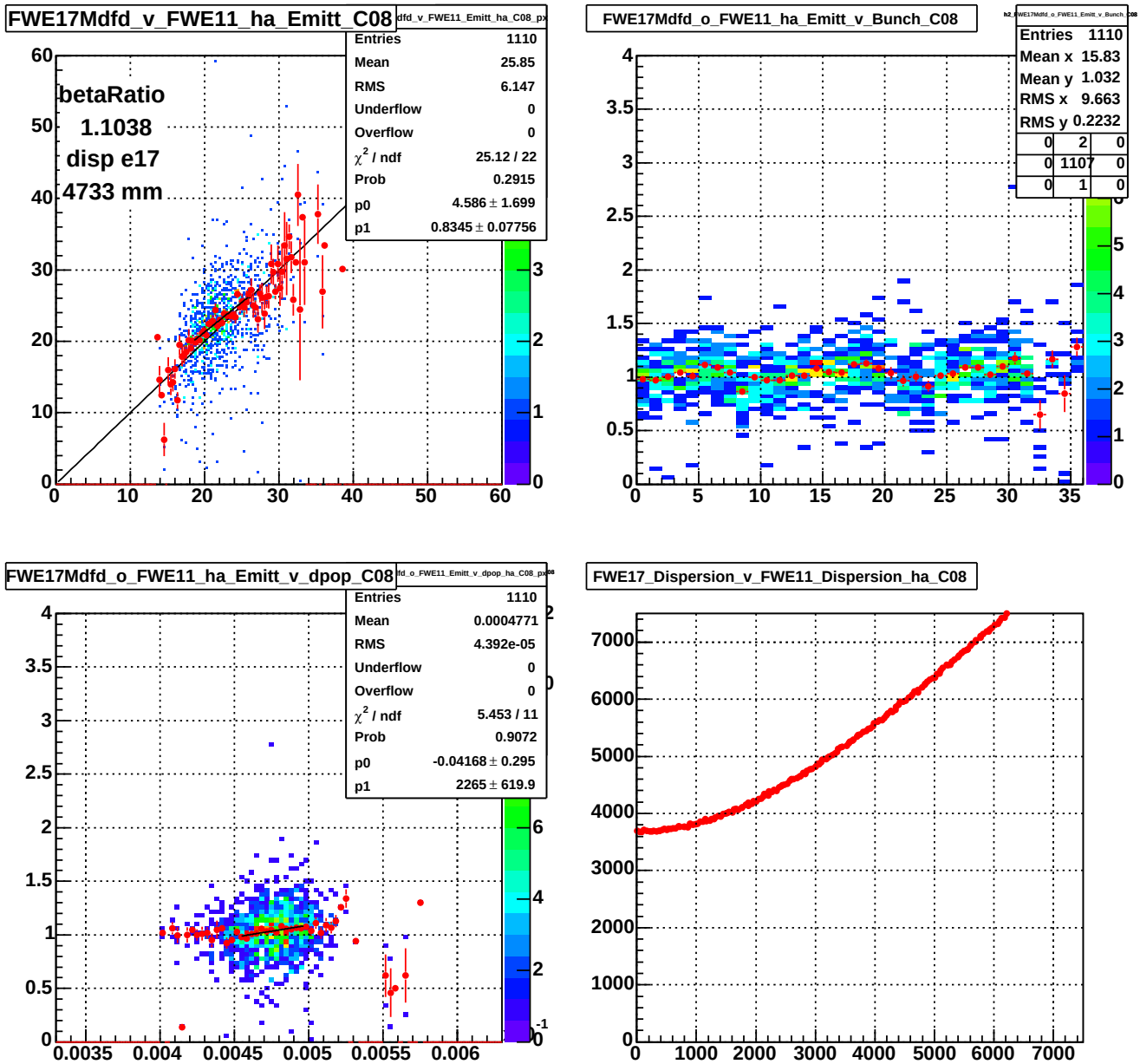

Figure 12: Antiproton beam, horizontal detectors, modified lattice: Stores 2676-2805, 150 GeV Case Before Ramp: Comparisons of Emittance measurements as done by Flying Wire (FW) Detector at E17 and Flying Wire Detector at E11 using fitted lattice parameters: Bunch emittance (in $\pi \cdot mm \cdot mrad$) as measured by FW E17 Detector versus bunch emittance as measured by the FW E11 Detector with an overlaid horizontal profile distribution with a straight line fit and the ideal prediction; bunch emittance as measured by FW E17 Detector over bunch emittance as measured by the FW E11 Detector versus bunch number together with an overlaid horizontal profile; bunch emittance as measured by FW E17 Detector over bunch emittance as measured by the FW E11 Detector versus recalculated $\delta p/p$ (based on δt the T:SBD[A,P]WS ACNET variable) with an overlaid horizontal profile with a straight line fit; fit based E17 dispersion function as a function of the E11 dispersion function.

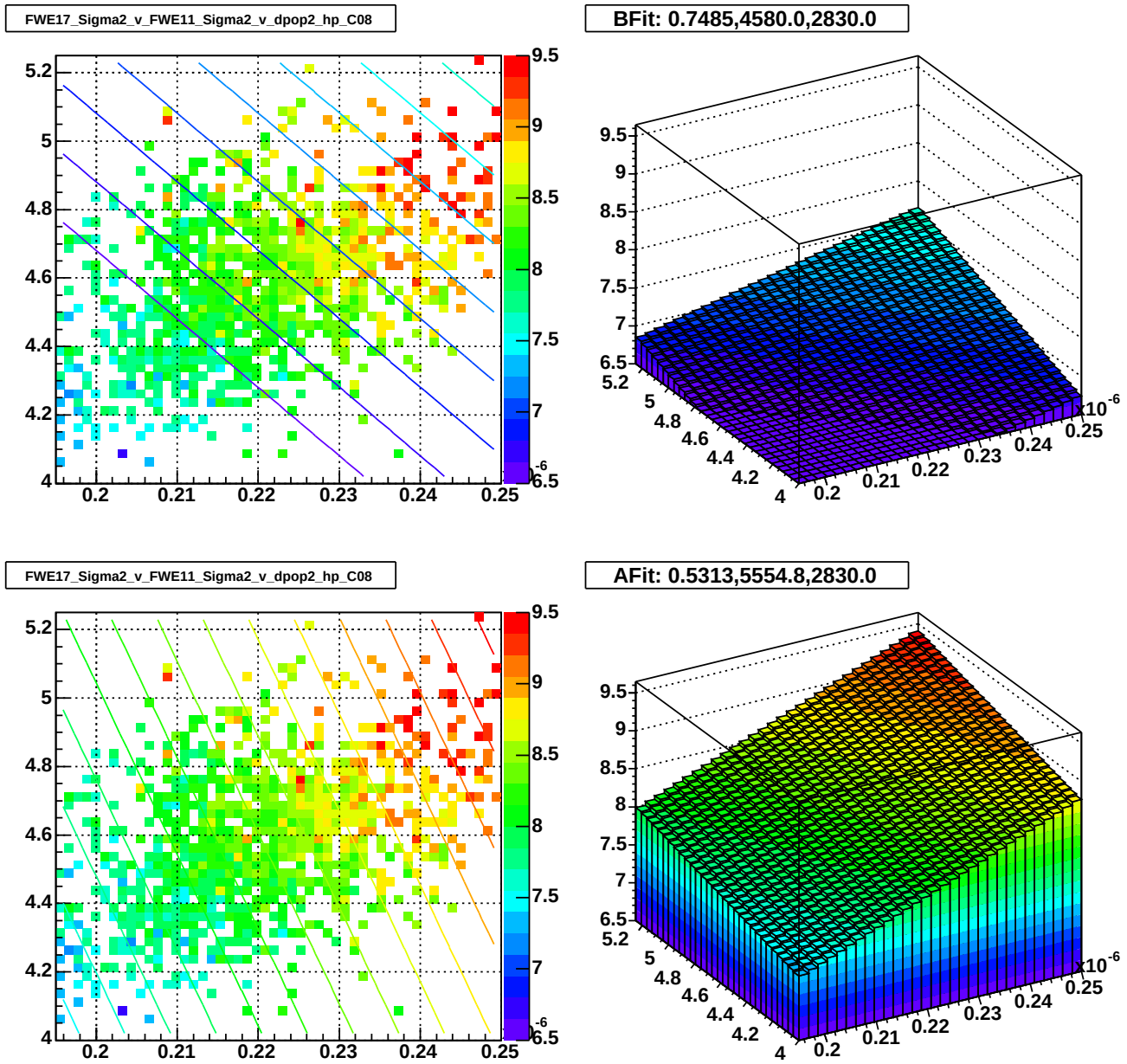

Figure 13: Proton beam, horizontal detectors, nominal lattice: Stores 2676-2805, 150 GeV Case Before Ramp: Comparisons of Sigma squared of the bunch width distribution measurements as done by Flying Wire (FW) E17 Detector with predictions based on the FW E11 Detector measurement: Sigma squared of the bunch width distribution (in mm^2) as measured by the FW E17 Detector as a function of sigma squared of the bunch width distribution (in mm^2) as measured by the FW E11 Detector versus recalculated $\delta p/p$ squared (based on δt the T:SBD[A,P]WS ACNET variable) with an overlaid contour of the prediction based on the nominal lattice functions; Prediction of sigma squared of the bunch width distribution (in mm^2) for E17 Detector as a function of sigma squared of the bunch width distribution (in mm^2) as measured by the FW E11 Detector versus recalculated $\delta p/p$ squared based on the nominal lattice functions; two lower plots have the same data points but have contours based on the fitted lattice functions.

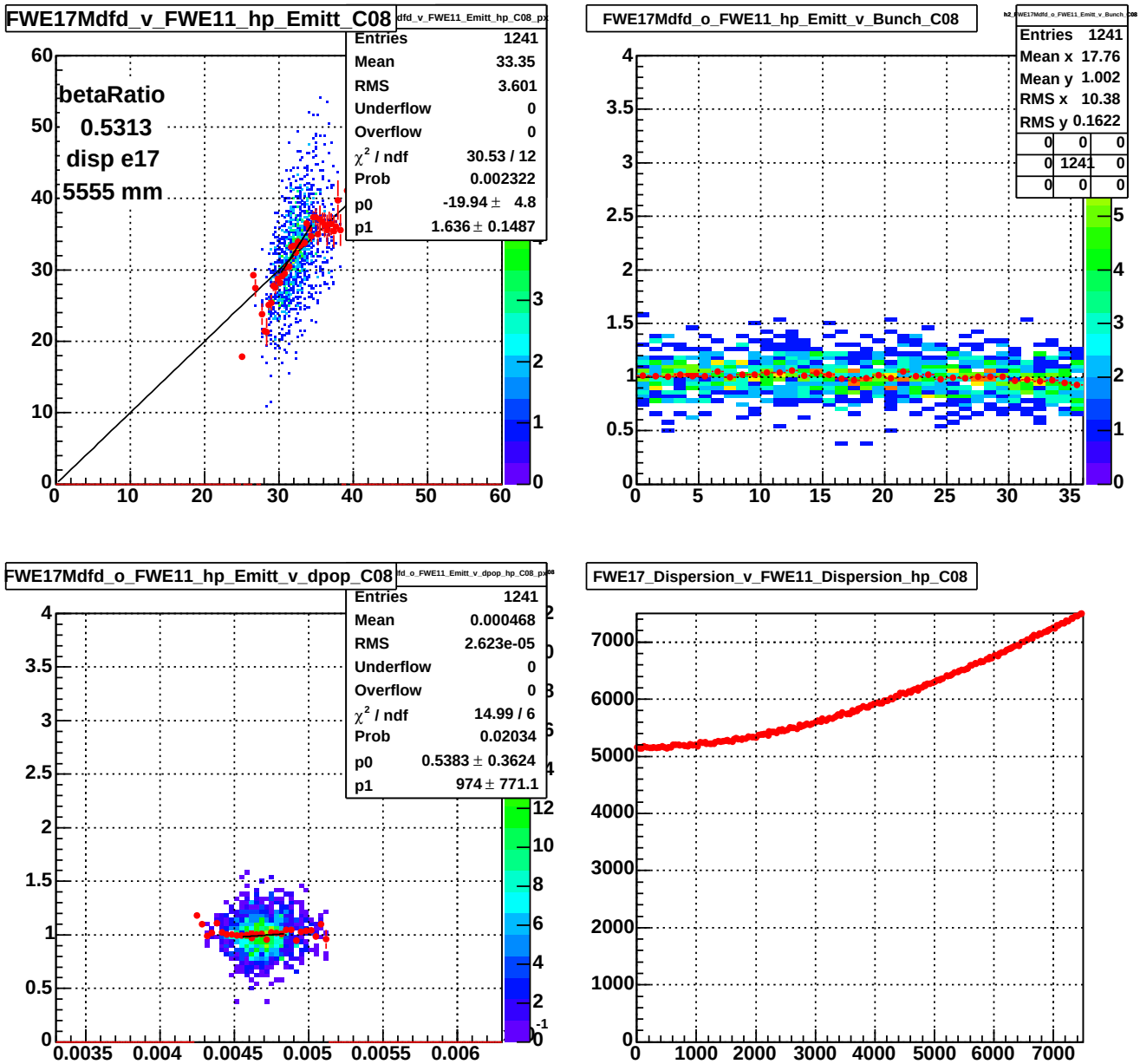

Figure 14: Proton beam, horizontal detectors, modified lattice: Stores 2676-2805, 150 GeV Case Before Ramp: Comparisons of Emittance measurements as done by Flying Wire (FW) Detector at E17 and Flying Wire Detector at E11 using fitted lattice parameters: Bunch emittance (in $\pi \cdot mm \cdot mrad$) as measured by FW E17 Detector versus bunch emittance as measured by the FW E11 Detector with an overlaid horizontal profile distribution with a straight line fit and the ideal prediction; bunch emittance as measured by FW E17 Detector over bunch emittance as measured by the FW E11 Detector versus bunch number together with an overlaid horizontal profile; bunch emittance as measured by FW E17 Detector over bunch emittance as measured by the FW E11 Detector versus recalculated $\delta p/p$ (based on δt the T:SBD[A,P]WS ACNET variable) with an overlaid horizontal profile with a straight line fit; fit based E17 dispersion function as a function of the E11 dispersion function.

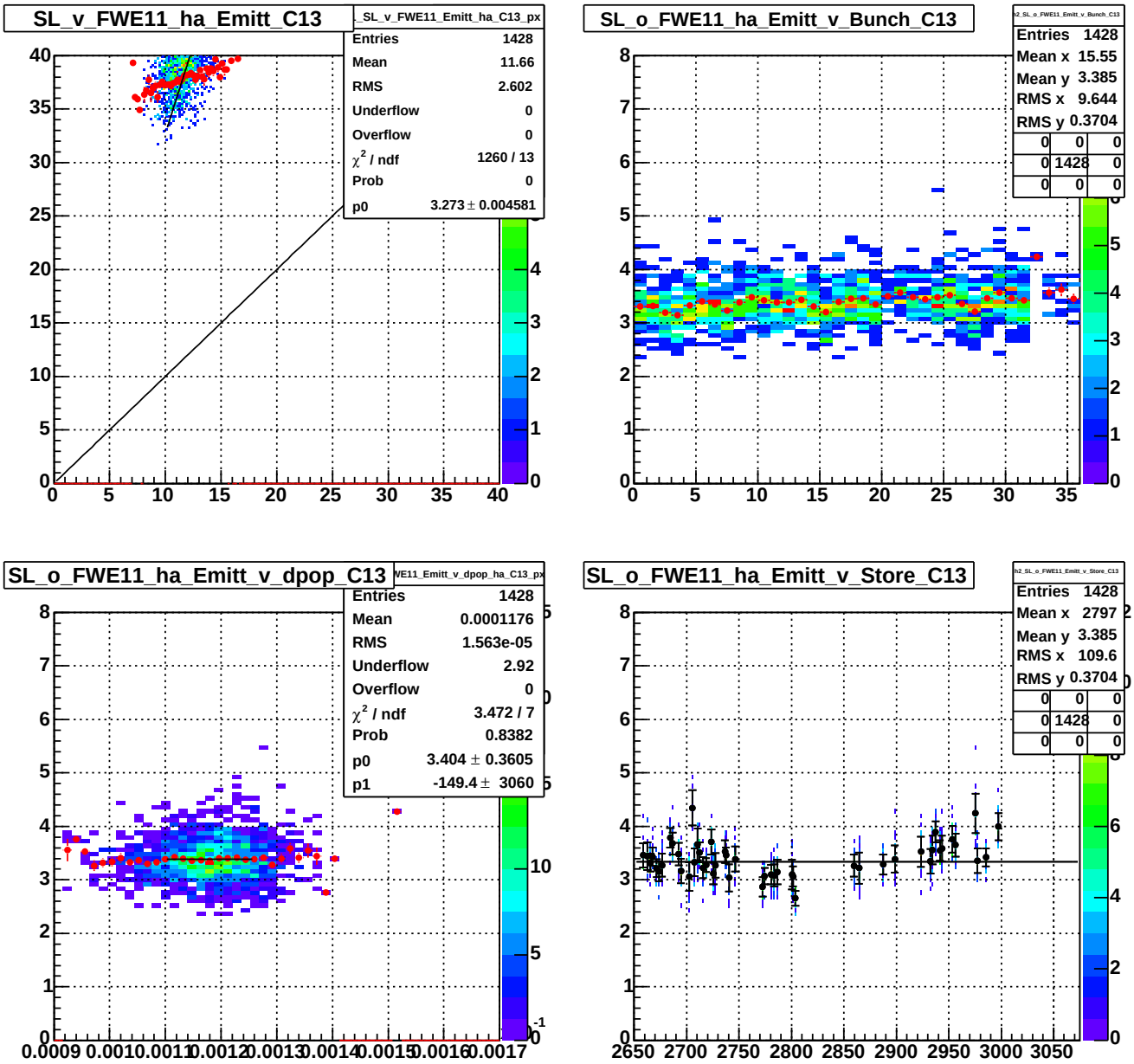

Figure 15: Antiproton beam, horizontal detectors, nominal lattice: Stores 2650-2997, 980 GeV Case Remove Halo: Comparisons of Emittance measurements as done by Synchrotron Light (SL) Detector at C11 and Flying Wire (FW) Detector at E11: Bunch emittance (in $\pi \cdot mm \cdot mrad$) as measured by SL C11 Detector versus bunch emittance as measured by the FW E11 Detector with an overlaid horizontal profile distribution with a straight line fit and the ideal prediction; bunch emittance as measured by SL C11 Detector over bunch emittance as measured by the FW E11 Detector versus bunch number together with an overlaid horizontal profile; bunch emittance as measured by SL C11 Detector over bunch emittance as measured by the FW E11 Detector versus recalculated $\delta p/p$ (based on δt the T:SBD[A,P]WS ACNET variable) with an overlaid horizontal profile with a straight line fit; bunch emittance as measured by SL C11 Detector over bunch emittance as measured by the FW E11 Detector versus store number with overlaid averaged ratios for each store and a horizontal line fit.

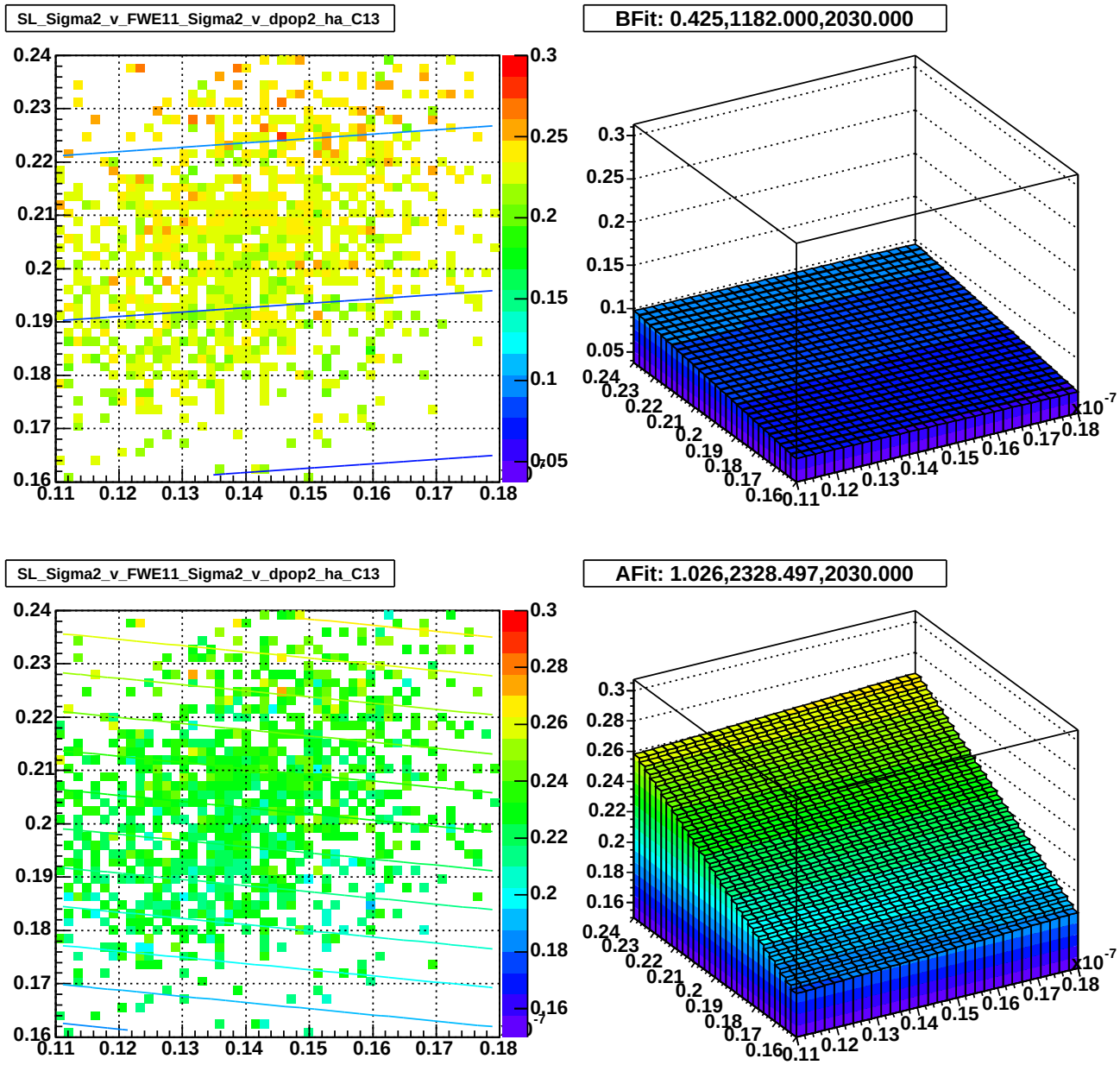

Figure 16: Antiproton beam, horizontal detectors, nominal lattice: Stores 2650-2997, 980 GeV Case Remove Halo: Comparisons of Sigma squared of the bunch width distribution measurements as done by Synchrotron Light (SL) C11 Detector with predictions based on the Flying Wire (FW) E11 Detector measurement: Sigma squared of the bunch width distribution (in mm^2) as measured by the SL C11 Detector as a function of sigma squared of the bunch width distribution (in mm^2) as measured by the FW E11 Detector versus recalculated $\delta p/p$ squared (based on δt the T:SBD[A,P]WS ACNET variable) with an overlaid contour of the prediction based on the nominal lattice functions; Prediction of sigma squared of the bunch width distribution (in mm^2) for SL C11 Detector as a function of sigma squared of the bunch width distribution (in mm^2) as measured by the FW E11 Detector versus recalculated $\delta p/p$ squared based on the nominal lattice functions; two lower plots have the same data points but have contours based on the fitted lattice functions.

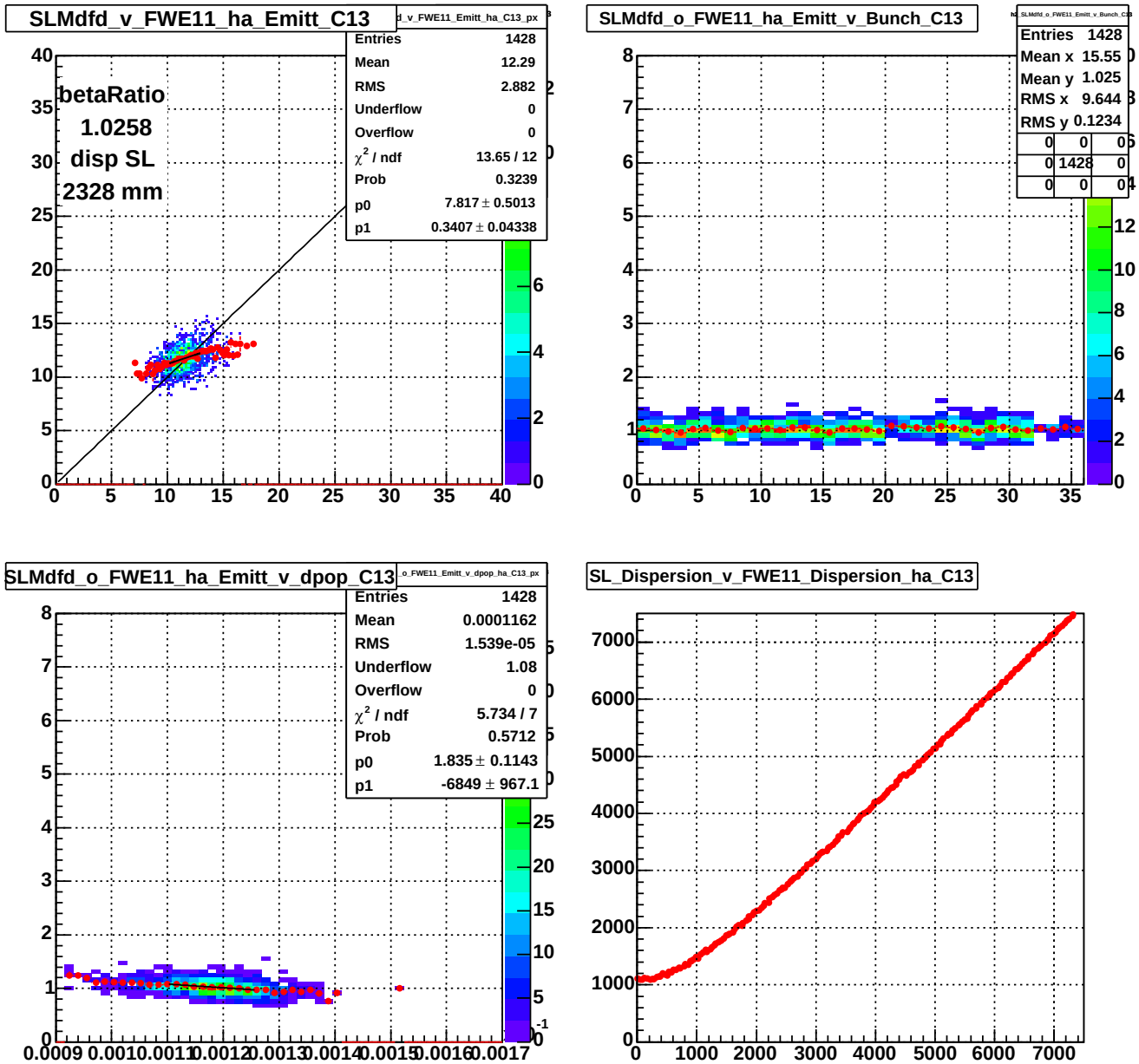

Figure 17: Antiproton beam, horizontal detectors, modified lattice: Stores 2650-2997, 980 GeV Case Remove Halo: Comparisons of Emittance measurements as done by Synchrotron Light (SL) Detector at C11 and Flying Wire (FW) Detector at E11 using fitted lattice parameters and formula with dispersion term both in the horizontal and in the vertical cases: Bunch emittance (in $\pi \cdot mm \cdot mrad$) as measured by SL C11 Detector versus bunch emittance as measured by the FW E11 Detector with an overlaid horizontal profile distribution with a straight line fit and the ideal prediction; bunch emittance as measured by SL C11 Detector over bunch emittance as measured by the FW E11 Detector versus bunch number together with an overlaid horizontal profile; bunch emittance as measured by SL C11 Detector over bunch emittance as measured by the FW E11 Detector versus recalculated $\delta p/p$ (based on δt the T:SBD[A,P]WS ACNET variable) with an overlaid horizontal profile with a straight line fit; fit based C11 dispersion function as a function of the E11 dispersion function.

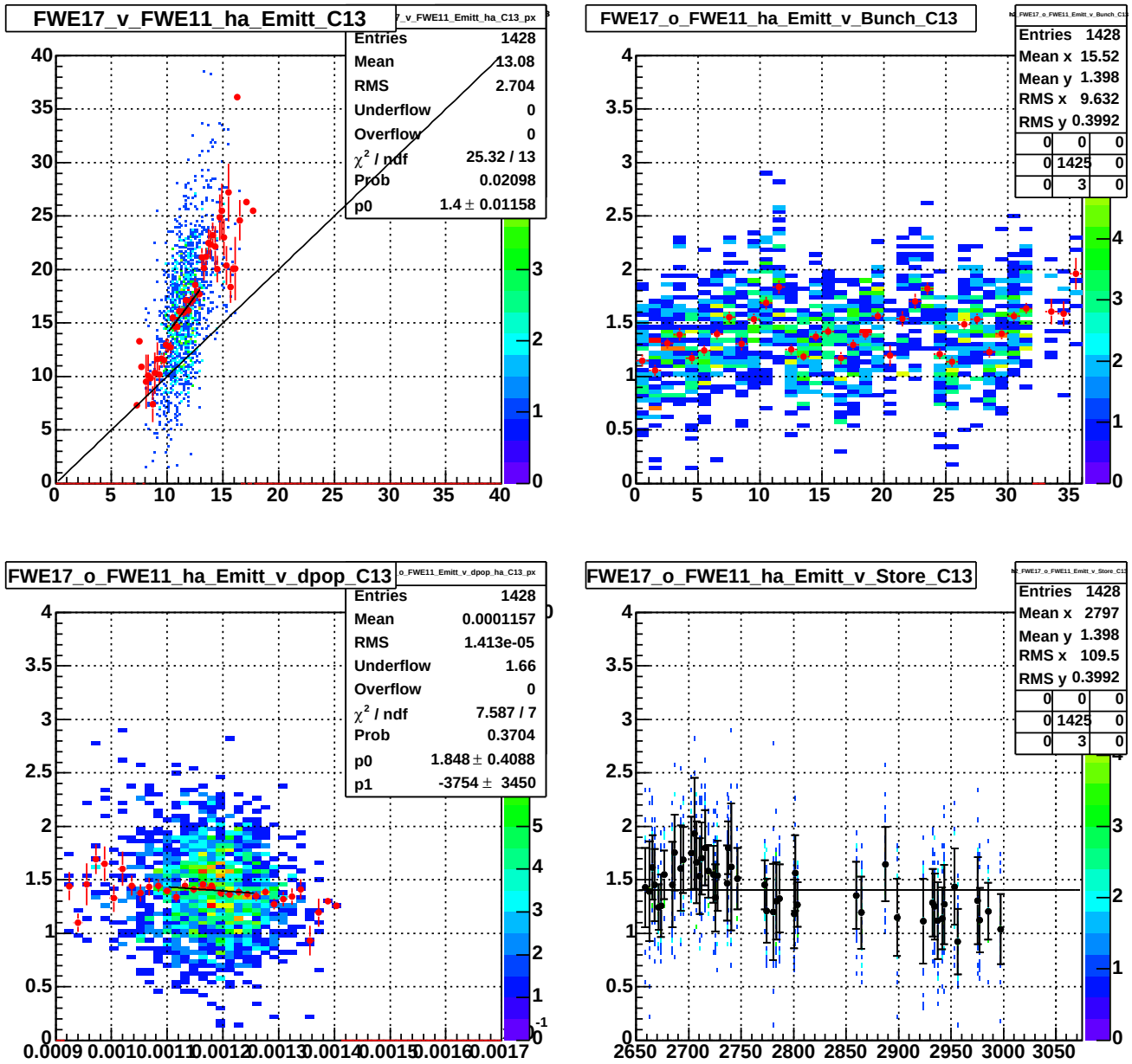

Figure 18: Antiproton beam, horizontal detectors, nominal lattice: Stores 2650-2997, 980 GeV Case Remove Halo: Comparisons of Emittance measurements as done by Flying Wire (FW) Detector at E17 and Flying Wire Detector at E11: Bunch emittance (in $\pi \cdot mm \cdot mrad$) as measured by FW E17 Detector versus bunch emittance as measured by the FW E11 Detector with an overlaid horizontal profile distribution with a straight line fit and the ideal prediction; bunch emittance as measured by FW E17 Detector over bunch emittance as measured by the FW E11 Detector versus bunch number together with an overlaid horizontal profile; bunch emittance as measured by FW E17 Detector over bunch emittance as measured by the FW E11 Detector versus recalculated $\delta p/p$ (based on δt the T:SBD[A,P]WS ACNET variable) with an overlaid horizontal profile with a straight line fit; bunch emittance as measured by FW E17 Detector over bunch emittance as measured by the FW E11 Detector versus store number with overlaid averaged ratios for each store and a horizontal line fit.

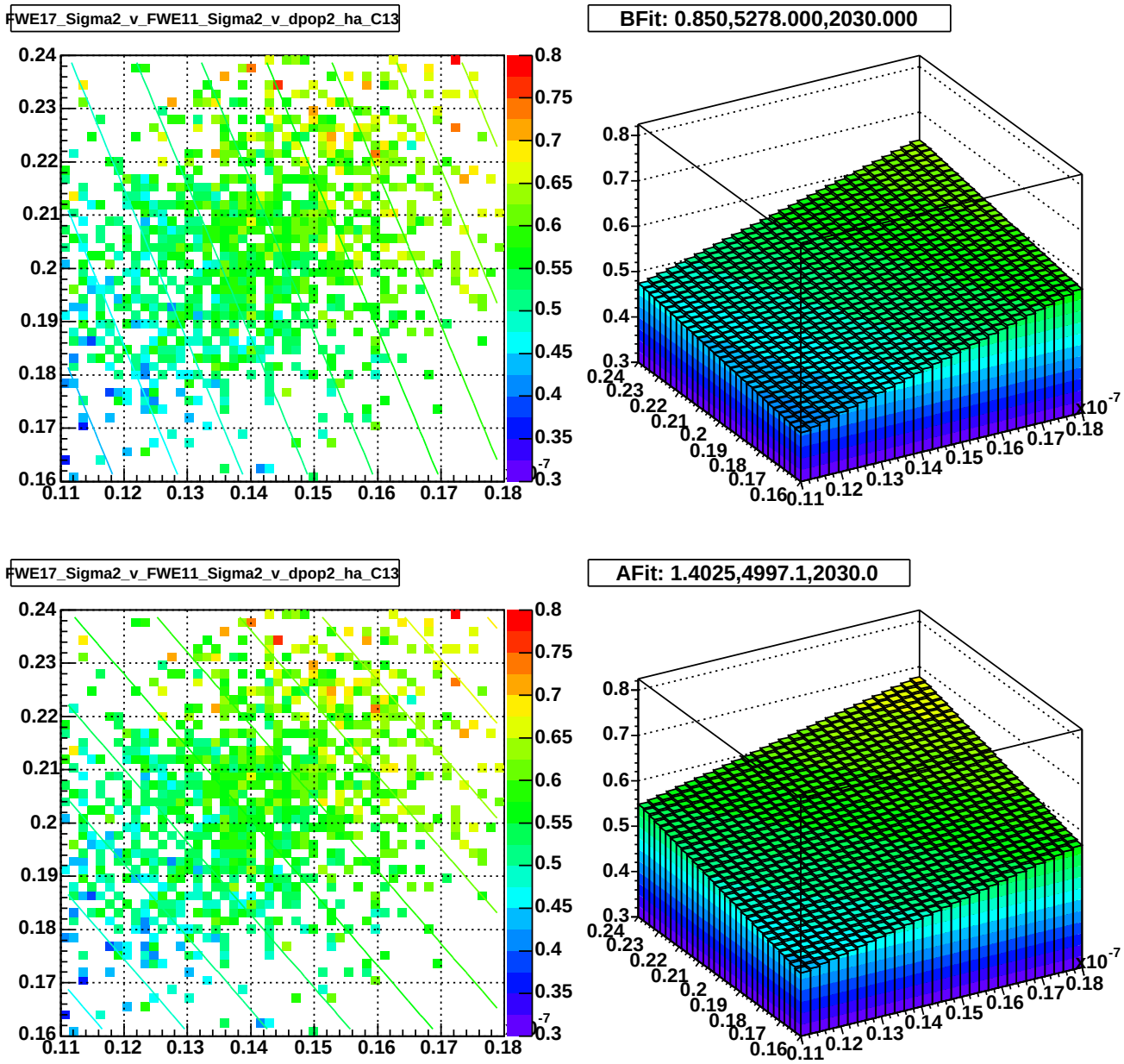

Figure 19: Antiproton beam, horizontal detectors, nominal lattice: Stores 2650-2997, 980 GeV Case Remove Halo: Comparisons of Sigma squared of the bunch width distribution measurements as done by Flying Wire (FW) E17 Detector with predictions based on the FW E11 Detector measurement: Sigma squared of the bunch width distribution (in mm^2) as measured by the FW E17 Detector as a function of sigma squared of the bunch width distribution (in mm^2) as measured by the FW E11 Detector versus recalculated $\delta p/p$ squared (based on δt the T:SBD[A,P]WS ACNET variable) with an overlaid contour of the prediction based on the nominal lattice functions; Prediction of sigma squared of the bunch width distribution (in mm^2) for E17 Detector as a function of sigma squared of the bunch width distribution (in mm^2) as measured by the FW E11 Detector versus recalculated $\delta p/p$ squared based on the nominal lattice functions; two lower plots have the same data points but have contours based on the fitted lattice functions.

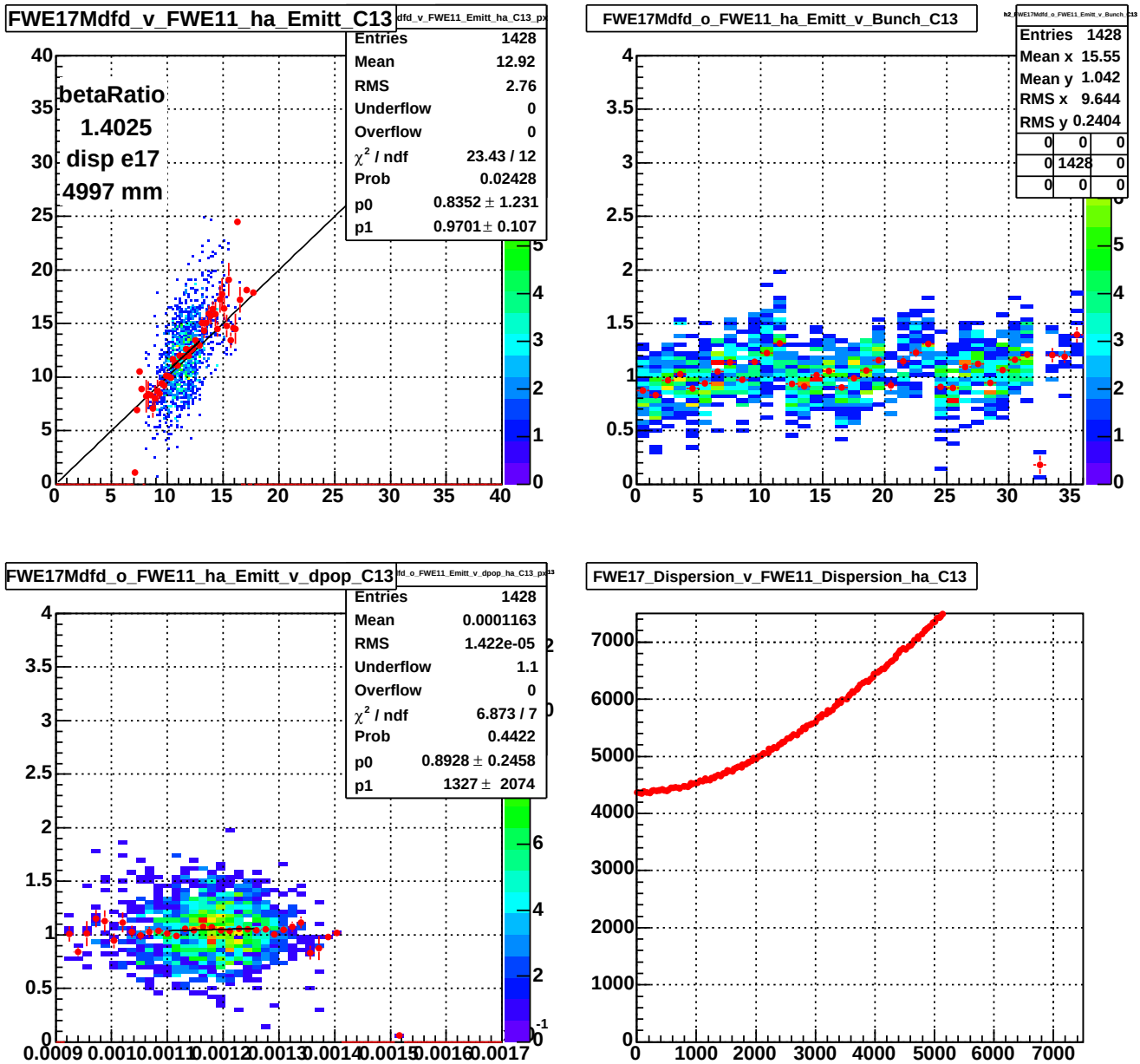

Figure 20: Antiproton beam, horizontal detectors, modified lattice: Stores 2650-2997, 980 GeV Case Remove Halo: Comparisons of Emittance measurements as done by Flying Wire (FW) Detector at E17 and Flying Wire Detector at E11 using fitted lattice parameters: Bunch emittance (in $\pi \cdot mm \cdot mrad$) as measured by FW E17 Detector versus bunch emittance as measured by the FW E11 Detector with an overlaid horizontal profile distribution with a straight line fit and the ideal prediction; bunch emittance as measured by FW E17 Detector over bunch emittance as measured by the FW E11 Detector versus bunch number together with an overlaid horizontal profile; bunch emittance as measured by FW E17 Detector over bunch emittance as measured by the FW E11 Detector versus recalculated $\delta p/p$ (based on δt the T:SBD[A,P]WS ACNET variable) with an overlaid horizontal profile with a straight line fit; fit based E17 dispersion function as a function of the E11 dispersion function.

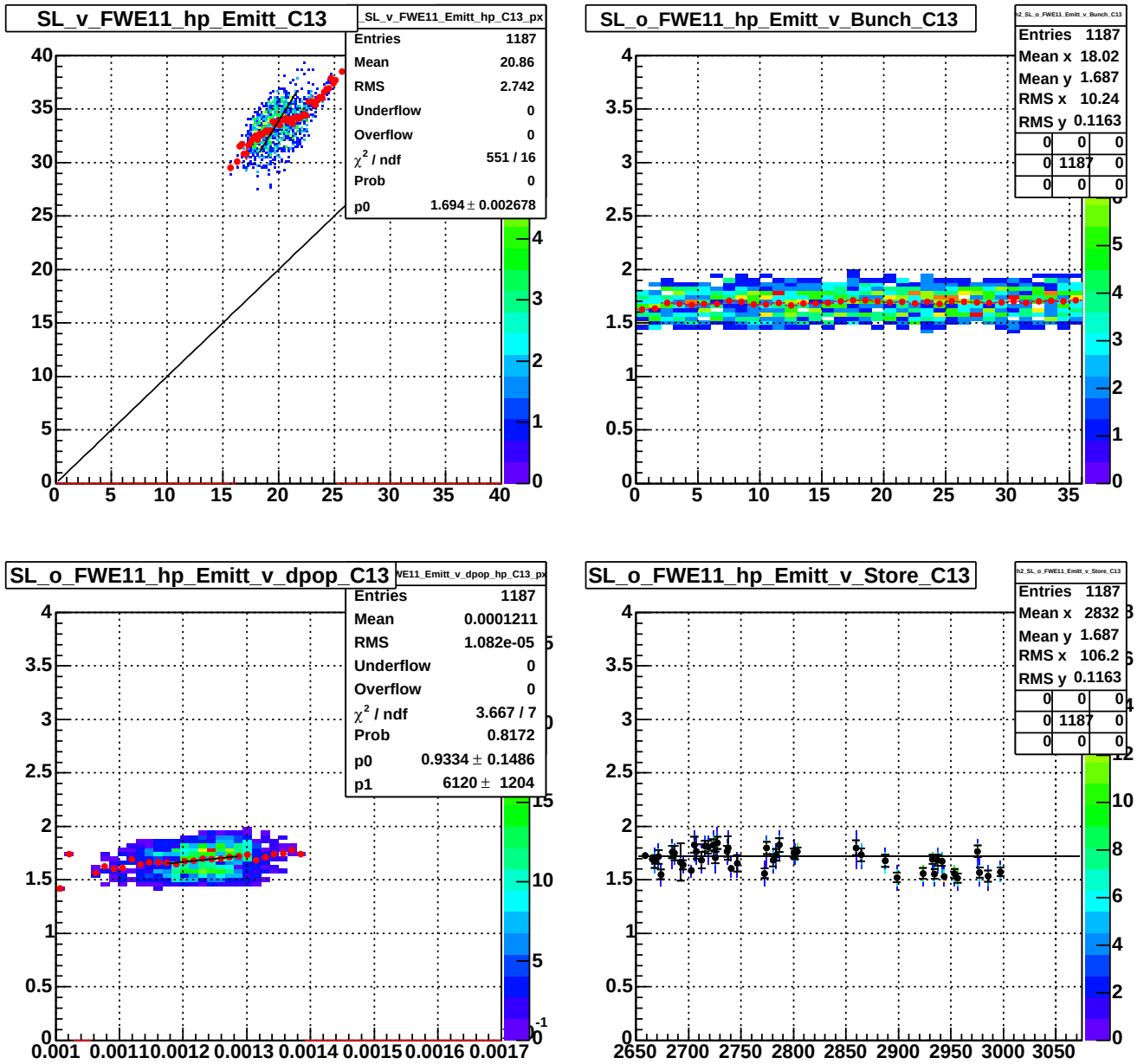

Figure 21: Proton beam, horizontal detectors, nominal lattice: Stores 2650-2997, 980 GeV Case Remove Halo: Comparisons of Emittance measurements as done by Synchrotron Light (SL) Detector at C11 and Flying Wire (FW) Detector at E11: Bunch emittance (in $\pi \cdot mm \cdot mrad$) as measured by SL C11 Detector versus bunch emittance as measured by the FW E11 Detector with an overlaid horizontal profile distribution with a straight line fit and the ideal prediction; bunch emittance as measured by SL C11 Detector over bunch emittance as measured by the FW E11 Detector versus bunch number together with an overlaid horizontal profile; bunch emittance as measured by SL C11 Detector over bunch emittance as measured by the FW E11 Detector versus recalculated $\delta p/p$ (based on δt the T:SBD[A,P]WS ACNET variable) with an overlaid horizontal profile with a straight line fit; bunch emittance as measured by SL C11 Detector over bunch emittance as measured by the FW E11 Detector versus store number with overlaid averaged ratios for each store and a horizontal line fit.

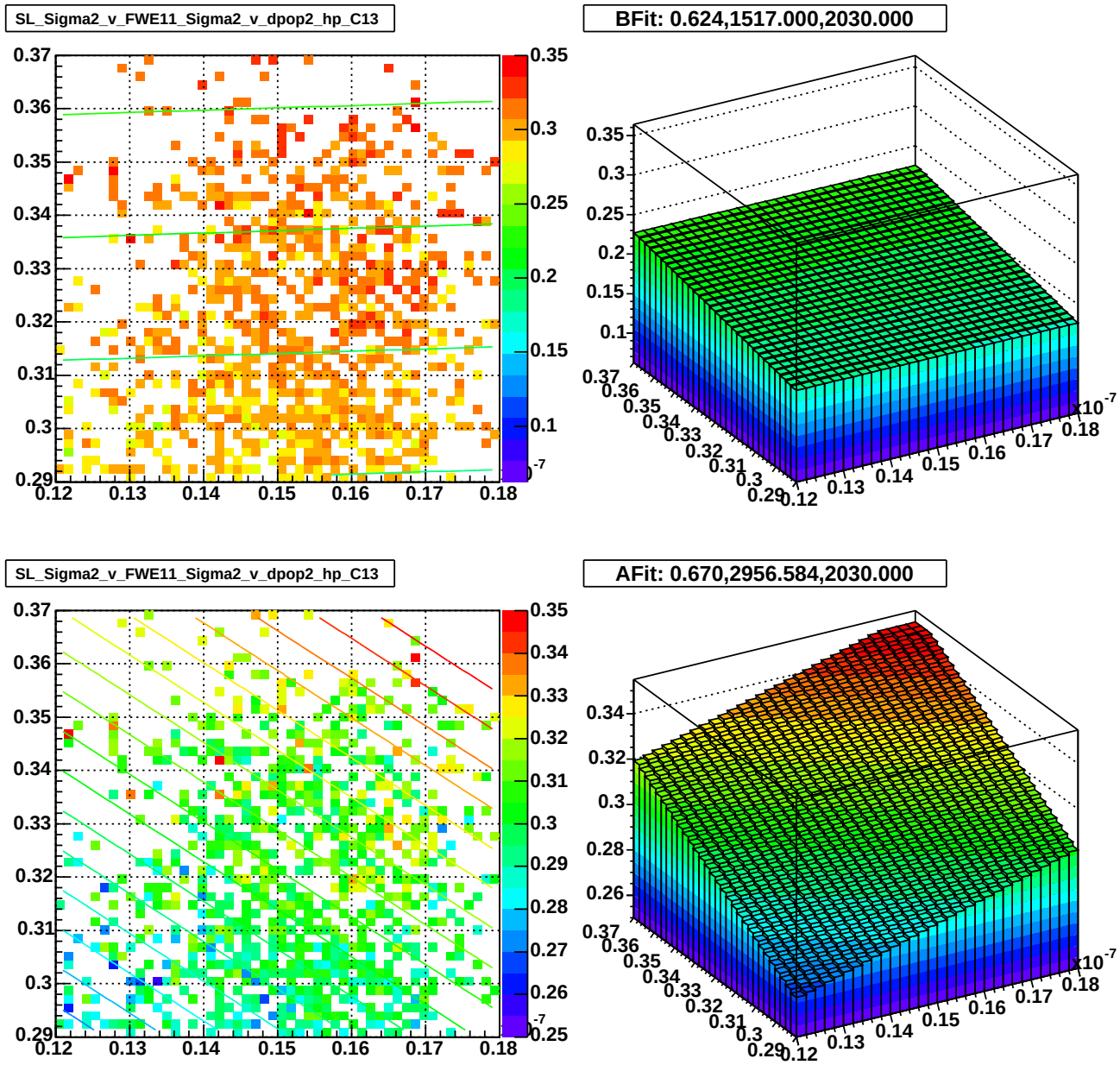

Figure 22: Proton beam, horizontal detectors, nominal lattice: Stores 2650-2997, 980 GeV Case Remove Halo: Comparisons of Sigma squared of the bunch width distribution measurements as done by Synchrotron Light (SL) C11 Detector with predictions based on the Flying Wire (FW) E11 Detector measurement: Sigma squared of the bunch width distribution (in mm^2) as measured by the SL C11 Detector as a function of sigma squared of the bunch width distribution (in mm^2) as measured by the FW E11 Detector versus recalculated $\delta p/p$ squared (based on δt the T:SBD[A,P]WS ACNET variable) with an overlaid contour of the prediction based on the nominal lattice functions; Prediction of sigma squared of the bunch width distribution (in mm^2) for SL C11 Detector as a function of sigma squared of the bunch width distribution (in mm^2) as measured by the FW E11 Detector versus recalculated $\delta p/p$ squared based on the nominal lattice functions; two lower plots have the same data points but have contours based on the fitted lattice functions.

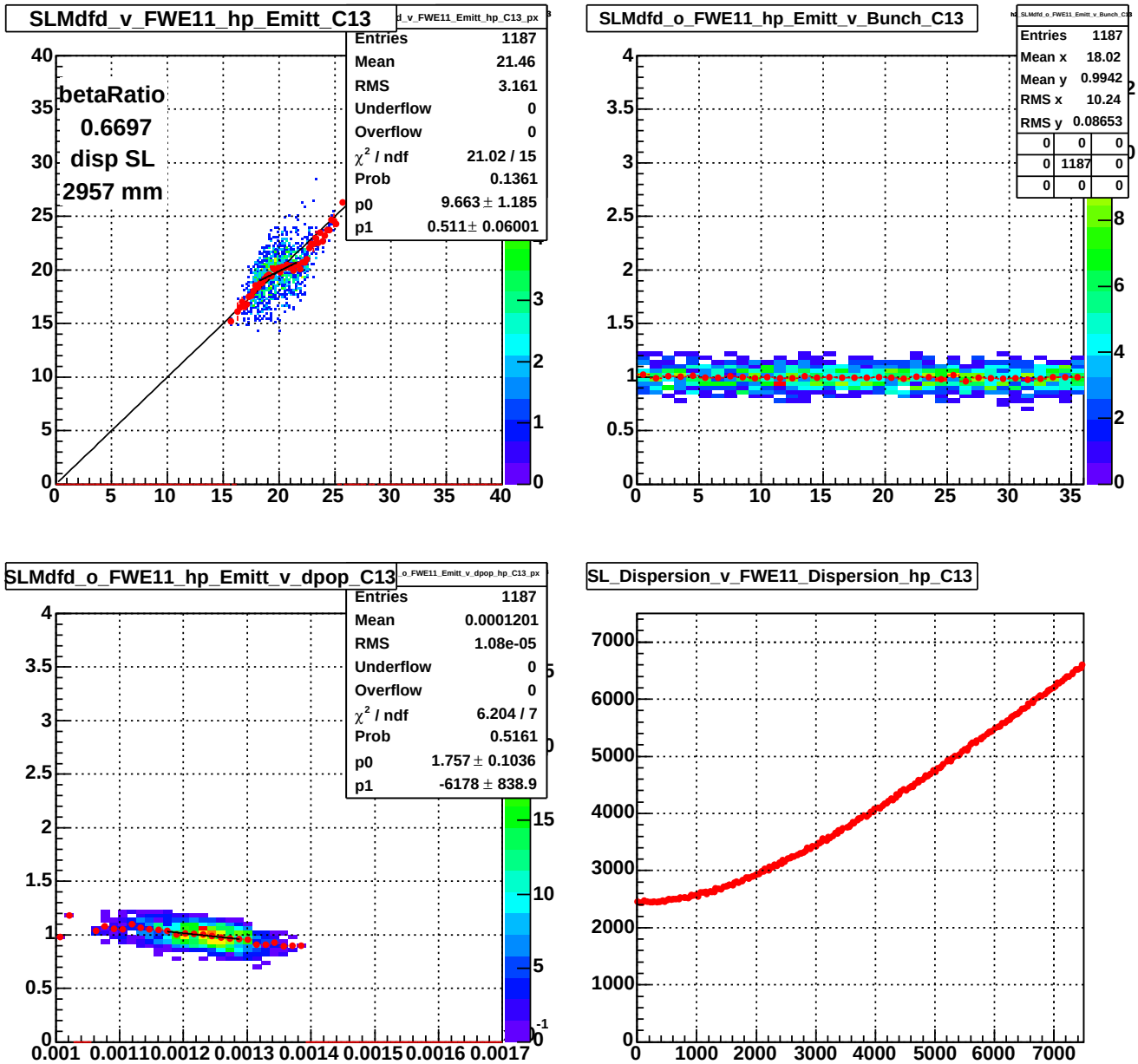

Figure 23: Proton beam, horizontal detectors, modified lattice: Stores 2650-2997, 980 GeV Case Remove Halo: Comparisons of Emittance measurements as done by Synchrotron Light (SL) Detector at C11 and Flying Wire (FW) Detector at E11 using fitted lattice parameters and formula with dispersion term both in the horizontal and in the vertical cases: Bunch emittance (in $\pi \cdot mm \cdot mrad$) as measured by SL C11 Detector versus bunch emittance as measured by the FW E11 Detector with an overlaid horizontal profile distribution with a straight line fit and the ideal prediction; bunch emittance as measured by SL C11 Detector over bunch emittance as measured by the FW E11 Detector versus bunch number together with an overlaid horizontal profile; bunch emittance as measured by SL C11 Detector over bunch emittance as measured by the FW E11 Detector versus recalculated $\delta p/p$ (based on δt the T:SBD[A,P]WS ACNET variable) with an overlaid horizontal profile with a straight line fit; fit based C11 dispersion function as a function of the E11 dispersion function.

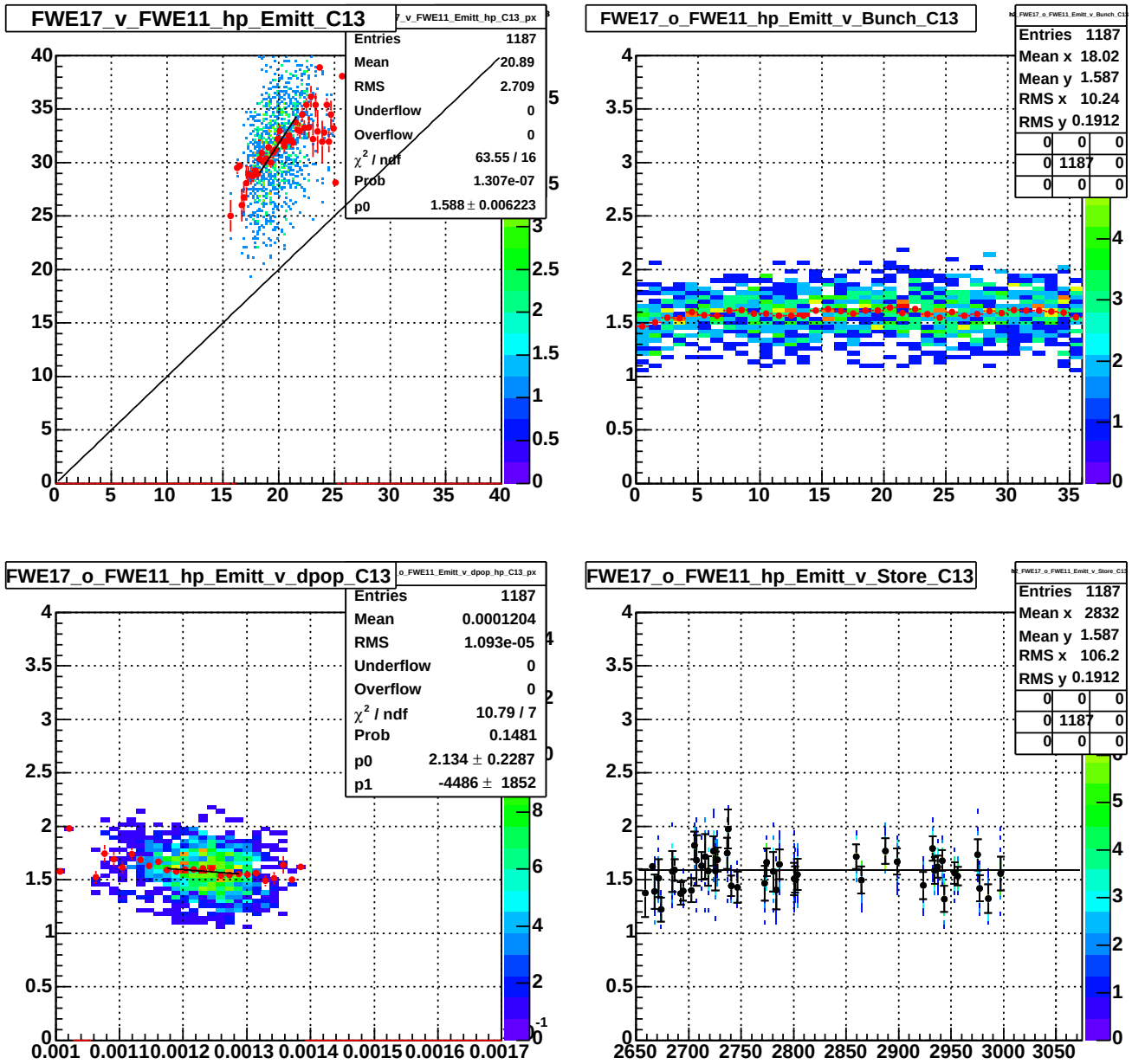

Figure 24: Proton beam, horizontal detectors, nominal lattice: Stores 2650-2997, 980 GeV Case Remove Halo: Comparisons of Emittance measurements as done by Flying Wire (FW) Detector at E17 and Flying Wire Detector at E11: Bunch emittance (in $\pi \cdot mm \cdot mrad$) as measured by FW E17 Detector versus bunch emittance as measured by the FW E11 Detector with an overlaid horizontal profile distribution with a straight line fit and the ideal prediction; bunch emittance as measured by FW E17 Detector over bunch emittance as measured by the FW E11 Detector versus bunch number together with an overlaid horizontal profile; bunch emittance as measured by FW E17 Detector over bunch emittance as measured by the FW E11 Detector versus recalculated $\delta p/p$ (based on δt the T:SBD[A,P]WS ACNET variable) with an overlaid horizontal profile with a straight line fit; bunch emittance as measured by FW E17 Detector over bunch emittance as measured by the FW E11 Detector versus store number with overlaid averaged ratios for each store and a horizontal line fit.

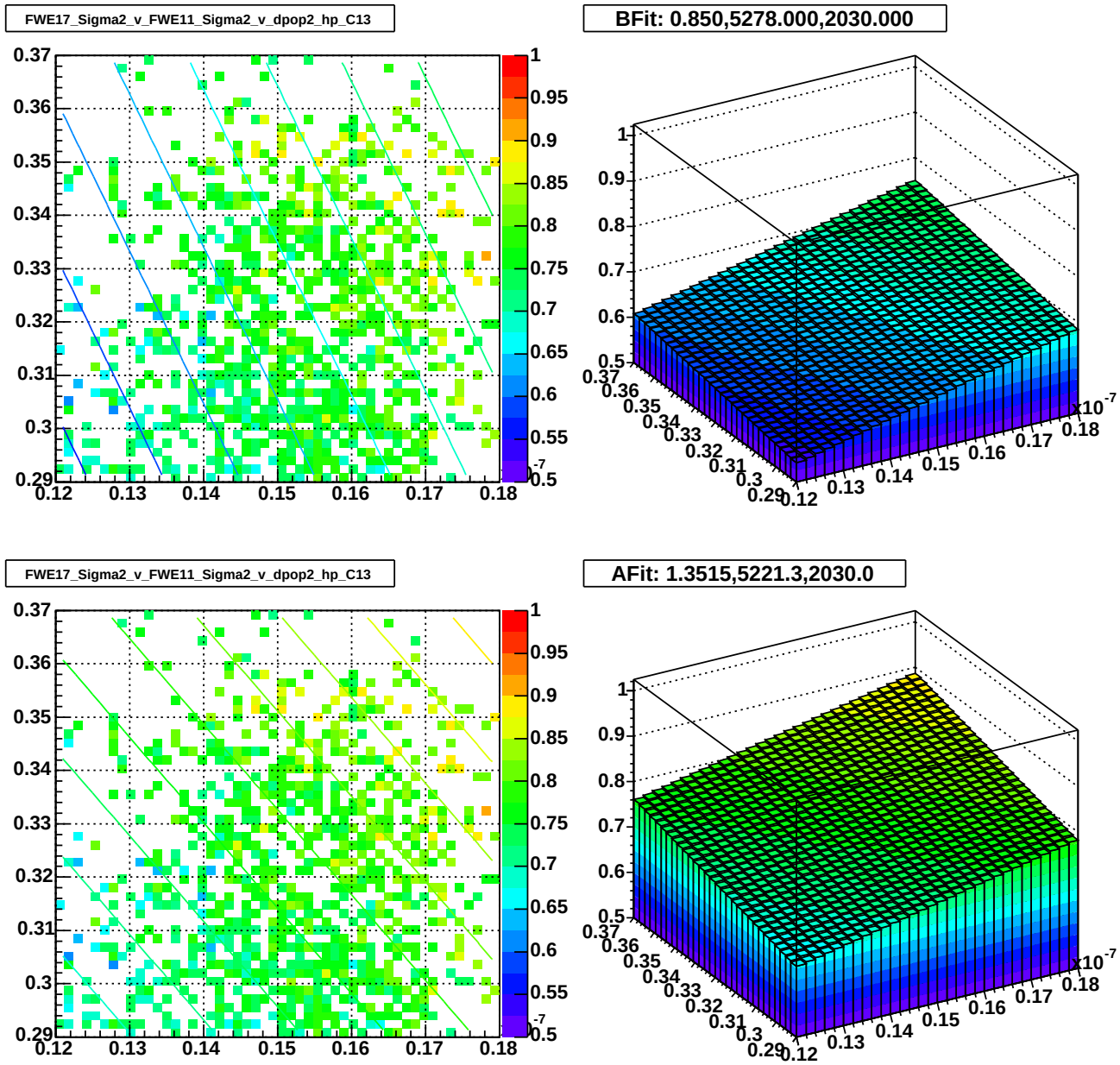

Figure 25: Proton beam, horizontal detectors, nominal lattice: Stores 2650-2997, 980 GeV Case Remove Halo: Comparisons of Sigma squared of the bunch width distribution measurements as done by Flying Wire (FW) E17 Detector with predictions based on the FW E11 Detector measurement: Sigma squared of the bunch width distribution (in mm^2) as measured by the FW E17 Detector as a function of sigma squared of the bunch width distribution (in mm^2) as measured by the FW E11 Detector versus recalculated $\delta p/p$ squared (based on δt the T:SBD[A,P]WS ACNET variable) with an overlaid contour of the prediction based on the nominal lattice functions; Prediction of sigma squared of the bunch width distribution (in mm^2) for E17 Detector as a function of sigma squared of the bunch width distribution (in mm^2) as measured by the FW E11 Detector versus recalculated $\delta p/p$ squared based on the nominal lattice functions; two lower plots have the same data points but have contours based on the fitted lattice functions.

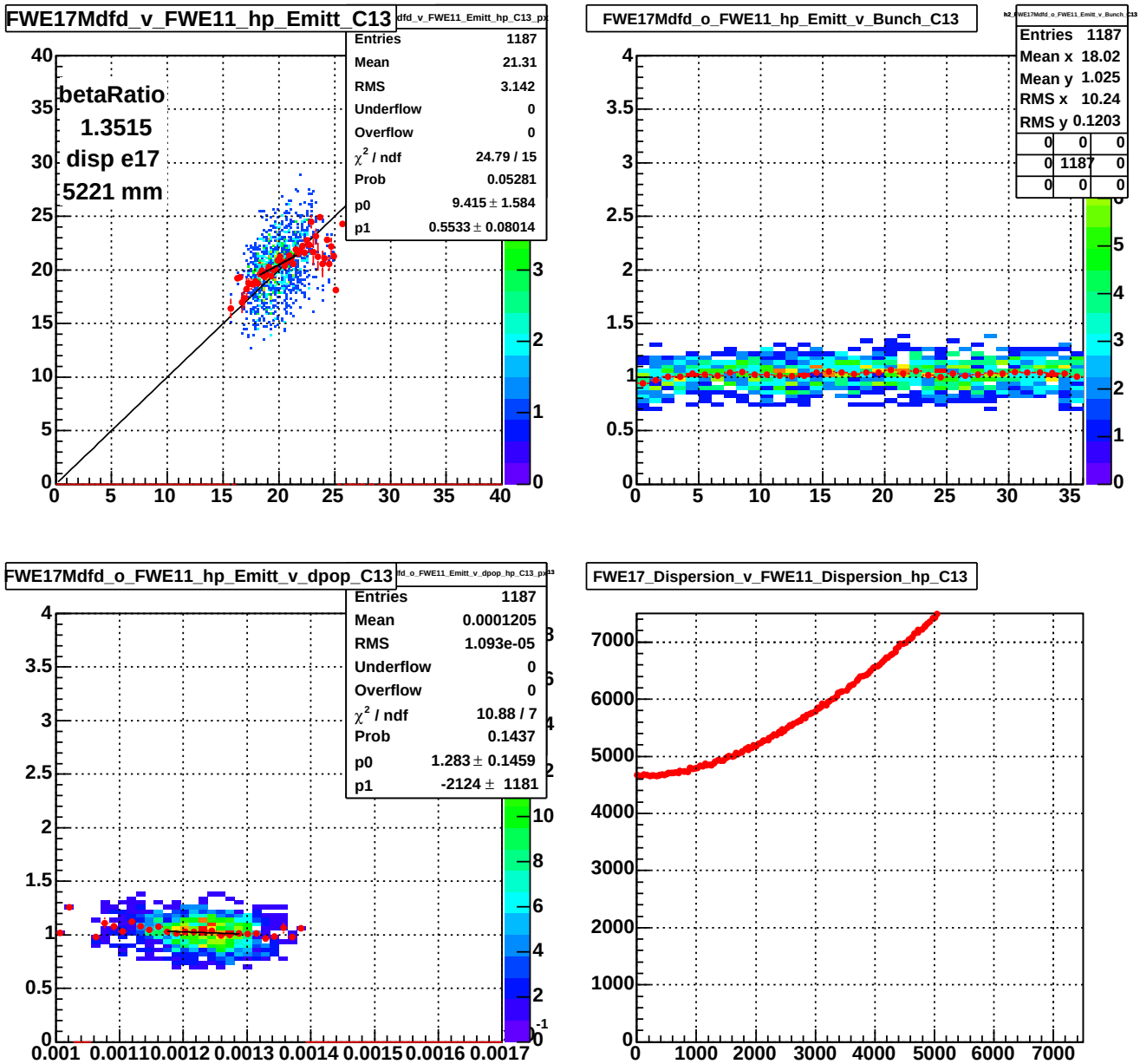

Figure 26: Proton beam, horizontal detectors, modified lattice: Stores 2650-2997, 980 GeV Case Remove Halo: Comparisons of Emittance measurements as done by Flying Wire (FW) Detector at E17 and Flying Wire Detector at E11 using fitted lattice parameters: Bunch emittance (in $\pi \cdot mm \cdot mrad$) as measured by FW E17 Detector versus bunch emittance as measured by the FW E11 Detector with an overlaid horizontal profile distribution with a straight line fit and the ideal prediction; bunch emittance as measured by FW E17 Detector over bunch emittance as measured by the FW E11 Detector versus bunch number together with an overlaid horizontal profile; bunch emittance as measured by FW E17 Detector over bunch emittance as measured by the FW E11 Detector versus recalculated $\delta p/p$ (based on δt the T:SBD[A,P]WS ACNET variable) with an overlaid horizontal profile with a straight line fit; fit based E17 dispersion function as a function of the E11 dispersion function.

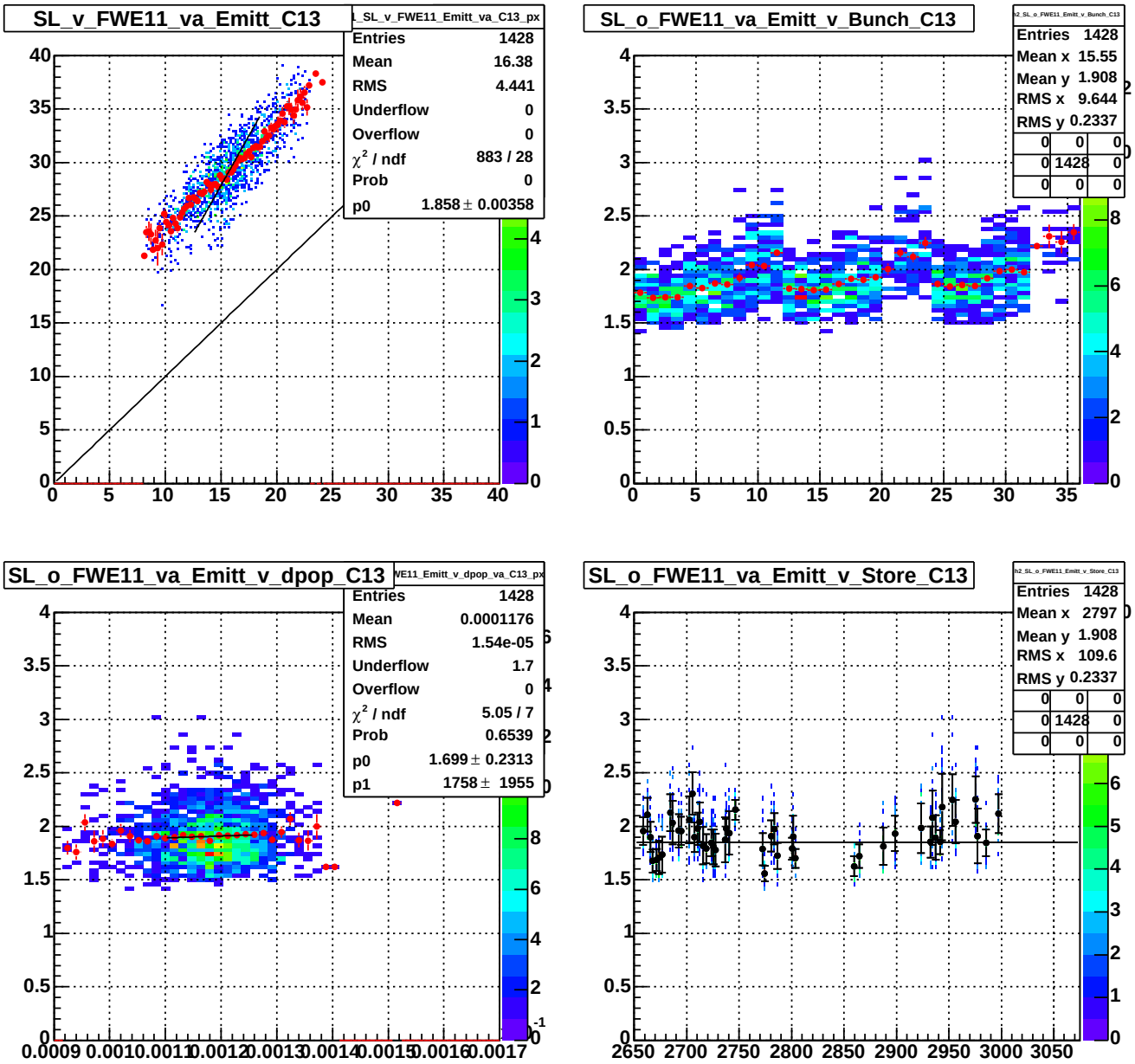

Figure 27: Antiproton beam, vertical detectors, nominal lattice: Stores 2650-2997, 980 GeV Case Remove Halo: Comparisons of Emittance measurements as done by Synchrotron Light (SL) Detector at C11 and Flying Wire (FW) Detector at E11: Bunch emittance (in $\pi \cdot mm \cdot mrad$) as measured by SL C11 Detector versus bunch emittance as measured by the FW E11 Detector with an overlaid horizontal profile distribution with a straight line fit and the ideal prediction; bunch emittance as measured by SL C11 Detector over bunch emittance as measured by the FW E11 Detector versus bunch number together with an overlaid horizontal profile; bunch emittance as measured by SL C11 Detector over bunch emittance as measured by the FW E11 Detector versus recalculated $\delta p/p$ (based on δt the T:SBD[A,P]WS ACNET variable) with an overlaid horizontal profile with a straight line fit; bunch emittance as measured by SL C11 Detector over bunch emittance as measured by the FW E11 Detector versus store number with overlaid averaged ratios for each store and a horizontal line fit.

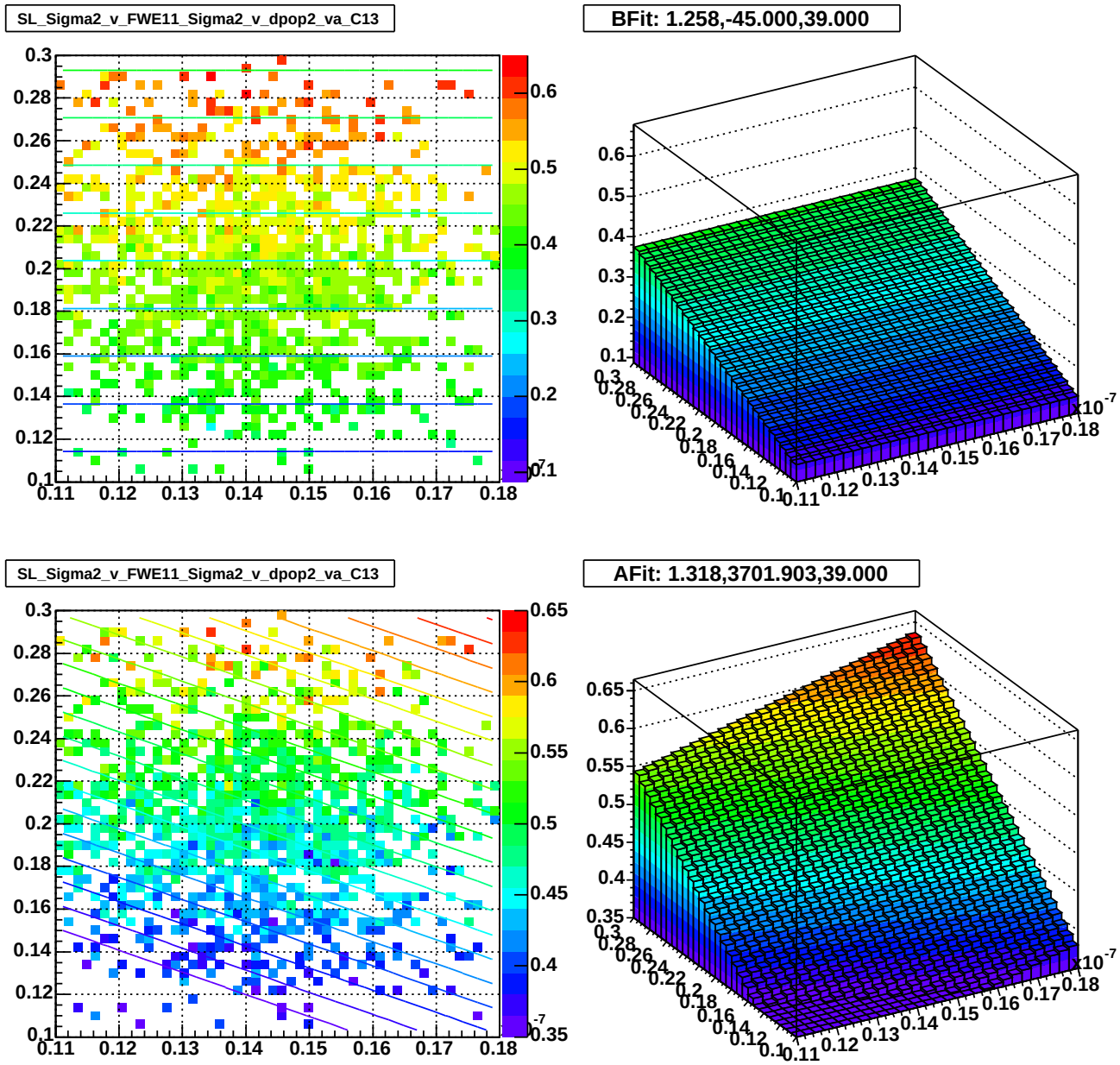

Figure 28: Antiproton beam, vertical detectors, nominal lattice: Stores 2650-2997, 980 GeV Case Remove Halo: Comparisons of Sigma squared of the bunch width distribution measurements as done by Synchrotron Light (SL) C11 Detector with predictions based on the Flying Wire (FW) E11 Detector measurement: Sigma squared of the bunch width distribution (in mm^2) as measured by the SL C11 Detector as a function of sigma squared of the bunch width distribution (in mm^2) as measured by the FW E11 Detector versus recalculated $\delta p/p$ squared (based on δt the T:SBD[A,P]WS ACNET variable) with an overlaid contour of the prediction based on the nominal lattice functions; Prediction of sigma squared of the bunch width distribution (in mm^2) for SL C11 Detector as a function of sigma squared of the bunch width distribution (in mm^2) as measured by the FW E11 Detector versus recalculated $\delta p/p$ squared based on the nominal lattice functions; two lower plots have the same data points but have contours based on the fitted lattice functions.

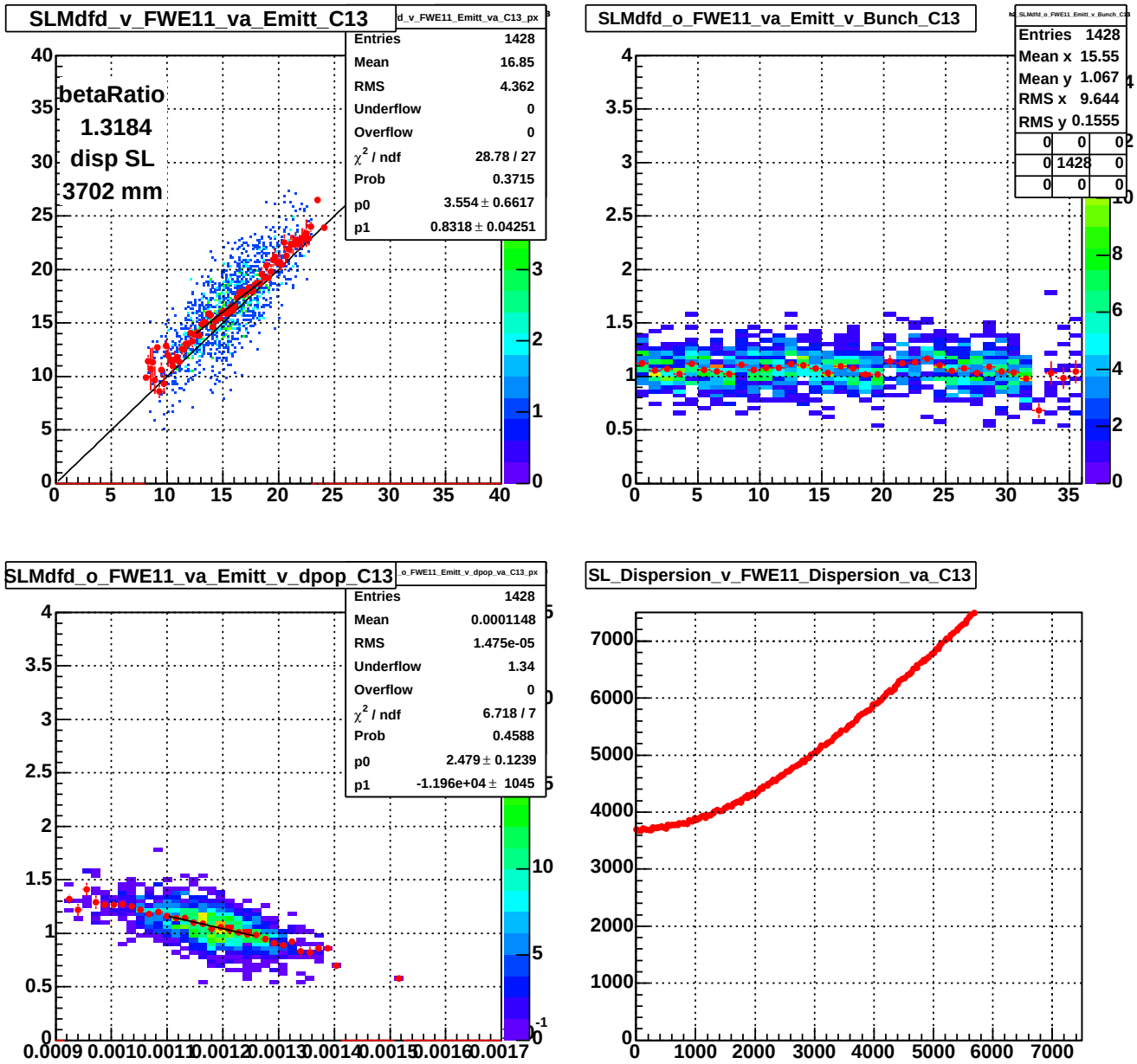

Figure 29: Antiproton beam, vertical detectors, modified lattice: Stores 2650-2997, 980 GeV Case Remove Halo: Comparisons of Emittance measurements as done by Synchrotron Light (SL) Detector at C11 and Flying Wire (FW) Detector at E11 using fitted lattice parameters and formula with dispersion term both in the horizontal and in the vertical cases: Bunch emittance (in $\pi \cdot mm \cdot mrad$) as measured by SL C11 Detector versus bunch emittance as measured by the FW E11 Detector with an overlaid horizontal profile distribution with a straight line fit and the ideal prediction; bunch emittance as measured by SL C11 Detector over bunch emittance as measured by the FW E11 Detector versus bunch number together with an overlaid horizontal profile; bunch emittance as measured by SL C11 Detector over bunch emittance as measured by the FW E11 Detector versus recalculated $\delta p/p$ (based on δt the T:SBD[A,P]WS ACNET variable) with an overlaid horizontal profile with a straight line fit; fit based C11 dispersion function as a function of the E11 dispersion function.

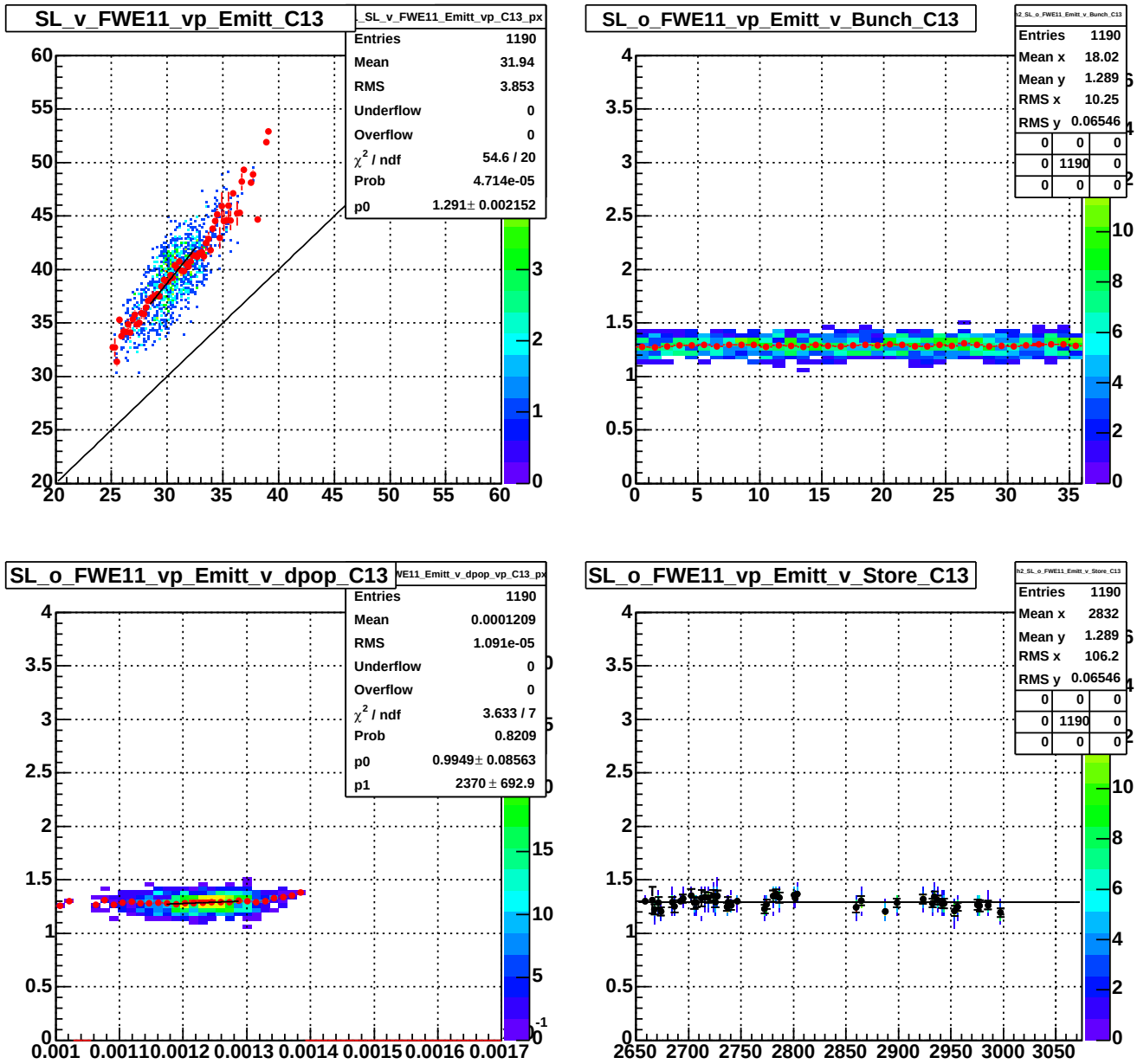

Figure 30: Proton beam, vertical detectors, nominal lattice: Stores 2650-2997, 980 GeV Case Remove Halo: Comparisons of Emittance measurements as done by Synchrotron Light (SL) Detector at C11 and Flying Wire (FW) Detector at E11: Bunch emittance (in $\pi \cdot mm \cdot mrad$) as measured by SL C11 Detector versus bunch emittance as measured by the FW E11 Detector with an overlaid horizontal profile distribution with a straight line fit and the ideal prediction; bunch emittance as measured by SL C11 Detector over bunch emittance as measured by the FW E11 Detector versus bunch number together with an overlaid horizontal profile; bunch emittance as measured by SL C11 Detector over bunch emittance as measured by the FW E11 Detector versus recalculated $\delta p/p$ (based on δt the T:SBD[A,P]WS ACNET variable) with an overlaid horizontal profile with a straight line fit; bunch emittance as measured by SL C11 Detector over bunch emittance as measured by the FW E11 Detector versus store number with overlaid averaged ratios for each store and a horizontal line fit.

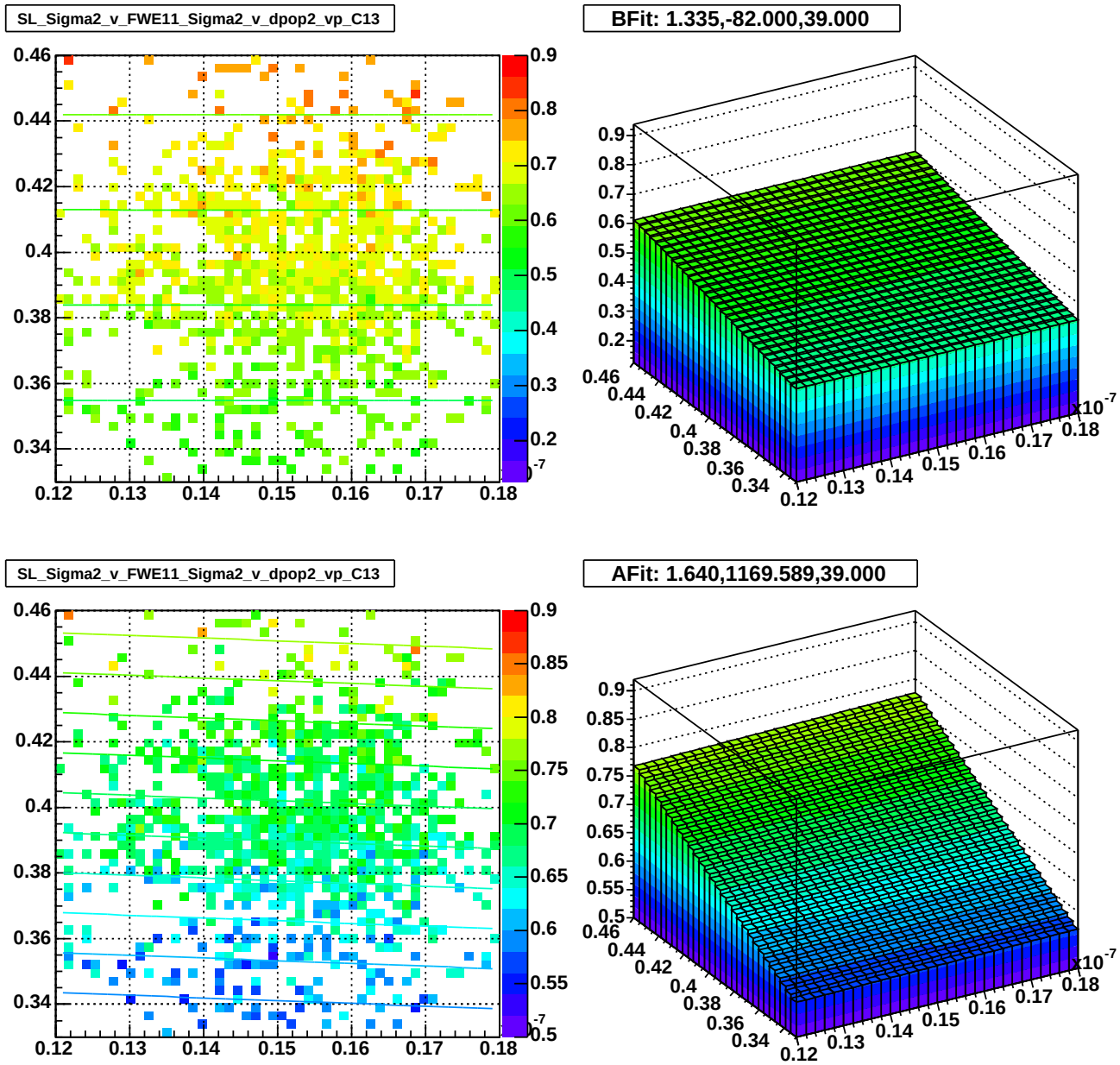

Figure 31: Proton beam, vertical detectors, nominal lattice: Stores 2650-2997, 980 GeV Case Remove Halo: Comparisons of Sigma squared of the bunch width distribution measurements as done by Synchrotron Light (SL) C11 Detector with predictions based on the Flying Wire (FW) E11 Detector measurement: Sigma squared of the bunch width distribution (in mm^2) as measured by the SL C11 Detector as a function of sigma squared of the bunch width distribution (in mm^2) as measured by the FW E11 Detector versus recalculated $\delta p/p$ squared (based on δt the T:SBD[A,P]WS ACNET variable) with an overlaid contour of the prediction based on the nominal lattice functions; Prediction of sigma squared of the bunch width distribution (in mm^2) for SL C11 Detector as a function of sigma squared of the bunch width distribution (in mm^2) as measured by the FW E11 Detector versus recalculated $\delta p/p$ squared based on the nominal lattice functions; two lower plots have the same data points but have contours based on the fitted lattice functions.

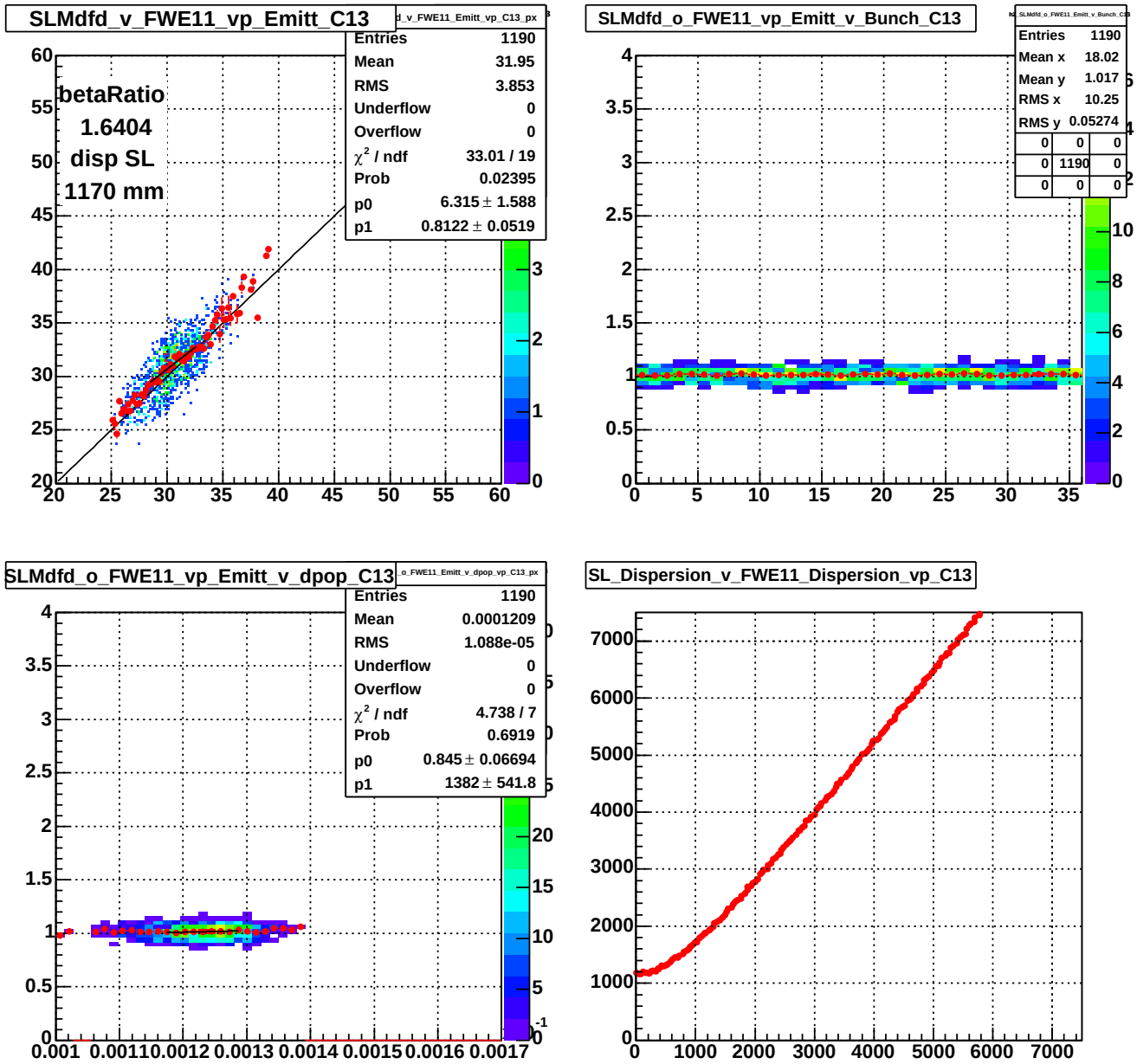

Figure 32: Proton beam, vertical detectors, modified lattice: Stores 2650-2997, 980 GeV Case Remove Halo: Comparisons of Emittance measurements as done by Synchrotron Light (SL) Detector at C11 and Flying Wire (FW) Detector at E11 using fitted lattice parameters and formula with dispersion term both in the horizontal and in the vertical cases: Bunch emittance (in $\pi \cdot mm \cdot mrad$) as measured by SL C11 Detector versus bunch emittance as measured by the FW E11 Detector with an overlaid horizontal profile distribution with a straight line fit and the ideal prediction; bunch emittance as measured by SL C11 Detector over bunch emittance as measured by the FW E11 Detector versus bunch number together with an overlaid horizontal profile; bunch emittance as measured by SL C11 Detector over bunch emittance as measured by the FW E11 Detector versus recalculated $\delta p/p$ (based on δt the T:SBD[A,P]WS ACNET variable) with an overlaid horizontal profile with a straight line fit; fit based C11 dispersion function as a function of the E11 dispersion function.

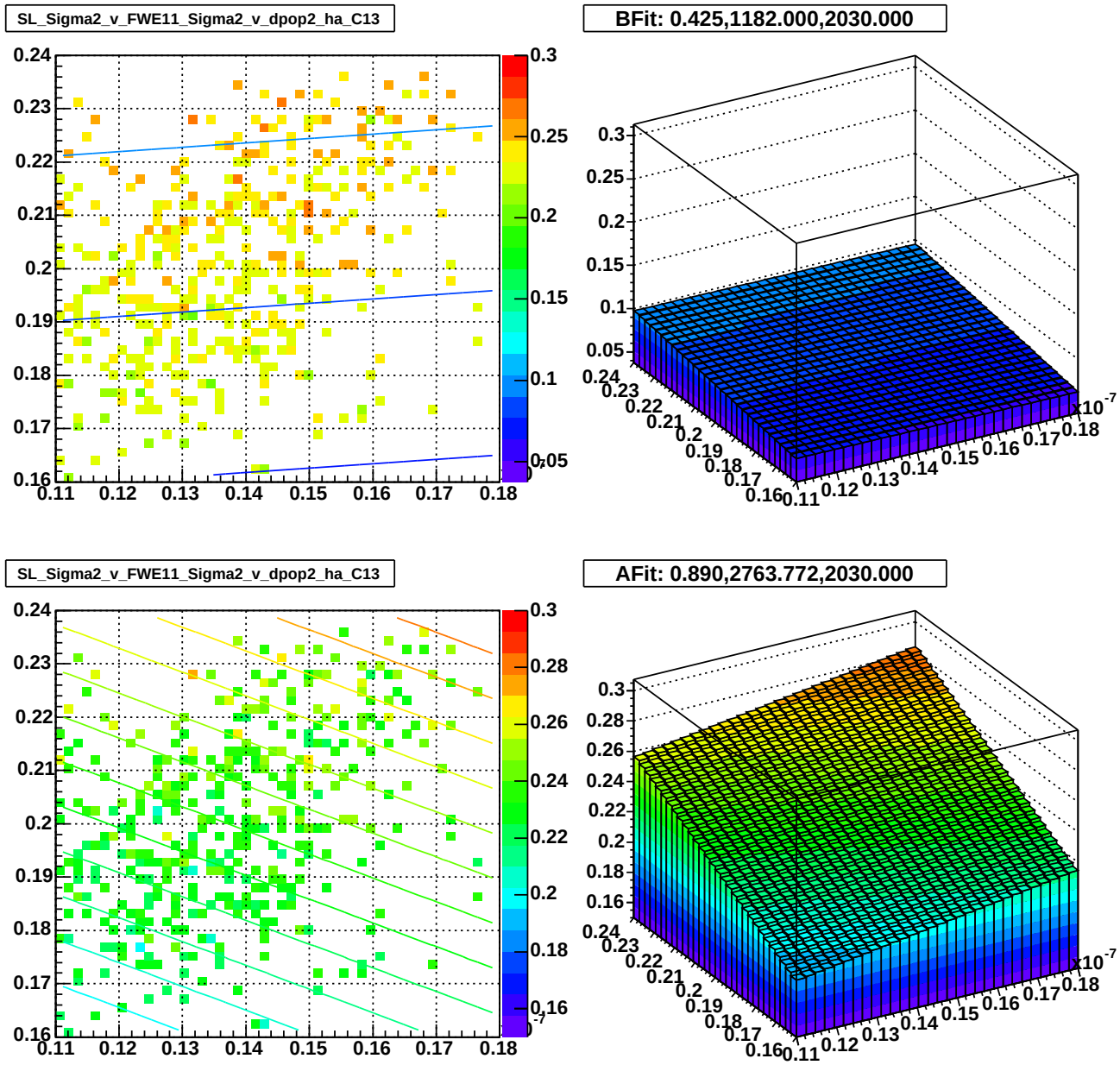

Figure 33: Antiproton beam, horizontal detectors, nominal lattice: Stores 2810-2997, 980 GeV Case Remove Halo: Comparisons of Sigma squared of the bunch width distribution measurements as done by Synchrotron Light (SL) C11 Detector with predictions based on the Flying Wire (FW) E11 Detector measurement: Sigma squared of the bunch width distribution (in mm^2) as measured by the SL C11 Detector as a function of sigma squared of the bunch width distribution (in mm^2) as measured by the FW E11 Detector versus recalculated $\delta p/p$ squared (based on δt the T:SBD[A,P]WS ACNET variable) with an overlaid contour of the prediction based on the nominal lattice functions; Prediction of sigma squared of the bunch width distribution (in mm^2) for SL C11 Detector as a function of sigma squared of the bunch width distribution (in mm^2) as measured by the FW E11 Detector versus recalculated $\delta p/p$ squared based on the nominal lattice functions; two lower plots have the same data points but have contours based on the fitted lattice functions.

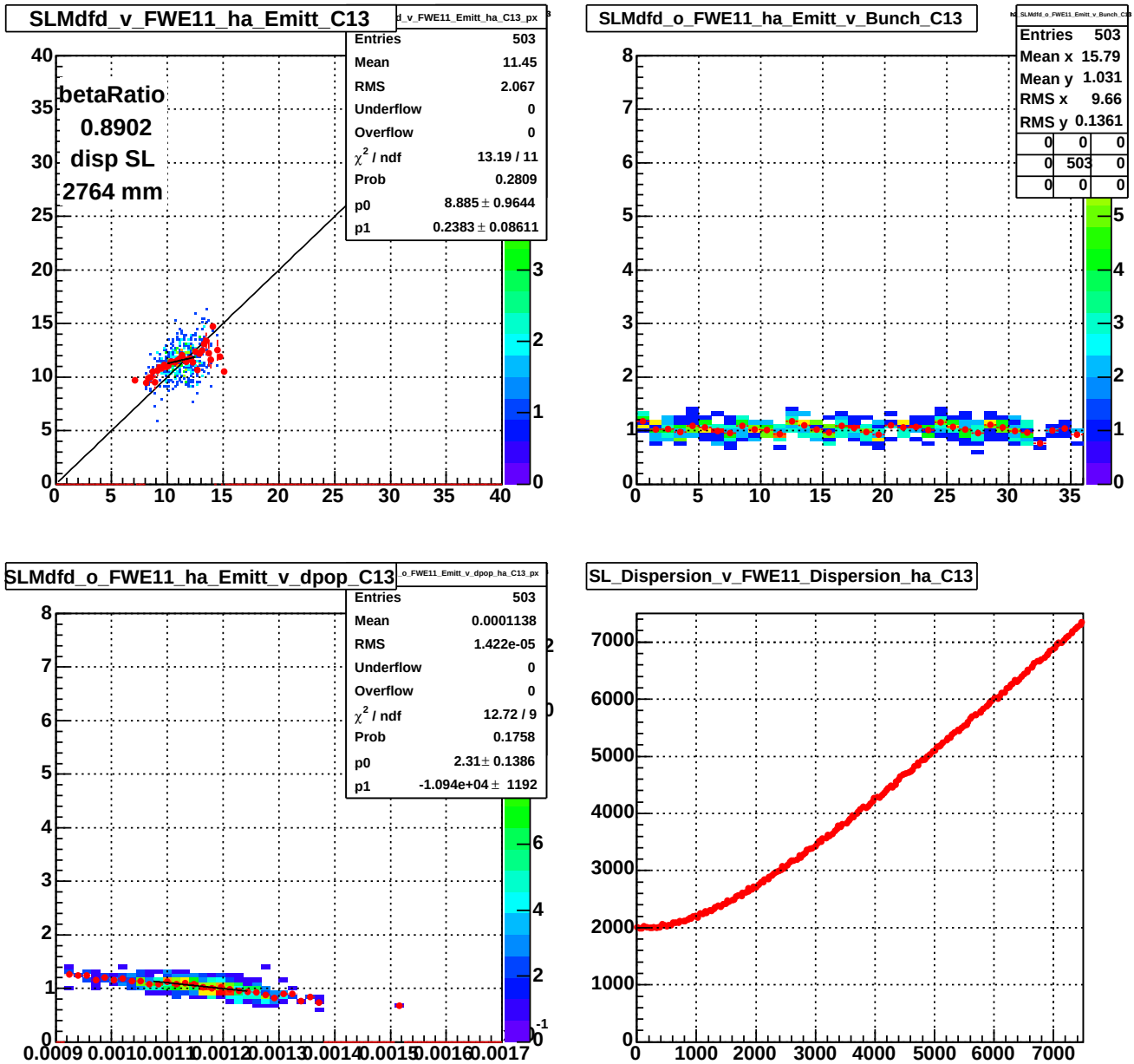

Figure 34: Antiproton beam, horizontal detectors, modified lattice: Stores 2810-2997, 980 GeV Case Remove Halo: Comparisons of Emittance measurements as done by Synchrotron Light (SL) Detector at C11 and Flying Wire (FW) Detector at E11 using fitted lattice parameters and formula with dispersion term both in the horizontal and in the vertical cases: Bunch emittance (in $\pi \cdot mm \cdot mrad$) as measured by SL C11 Detector versus bunch emittance as measured by the FW E11 Detector with an overlaid horizontal profile distribution with a straight line fit and the ideal prediction; bunch emittance as measured by SL C11 Detector over bunch emittance as measured by the FW E11 Detector versus bunch number together with an overlaid horizontal profile; bunch emittance as measured by SL C11 Detector over bunch emittance as measured by the FW E11 Detector versus recalculated $\delta p/p$ (based on δt the T:SBD[A,P]WS ACNET variable) with an overlaid horizontal profile with a straight line fit; fit based C11 dispersion function as a function of the E11 dispersion function.

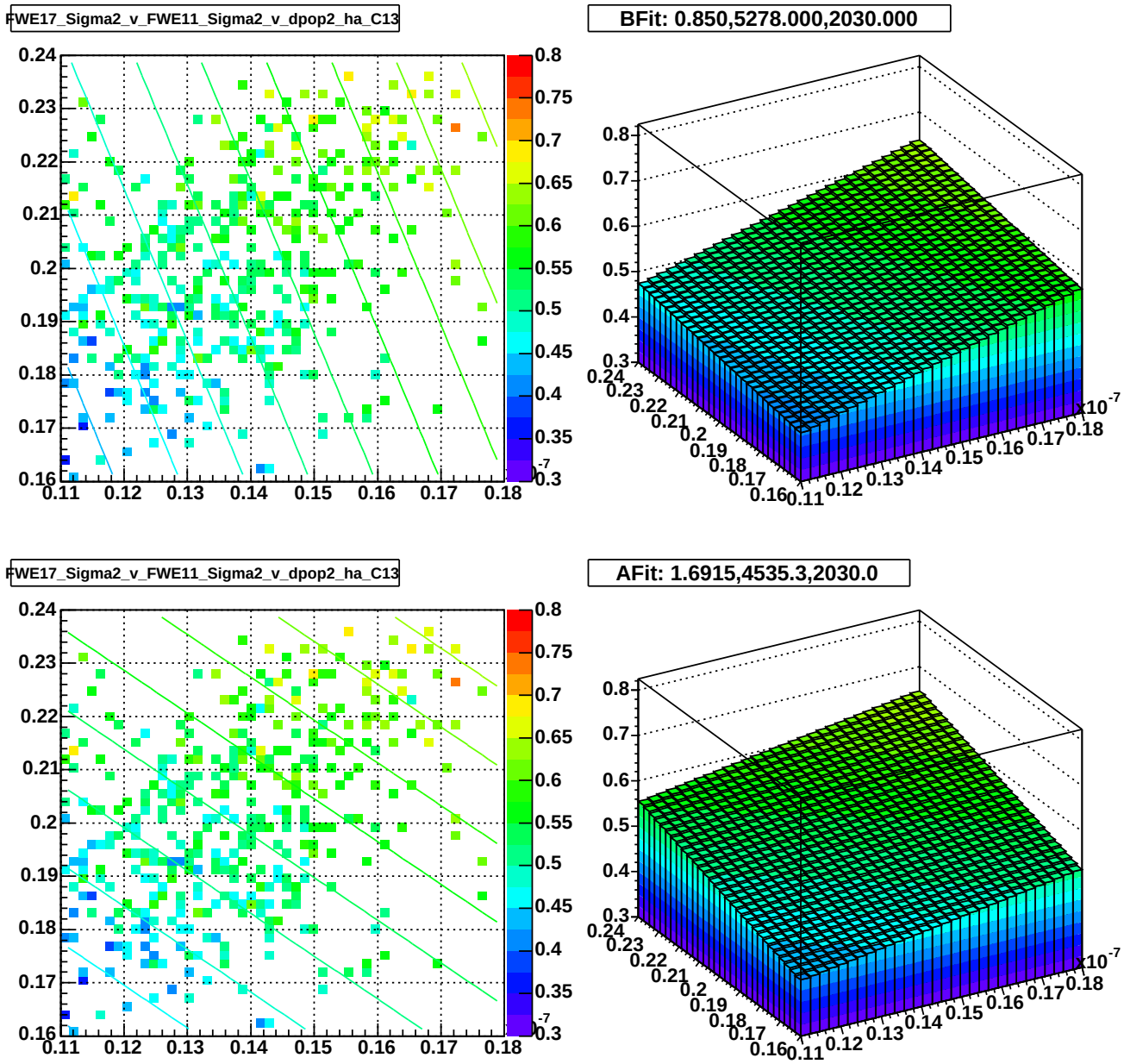

Figure 35: Antiproton beam, horizontal detectors, nominal lattice: Stores 2810-2997, 980 GeV Case Remove Halo: Comparisons of Sigma squared of the bunch width distribution measurements as done by Flying Wire (FW) E17 Detector with predictions based on the FW E11 Detector measurement: Sigma squared of the bunch width distribution (in mm^2) as measured by the FW E17 Detector as a function of sigma squared of the bunch width distribution (in mm^2) as measured by the FW E11 Detector versus recalculated $\delta p/p$ squared (based on δt the T:SBD[A,P]WS ACNET variable) with an overlaid contour of the prediction based on the nominal lattice functions; Prediction of sigma squared of the bunch width distribution (in mm^2) for E17 Detector as a function of sigma squared of the bunch width distribution (in mm^2) as measured by the FW E11 Detector versus recalculated $\delta p/p$ squared based on the nominal lattice functions; two lower plots have the same data points but have contours based on the fitted lattice functions.

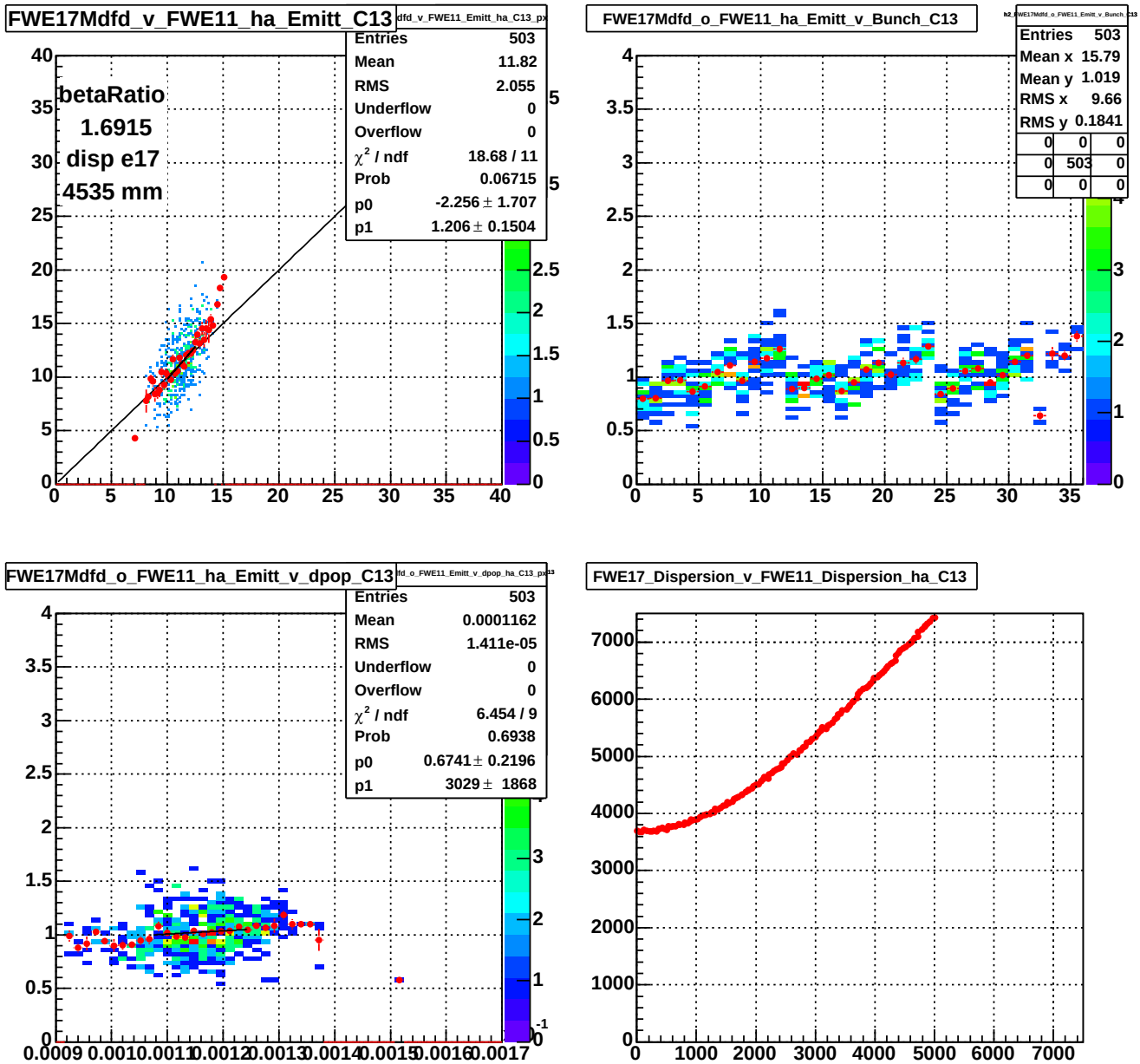

Figure 36: Antiproton beam, horizontal detectors, modified lattice: Stores 2810-2997, 980 GeV Case Remove Halo: Comparisons of Emittance measurements as done by Flying Wire (FW) Detector at E17 and Flying Wire Detector at E11 using fitted lattice parameters: Bunch emittance (in $\pi \cdot mm \cdot mrad$) as measured by FW E17 Detector versus bunch emittance as measured by the FW E11 Detector with an overlaid horizontal profile distribution with a straight line fit and the ideal prediction; bunch emittance as measured by FW E17 Detector over bunch emittance as measured by the FW E11 Detector versus bunch number together with an overlaid horizontal profile; bunch emittance as measured by FW E17 Detector over bunch emittance as measured by the FW E11 Detector versus recalculated $\delta p/p$ (based on δt the T:SBD[A,P]WS ACNET variable) with an overlaid horizontal profile with a straight line fit; fit based E17 dispersion function as a function of the E11 dispersion function.

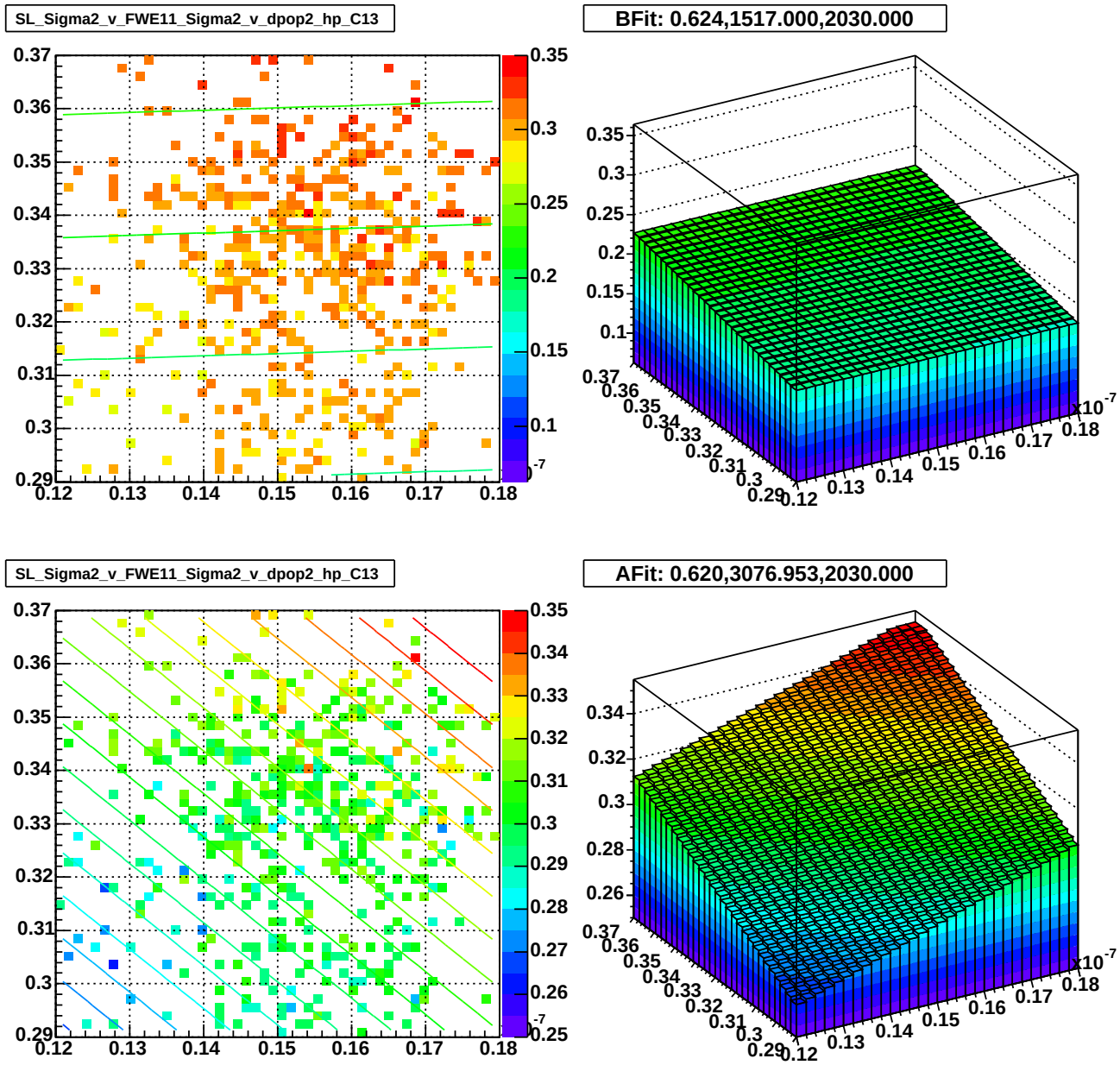

Figure 37: Proton beam, horizontal detectors, nominal lattice: Stores 2810-2997, 980 GeV Case Remove Halo: Comparisons of Sigma squared of the bunch width distribution measurements as done by Synchrotron Light (SL) C11 Detector with predictions based on the Flying Wire (FW) E11 Detector measurement: Sigma squared of the bunch width distribution (in mm^2) as measured by the SL C11 Detector as a function of sigma squared of the bunch width distribution (in mm^2) as measured by the FW E11 Detector versus recalculated $\delta p/p$ squared (based on δt the T:SBD[A,P]WS ACNET variable) with an overlaid contour of the prediction based on the nominal lattice functions; Prediction of sigma squared of the bunch width distribution (in mm^2) for SL C11 Detector as a function of sigma squared of the bunch width distribution (in mm^2) as measured by the FW E11 Detector versus recalculated $\delta p/p$ squared based on the nominal lattice functions; two lower plots have the same data points but have contours based on the fitted lattice functions.

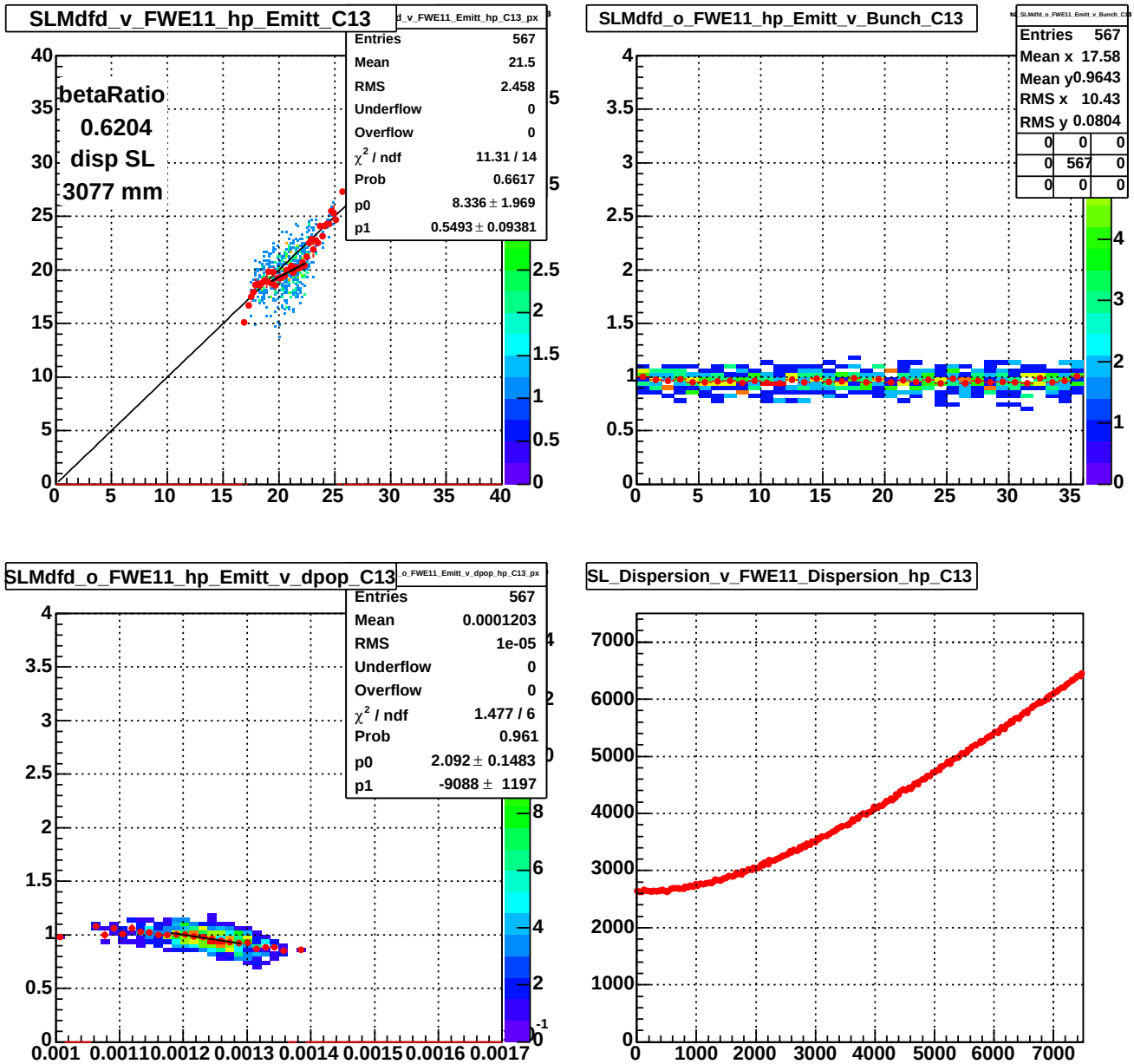

Figure 38: Proton beam, horizontal detectors, modified lattice: Stores 2810-2997, 980 GeV Case Remove Halo: Comparisons of Emittance measurements as done by Synchrotron Light (SL) Detector at C11 and Flying Wire (FW) Detector at E11 using fitted lattice parameters and formula with dispersion term both in the horizontal and in the vertical cases: Bunch emittance (in $\pi \cdot mm \cdot mrad$) as measured by SL C11 Detector versus bunch emittance as measured by the FW E11 Detector with an overlaid horizontal profile distribution with a straight line fit and the ideal prediction; bunch emittance as measured by SL C11 Detector over bunch emittance as measured by the FW E11 Detector versus bunch number together with an overlaid horizontal profile; bunch emittance as measured by SL C11 Detector over bunch emittance as measured by the FW E11 Detector versus recalculated $\delta p/p$ (based on δt the T:SBD[A,P]WS ACNET variable) with an overlaid horizontal profile with a straight line fit; fit based C11 dispersion function as a function of the E11 dispersion function.

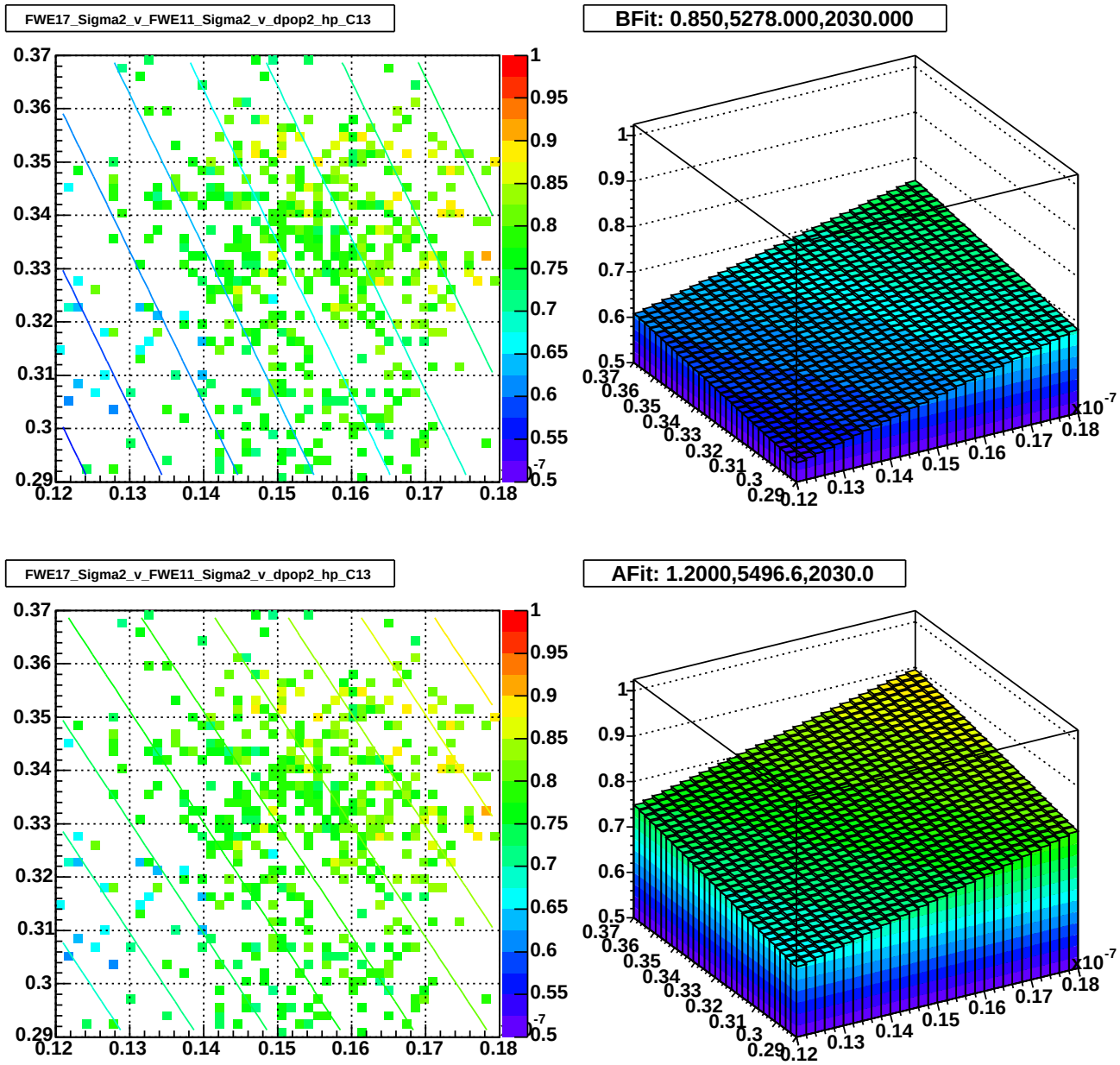

Figure 39: Proton beam, horizontal detectors, nominal lattice: Stores 2810-2997, 980 GeV Case Remove Halo: Comparisons of Sigma squared of the bunch width distribution measurements as done by Flying Wire (FW) E17 Detector with predictions based on the FW E11 Detector measurement: Sigma squared of the bunch width distribution (in mm^2) as measured by the FW E17 Detector as a function of sigma squared of the bunch width distribution (in mm^2) as measured by the FW E11 Detector versus recalculated $\delta p/p$ squared (based on δt the T:SBD[A,P]WS ACNET variable) with an overlaid contour of the prediction based on the nominal lattice functions; Prediction of sigma squared of the bunch width distribution (in mm^2) for E17 Detector as a function of sigma squared of the bunch width distribution (in mm^2) as measured by the FW E11 Detector versus recalculated $\delta p/p$ squared based on the nominal lattice functions; two lower plots have the same data points but have contours based on the fitted lattice functions.

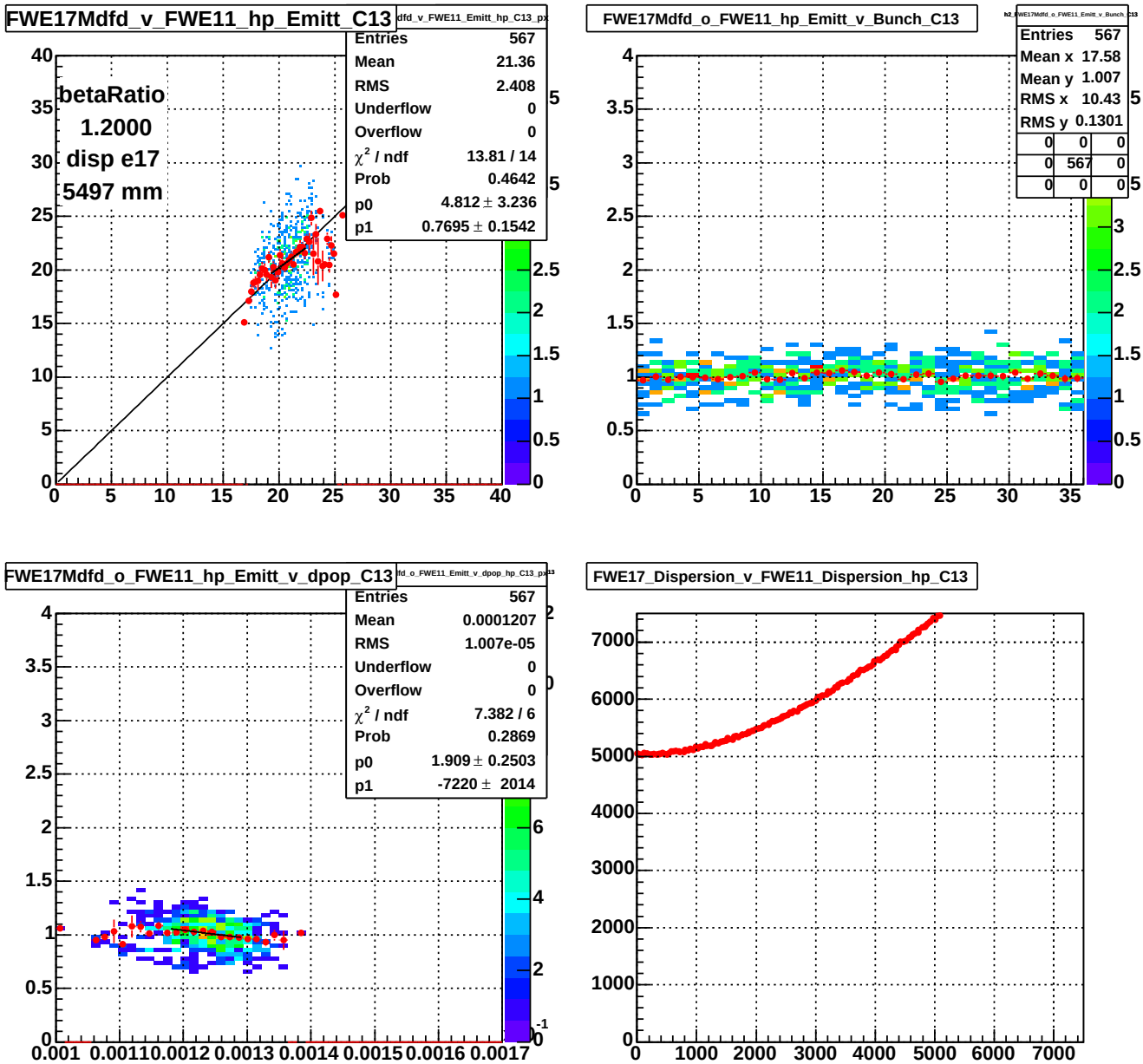

Figure 40: Proton beam, horizontal detectors, modified lattice: Stores 2810-2997, 980 GeV Case Remove Halo: Comparisons of Emittance measurements as done by Flying Wire (FW) Detector at E17 and Flying Wire Detector at E11 using fitted lattice parameters: Bunch emittance (in $\pi \cdot mm \cdot mrad$) as measured by FW E17 Detector versus bunch emittance as measured by the FW E11 Detector with an overlaid horizontal profile distribution with a straight line fit and the ideal prediction; bunch emittance as measured by FW E17 Detector over bunch emittance as measured by the FW E11 Detector versus bunch number together with an overlaid horizontal profile; bunch emittance as measured by FW E17 Detector over bunch emittance as measured by the FW E11 Detector versus recalculated $\delta p/p$ (based on δt the T:SBD[A,P]WS ACNET variable) with an overlaid horizontal profile with a straight line fit; fit based E17 dispersion function as a function of the E11 dispersion function.

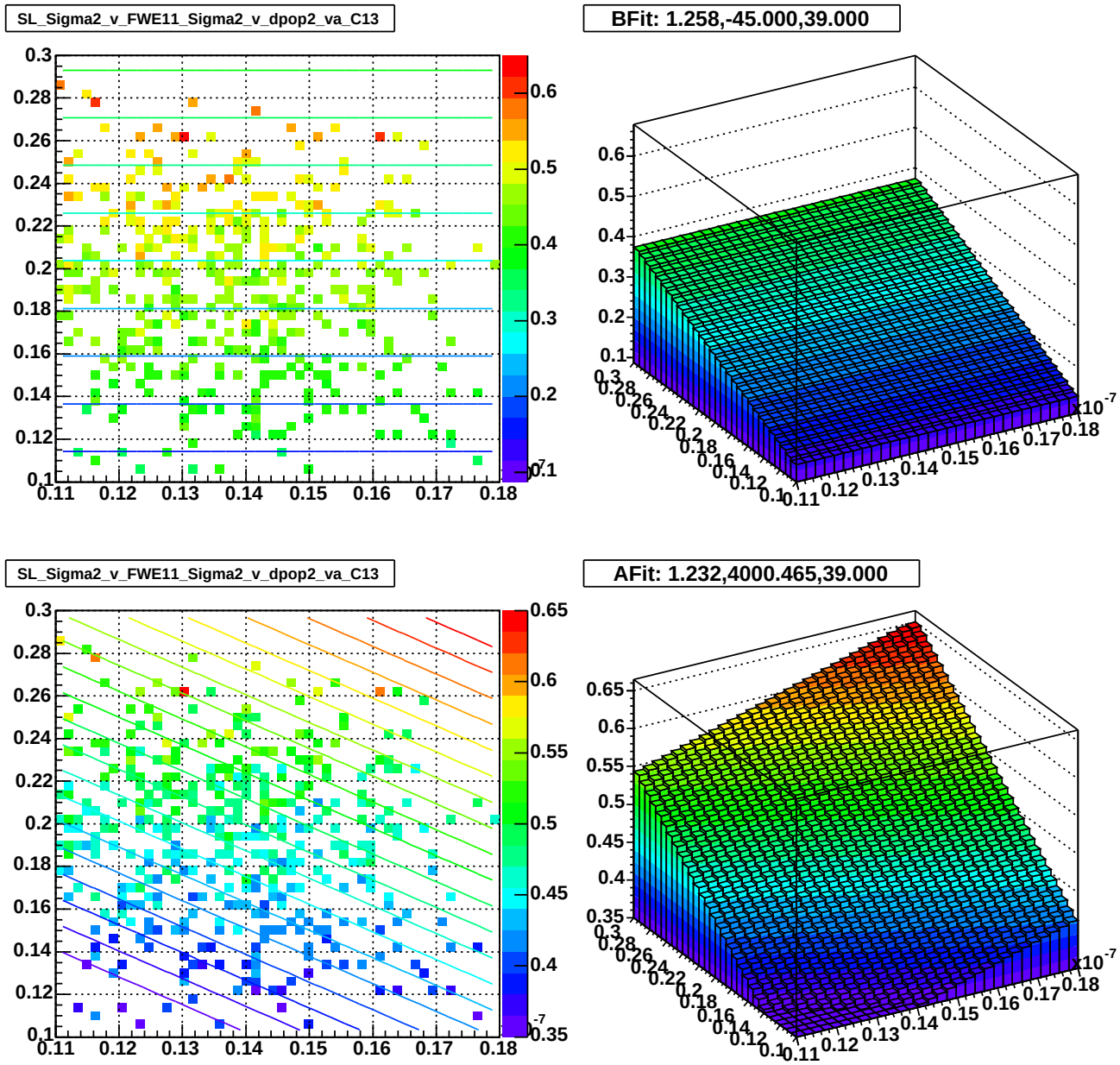

Figure 41: Antiproton beam, vertical detectors, nominal lattice: Stores 2810-2997, 980 GeV Case Remove Halo: Comparisons of Sigma squared of the bunch width distribution measurements as done by Synchrotron Light (SL) C11 Detector with predictions based on the Flying Wire (FW) E11 Detector measurement: Sigma squared of the bunch width distribution (in mm^2) as measured by the SL C11 Detector as a function of sigma squared of the bunch width distribution (in mm^2) as measured by the FW E11 Detector versus recalculated $\delta p/p$ squared (based on δt the T:SBD[A,P]WS ACNET variable) with an overlaid contour of the prediction based on the nominal lattice functions; Prediction of sigma squared of the bunch width distribution (in mm^2) for SL C11 Detector as a function of sigma squared of the bunch width distribution (in mm^2) as measured by the FW E11 Detector versus recalculated $\delta p/p$ squared based on the nominal lattice functions; two lower plots have the same data points but have contours based on the fitted lattice functions.

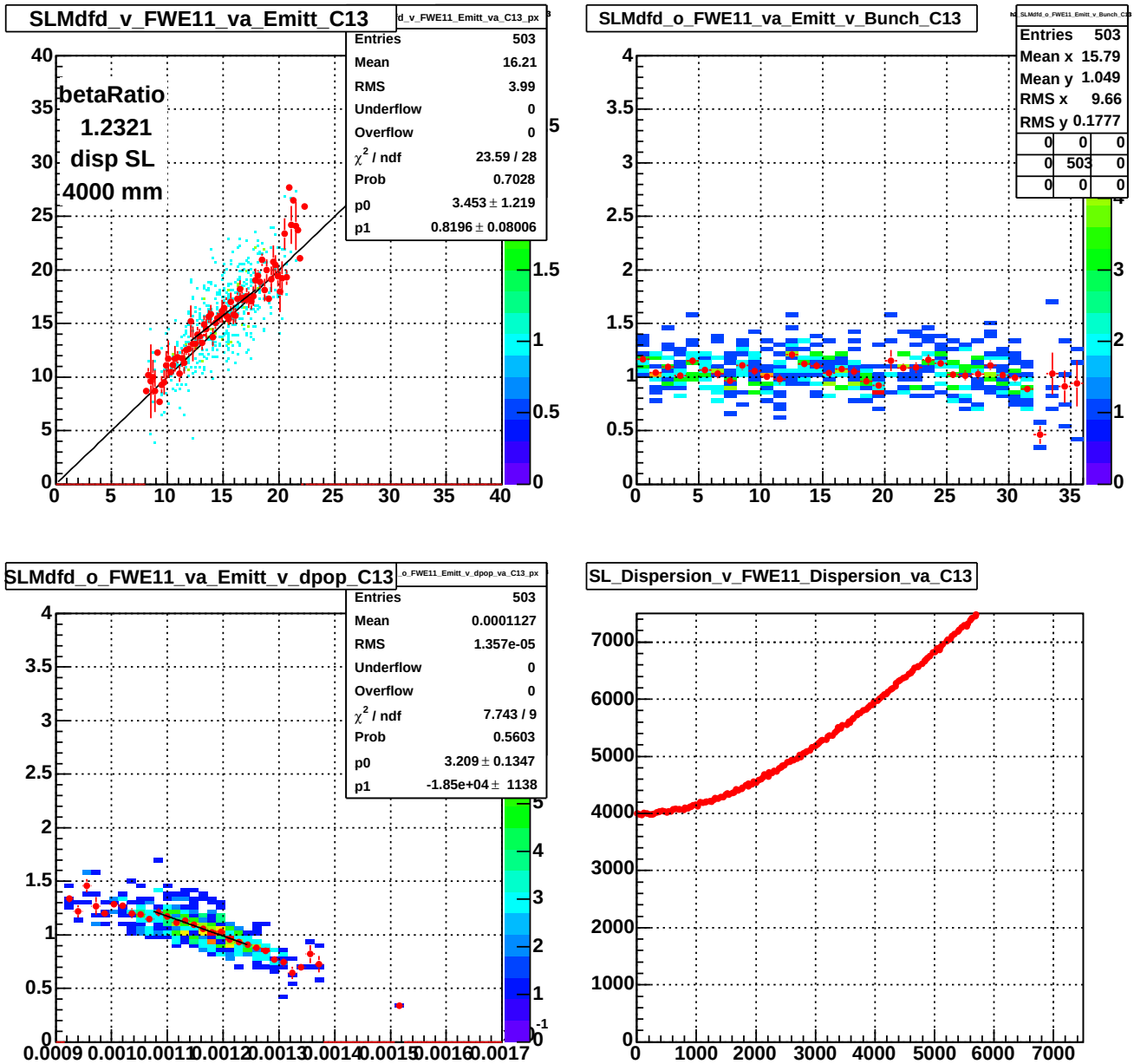

Figure 42: Antiproton beam, vertical detectors, modified lattice: Stores 2810-2997, 980 GeV Case Remove Halo: Comparisons of Emittance measurements as done by Synchrotron Light (SL) Detector at C11 and Flying Wire (FW) Detector at E11 using fitted lattice parameters and formula with dispersion term both in the horizontal and in the vertical cases: Bunch emittance (in $\pi \cdot mm \cdot mrad$) as measured by SL C11 Detector versus bunch emittance as measured by the FW E11 Detector with an overlaid horizontal profile distribution with a straight line fit and the ideal prediction; bunch emittance as measured by SL C11 Detector over bunch emittance as measured by the FW E11 Detector versus bunch number together with an overlaid horizontal profile; bunch emittance as measured by SL C11 Detector over bunch emittance as measured by the FW E11 Detector versus recalculated $\delta p/p$ (based on δt the T:SBD[A,P]WS ACNET variable) with an overlaid horizontal profile with a straight line fit; fit based C11 dispersion function as a function of the E11 dispersion function.

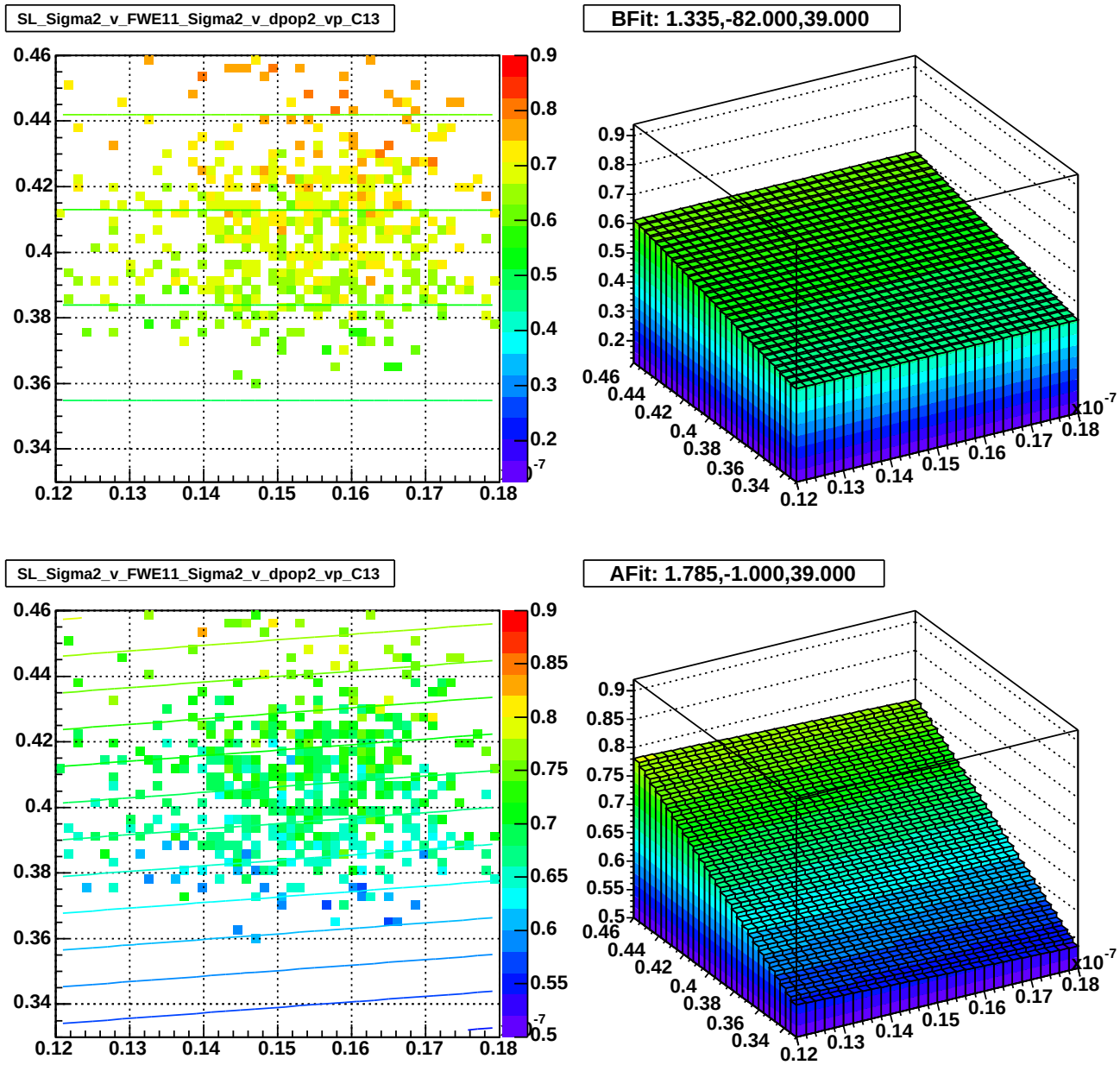

Figure 43: Proton beam, vertical detectors, nominal lattice: Stores 2810-2997, 980 GeV Case Remove Halo: Comparisons of Sigma squared of the bunch width distribution measurements as done by Synchrotron Light (SL) C11 Detector with predictions based on the Flying Wire (FW) E11 Detector measurement: Sigma squared of the bunch width distribution (in mm^2) as measured by the SL C11 Detector as a function of sigma squared of the bunch width distribution (in mm^2) as measured by the FW E11 Detector versus recalculated $\delta p/p$ squared (based on δt the T:SBD[A,P]WS ACNET variable) with an overlaid contour of the prediction based on the nominal lattice functions; Prediction of sigma squared of the bunch width distribution (in mm^2) for SL C11 Detector as a function of sigma squared of the bunch width distribution (in mm^2) as measured by the FW E11 Detector versus recalculated $\delta p/p$ squared based on the nominal lattice functions; two lower plots have the same data points but have contours based on the fitted lattice functions.

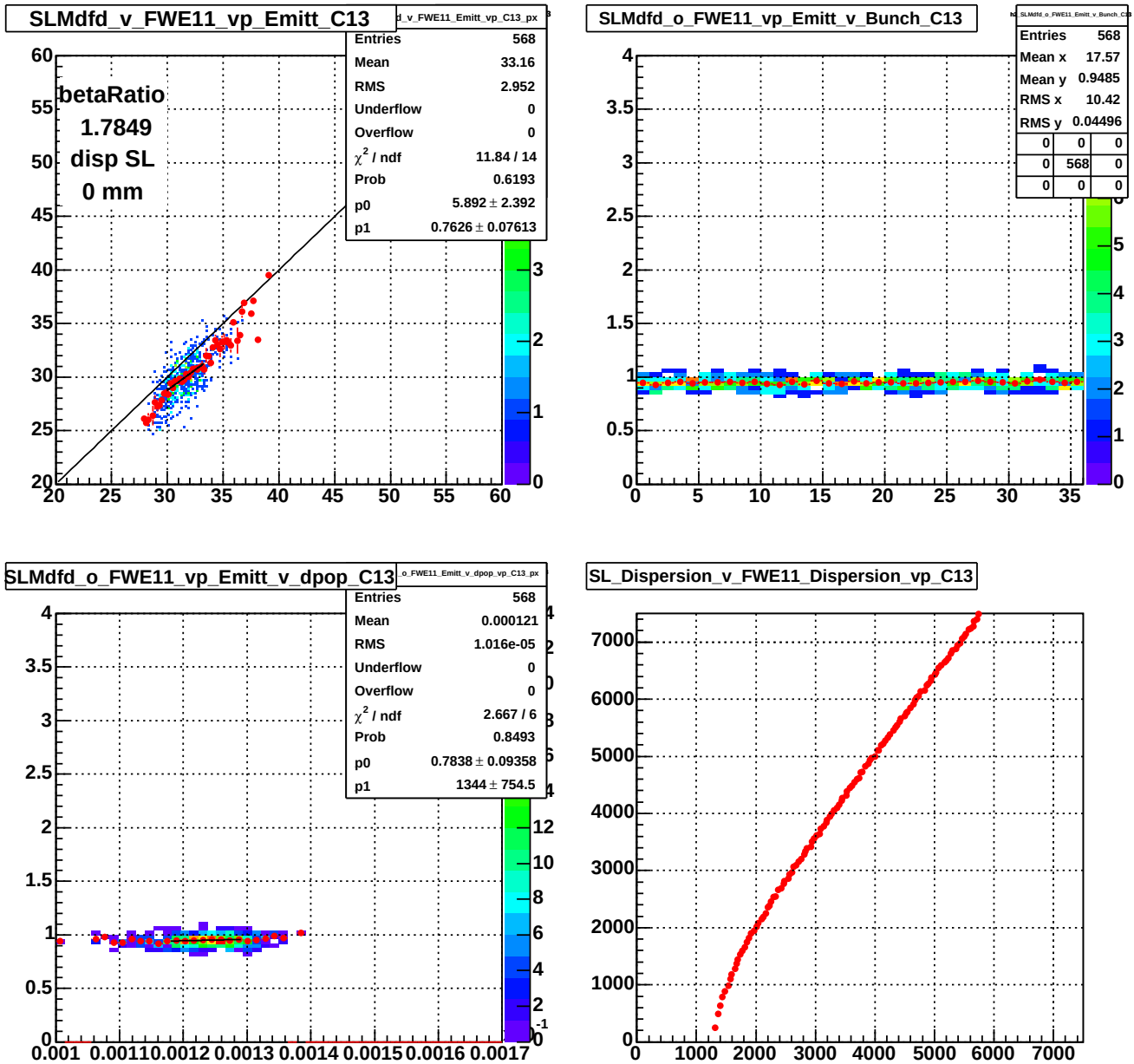

Figure 44: Proton beam, vertical detectors, modified lattice: Stores 2810-2997, 980 GeV Case Remove Halo: Comparisons of Emittance measurements as done by Synchrotron Light (SL) Detector at C11 and Flying Wire (FW) Detector at E11 using fitted lattice parameters and formula with dispersion term both in the horizontal and in the vertical cases: Bunch emittance (in $\pi \cdot mm \cdot mrad$) as measured by SL C11 Detector versus bunch emittance as measured by the FW E11 Detector with an overlaid horizontal profile distribution with a straight line fit and the ideal prediction; bunch emittance as measured by SL C11 Detector over bunch emittance as measured by the FW E11 Detector versus bunch number together with an overlaid horizontal profile; bunch emittance as measured by SL C11 Detector over bunch emittance as measured by the FW E11 Detector versus recalculated $\delta p/p$ (based on δt the T:SBD[A,P]WS ACNET variable) with an overlaid horizontal profile with a straight line fit; fit based C11 dispersion function as a function of the E11 dispersion function.

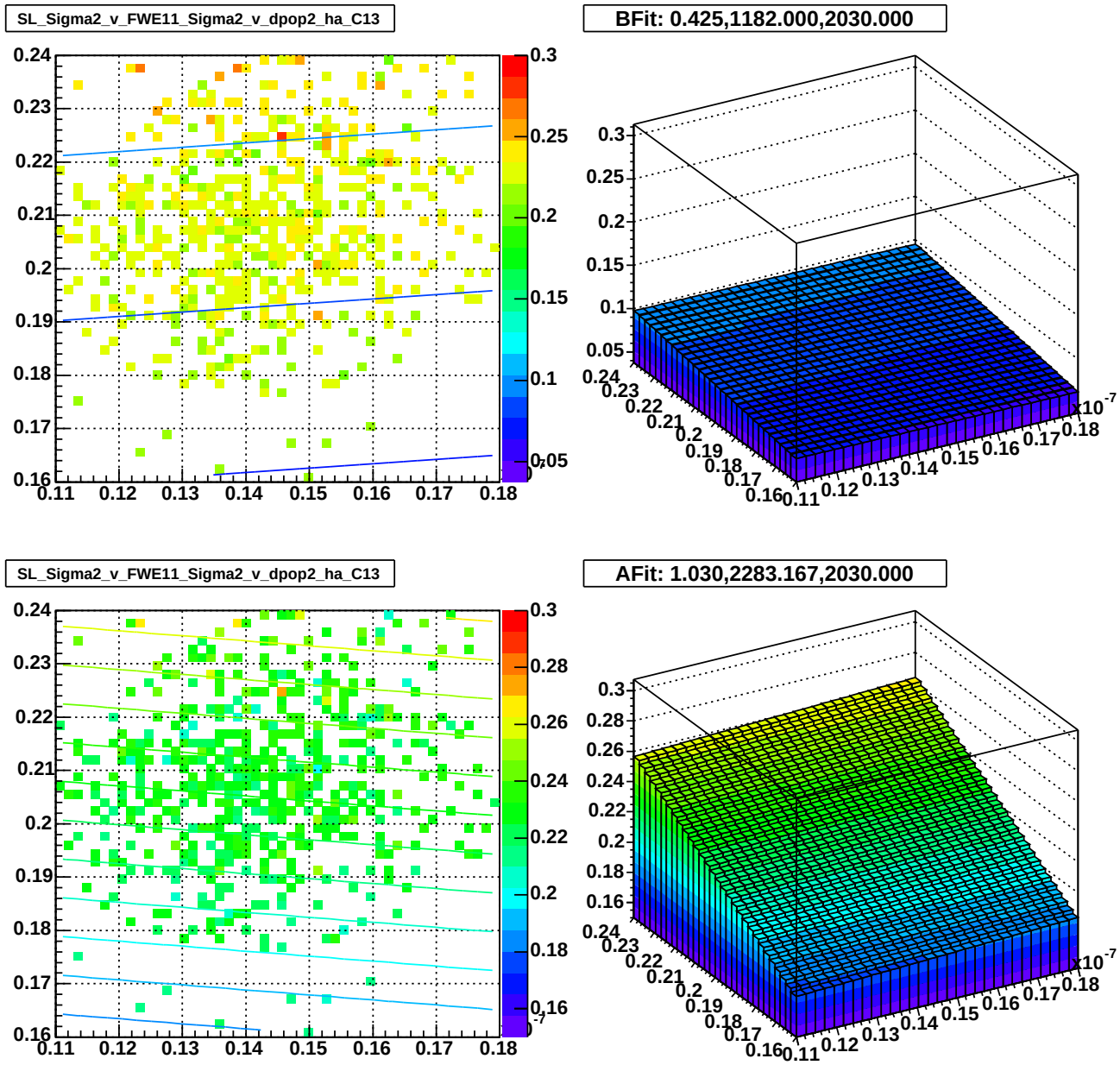

Figure 45: Antiproton beam, horizontal detectors, nominal lattice: Stores 2676-2805, 980 GeV Case Remove Halo: Comparisons of Sigma squared of the bunch width distribution measurements as done by Synchrotron Light (SL) C11 Detector with predictions based on the Flying Wire (FW) E11 Detector measurement: Sigma squared of the bunch width distribution (in mm^2) as measured by the SL C11 Detector as a function of sigma squared of the bunch width distribution (in mm^2) as measured by the FW E11 Detector versus recalculated $\delta p/p$ squared (based on δt the T:SBD[A,P]WS ACNET variable) with an overlaid contour of the prediction based on the nominal lattice functions; Prediction of sigma squared of the bunch width distribution (in mm^2) for SL C11 Detector as a function of sigma squared of the bunch width distribution (in mm^2) as measured by the FW E11 Detector versus recalculated $\delta p/p$ squared based on the nominal lattice functions; two lower plots have the same data points but have contours based on the fitted lattice functions.

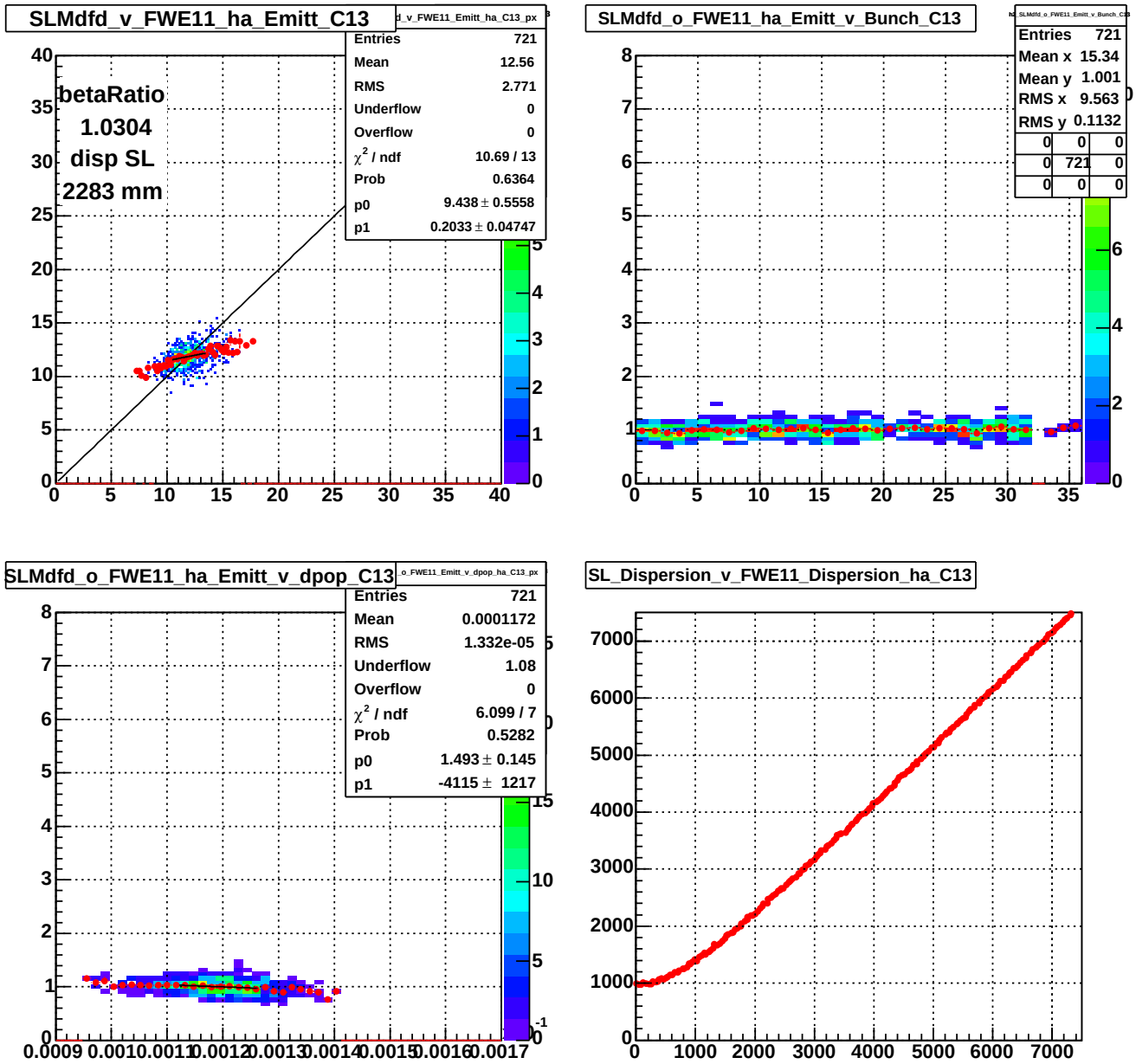

Figure 46: Antiproton beam, horizontal detectors, modified lattice: Stores 2676-2805, 980 GeV Case Remove Halo: Comparisons of Emittance measurements as done by Synchrotron Light (SL) Detector at C11 and Flying Wire (FW) Detector at E11 using fitted lattice parameters and formula with dispersion term both in the horizontal and in the vertical cases: Bunch emittance (in $\pi \cdot mm \cdot mrad$) as measured by SL C11 Detector versus bunch emittance as measured by the FW E11 Detector with an overlaid horizontal profile distribution with a straight line fit and the ideal prediction; bunch emittance as measured by SL C11 Detector over bunch emittance as measured by the FW E11 Detector versus bunch number together with an overlaid horizontal profile; bunch emittance as measured by SL C11 Detector over bunch emittance as measured by the FW E11 Detector versus recalculated $\delta p/p$ (based on δt the T:SBD[A,P]WS ACNET variable) with an overlaid horizontal profile with a straight line fit; fit based C11 dispersion function as a function of the E11 dispersion function.

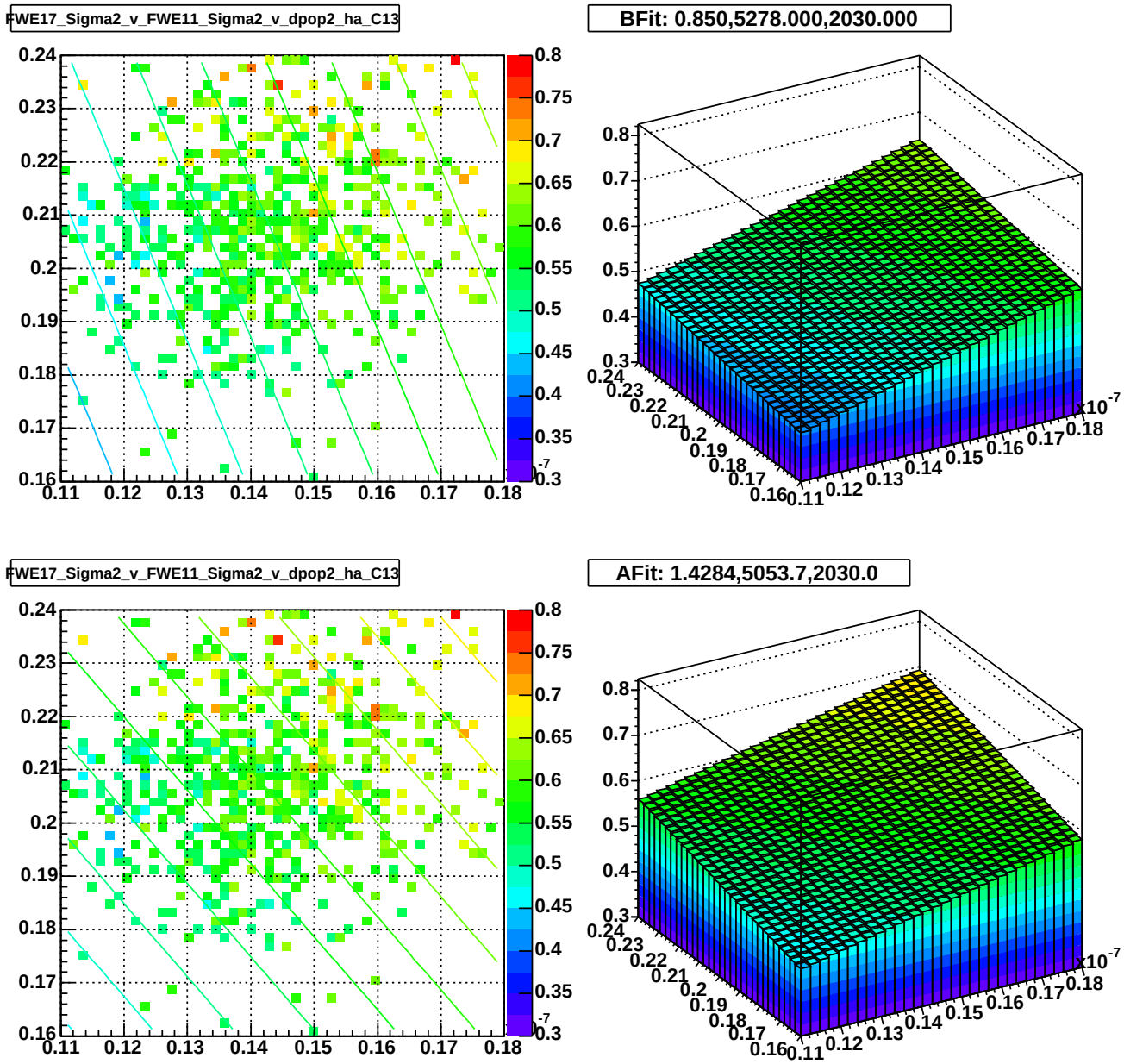

Figure 47: Antiproton beam, horizontal detectors, nominal lattice: Stores 2676-2805, 980 GeV Case Remove Halo: Comparisons of Sigma squared of the bunch width distribution measurements as done by Flying Wire (FW) E17 Detector with predictions based on the FW E11 Detector measurement: Sigma squared of the bunch width distribution (in mm^2) as measured by the FW E17 Detector as a function of sigma squared of the bunch width distribution (in mm^2) as measured by the FW E11 Detector versus recalculated $\delta p/p$ squared (based on δt the T:SBD[A,P]WS ACNET variable) with an overlaid contour of the prediction based on the nominal lattice functions; Prediction of sigma squared of the bunch width distribution (in mm^2) for E17 Detector as a function of sigma squared of the bunch width distribution (in mm^2) as measured by the FW E11 Detector versus recalculated $\delta p/p$ squared based on the nominal lattice functions; two lower plots have the same data points but have contours based on the fitted lattice functions.

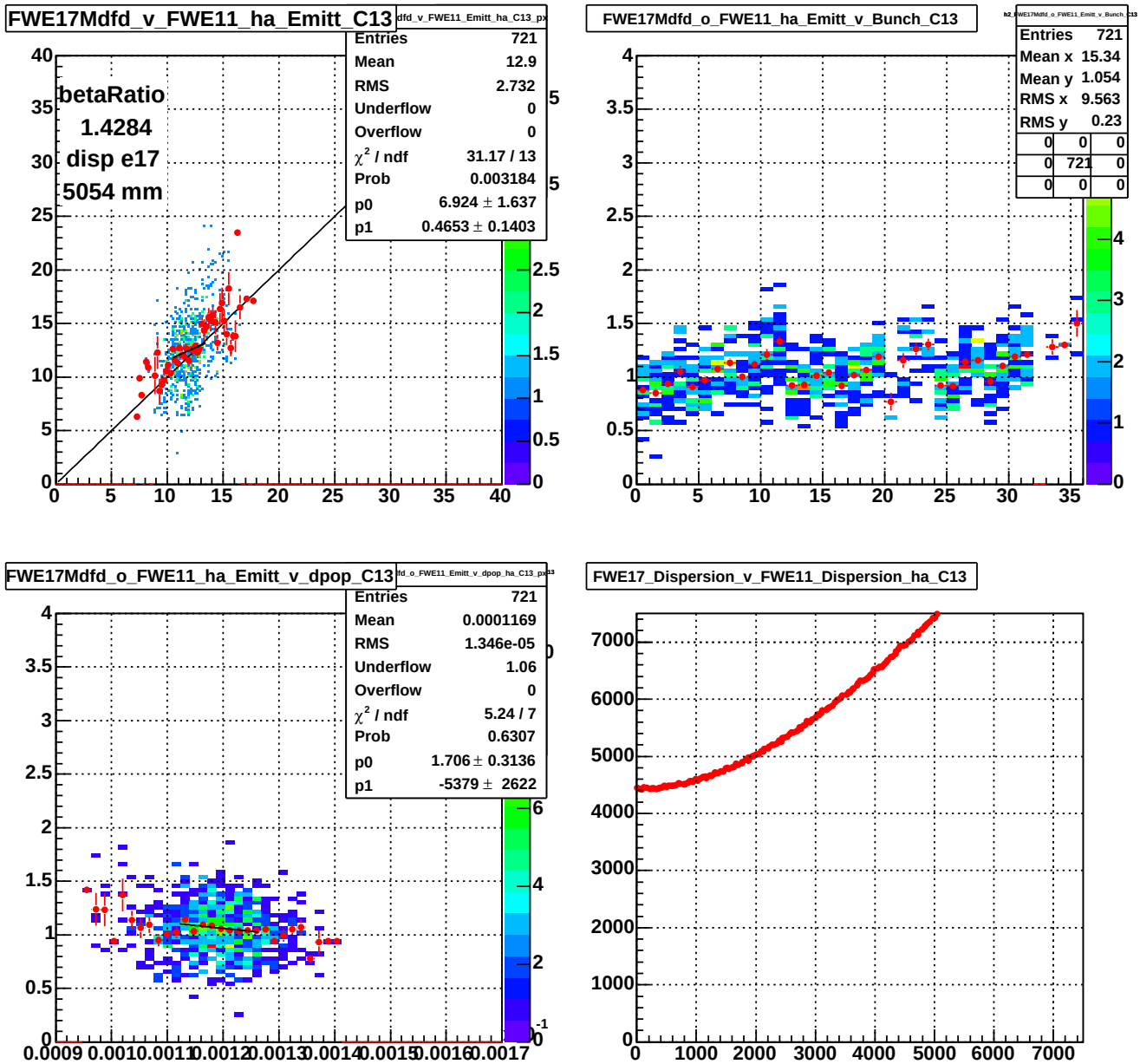

Figure 48: Antiproton beam, horizontal detectors, modified lattice: Stores 2676-2805, 980 GeV Case Remove Halo: Comparisons of Emittance measurements as done by Flying Wire (FW) Detector at E17 and Flying Wire Detector at E11 using fitted lattice parameters: Bunch emittance (in $\pi \cdot mm \cdot mrad$) as measured by FW E17 Detector versus bunch emittance as measured by the FW E11 Detector with an overlaid horizontal profile distribution with a straight line fit and the ideal prediction; bunch emittance as measured by FW E17 Detector over bunch emittance as measured by the FW E11 Detector versus bunch number together with an overlaid horizontal profile; bunch emittance as measured by FW E17 Detector over bunch emittance as measured by the FW E11 Detector versus recalculated $\delta p/p$ (based on δt the T:SBD[A,P]WS ACNET variable) with an overlaid horizontal profile with a straight line fit; fit based E17 dispersion function as a function of the E11 dispersion function.

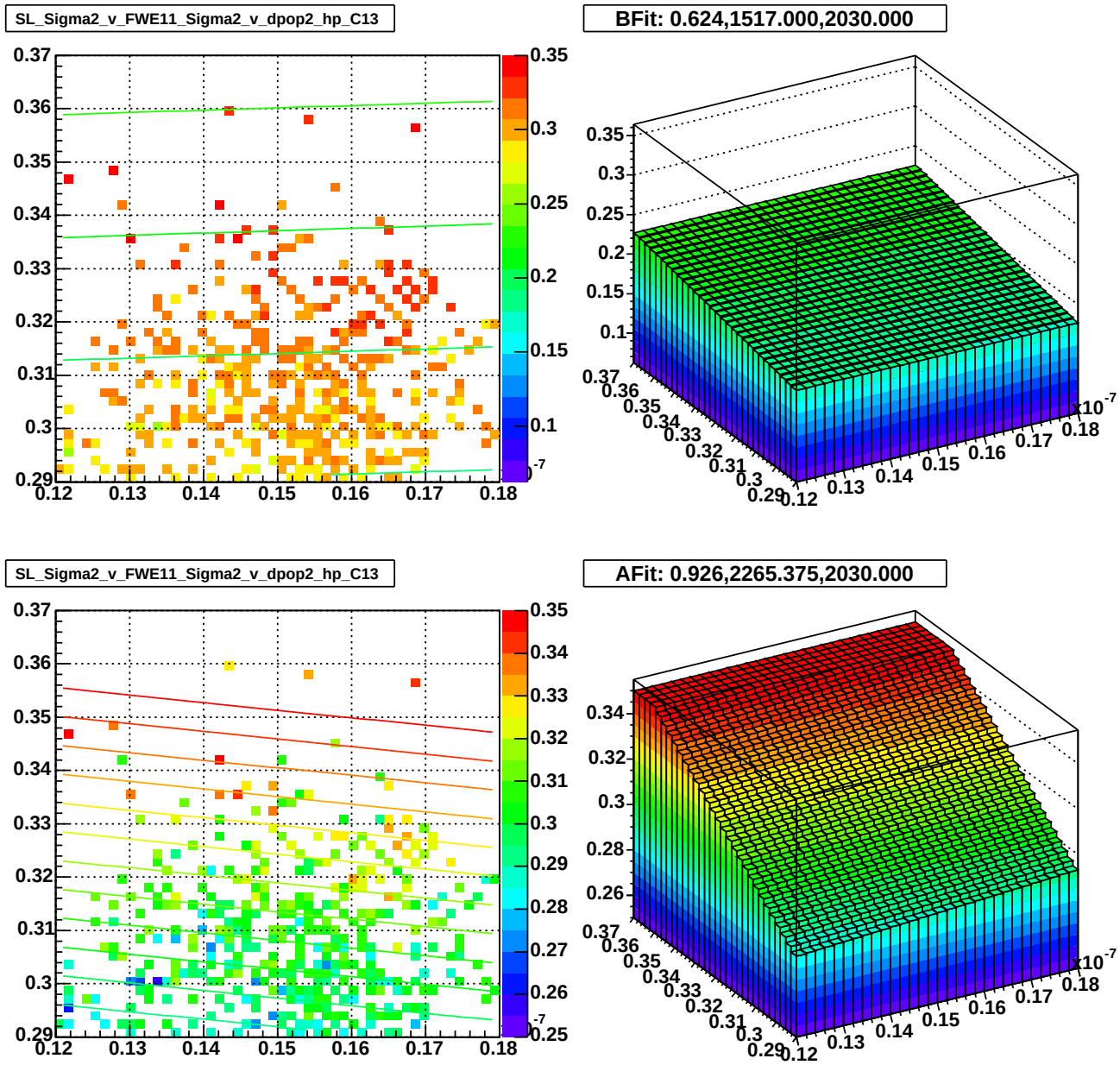

Figure 49: Proton beam, horizontal detectors, nominal lattice: Stores 2676-2805, 980 GeV Case Remove Halo: Comparisons of Sigma squared of the bunch width distribution measurements as done by Synchrotron Light (SL) C11 Detector with predictions based on the Flying Wire (FW) E11 Detector measurement: Sigma squared of the bunch width distribution (in mm^2) as measured by the SL C11 Detector as a function of sigma squared of the bunch width distribution (in mm^2) as measured by the FW E11 Detector versus recalculated $\delta p/p$ squared (based on δt the T:SBD[A,P]WS ACNET variable) with an overlaid contour of the prediction based on the nominal lattice functions; Prediction of sigma squared of the bunch width distribution (in mm^2) for SL C11 Detector as a function of sigma squared of the bunch width distribution (in mm^2) as measured by the FW E11 Detector versus recalculated $\delta p/p$ squared based on the nominal lattice functions; two lower plots have the same data points but have contours based on the fitted lattice functions.

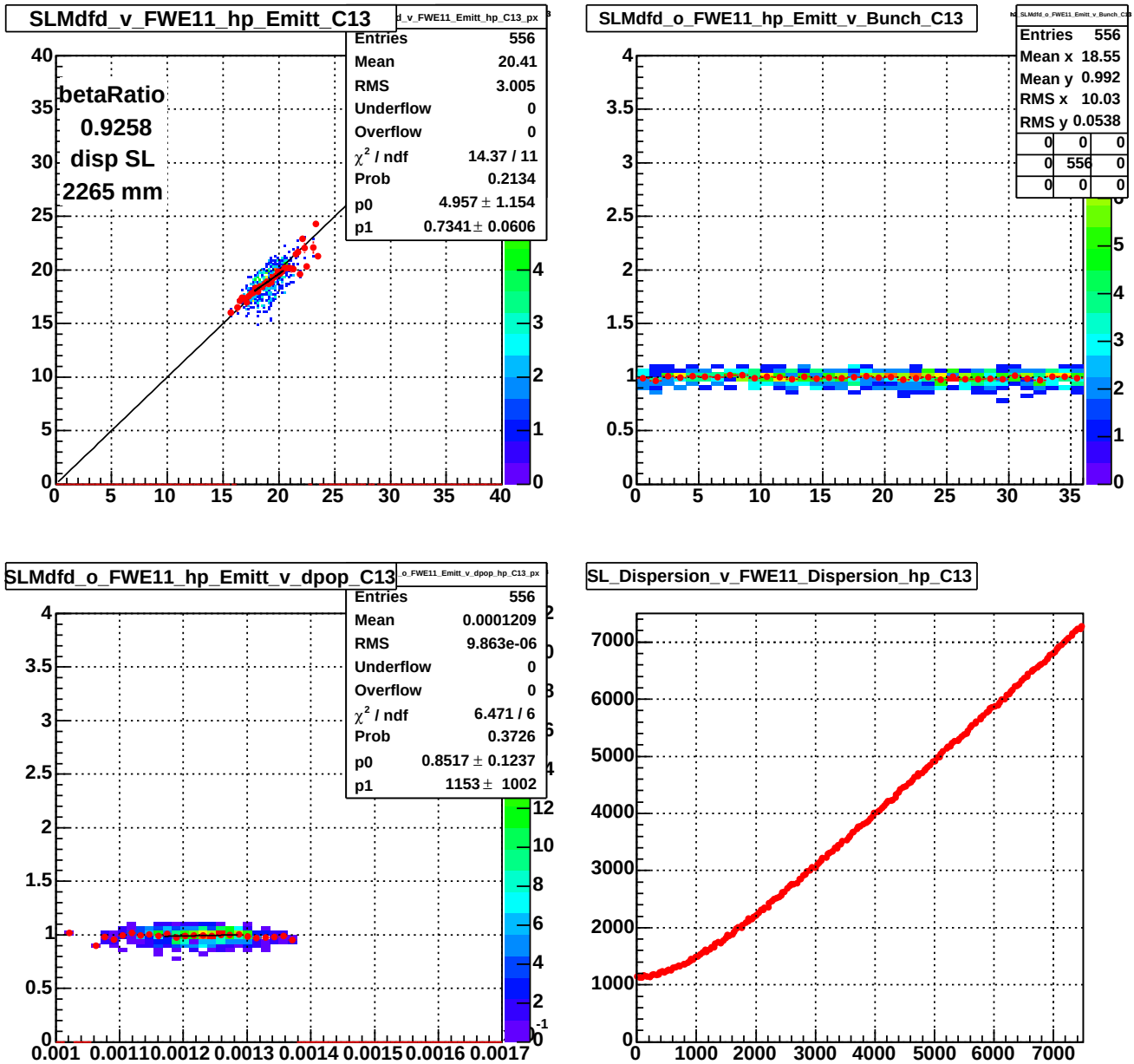

Figure 50: Proton beam, horizontal detectors, modified lattice: Stores 2676-2805, 980 GeV Case Remove Halo: Comparisons of Emittance measurements as done by Synchrotron Light (SL) Detector at C11 and Flying Wire (FW) Detector at E11 using fitted lattice parameters and formula with dispersion term both in the horizontal and in the vertical cases: Bunch emittance (in $\pi \cdot mm \cdot mrad$) as measured by SL C11 Detector versus bunch emittance as measured by the FW E11 Detector with an overlaid horizontal profile distribution with a straight line fit and the ideal prediction; bunch emittance as measured by SL C11 Detector over bunch emittance as measured by the FW E11 Detector versus bunch number together with an overlaid horizontal profile; bunch emittance as measured by SL C11 Detector over bunch emittance as measured by the FW E11 Detector versus recalculated $\delta p/p$ (based on δt the T:SBD[A,P]WS ACNET variable) with an overlaid horizontal profile with a straight line fit; fit based C11 dispersion function as a function of the E11 dispersion function.

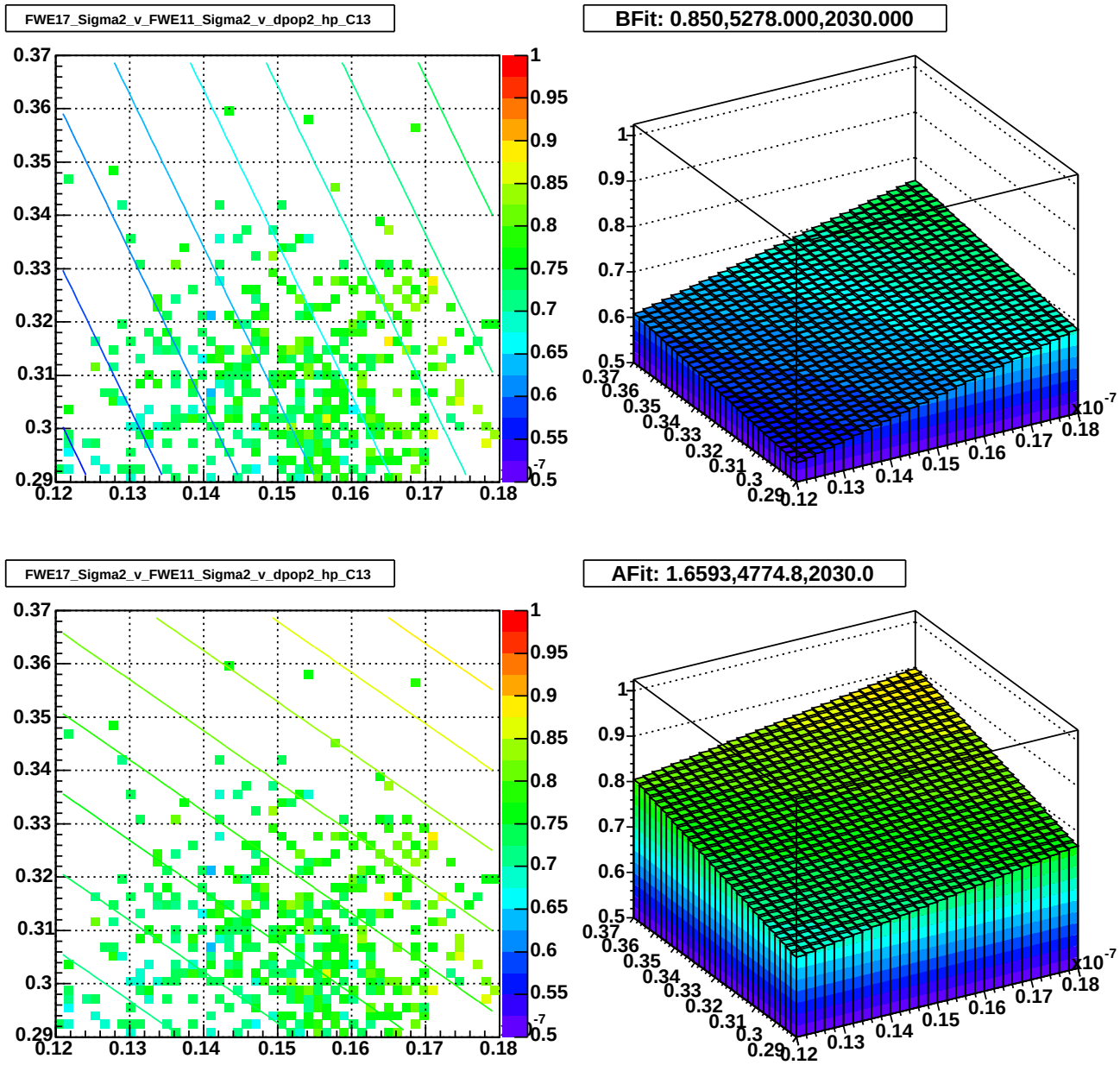

Figure 51: Proton beam, horizontal detectors, nominal lattice: Stores 2676-2805, 980 GeV Case Remove Halo: Comparisons of Sigma squared of the bunch width distribution measurements as done by Flying Wire (FW) E17 Detector with predictions based on the FW E11 Detector measurement: Sigma squared of the bunch width distribution (in mm^2) as measured by the FW E17 Detector as a function of sigma squared of the bunch width distribution (in mm^2) as measured by the FW E11 Detector versus recalculated $\delta p/p$ squared (based on δt the T:SBD[A,P]WS ACNET variable) with an overlaid contour of the prediction based on the nominal lattice functions; Prediction of sigma squared of the bunch width distribution (in mm^2) for E17 Detector as a function of sigma squared of the bunch width distribution (in mm^2) as measured by the FW E11 Detector versus recalculated $\delta p/p$ squared based on the nominal lattice functions; two lower plots have the same data points but have contours based on the fitted lattice functions.

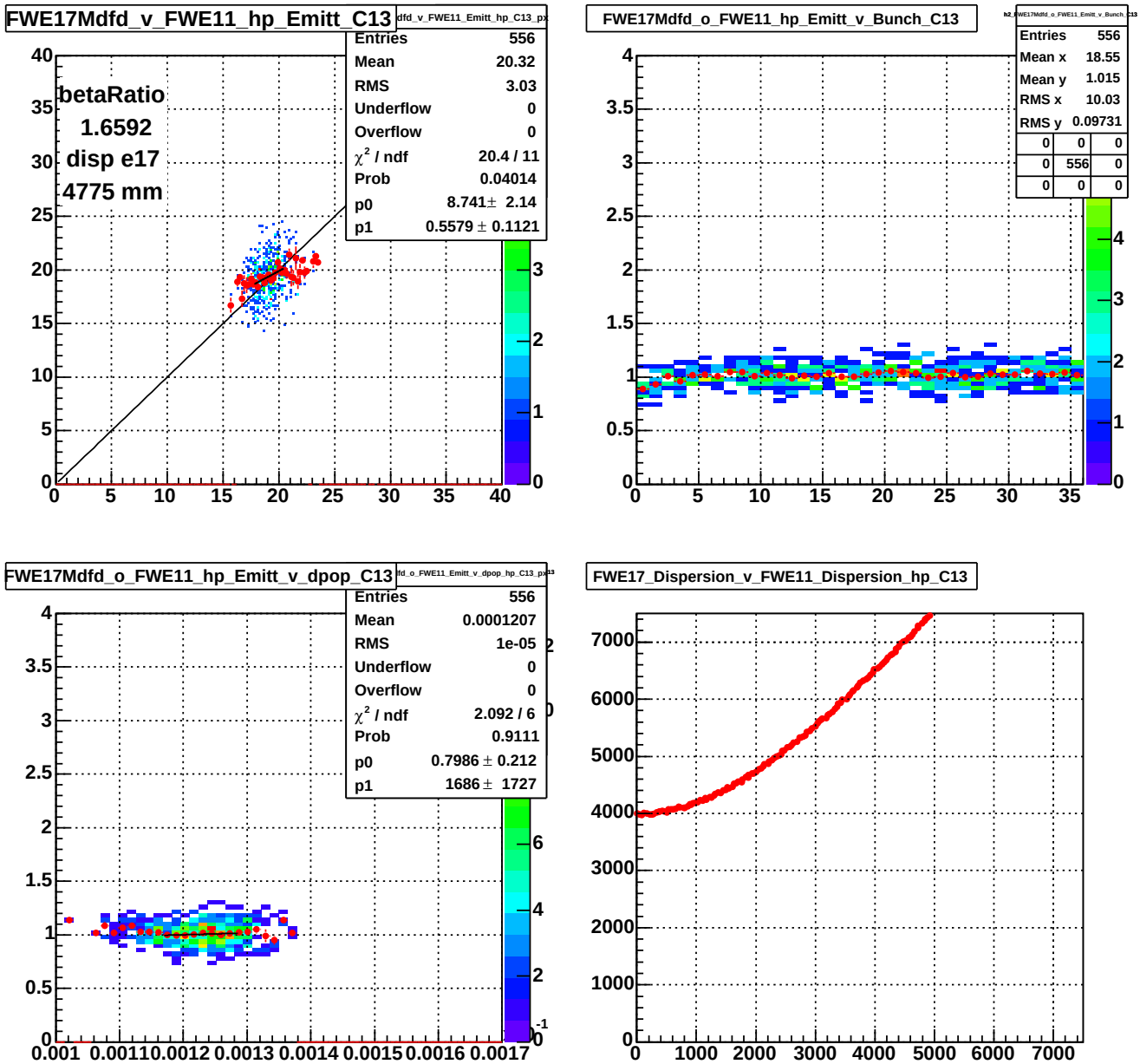

Figure 52: Proton beam, horizontal detectors, modified lattice: Stores 2676-2805, 980 GeV Case Remove Halo: Comparisons of Emittance measurements as done by Flying Wire (FW) Detector at E17 and Flying Wire Detector at E11 using fitted lattice parameters: Bunch emittance (in $\pi \cdot mm \cdot mrad$) as measured by FW E17 Detector versus bunch emittance as measured by the FW E11 Detector with an overlaid horizontal profile distribution with a straight line fit and the ideal prediction; bunch emittance as measured by FW E17 Detector over bunch emittance as measured by the FW E11 Detector versus bunch number together with an overlaid horizontal profile; bunch emittance as measured by FW E17 Detector over bunch emittance as measured by the FW E11 Detector versus recalculated $\delta p/p$ (based on δt the T:SBD[A,P]WS ACNET variable) with an overlaid horizontal profile with a straight line fit; fit based E17 dispersion function as a function of the E11 dispersion function.

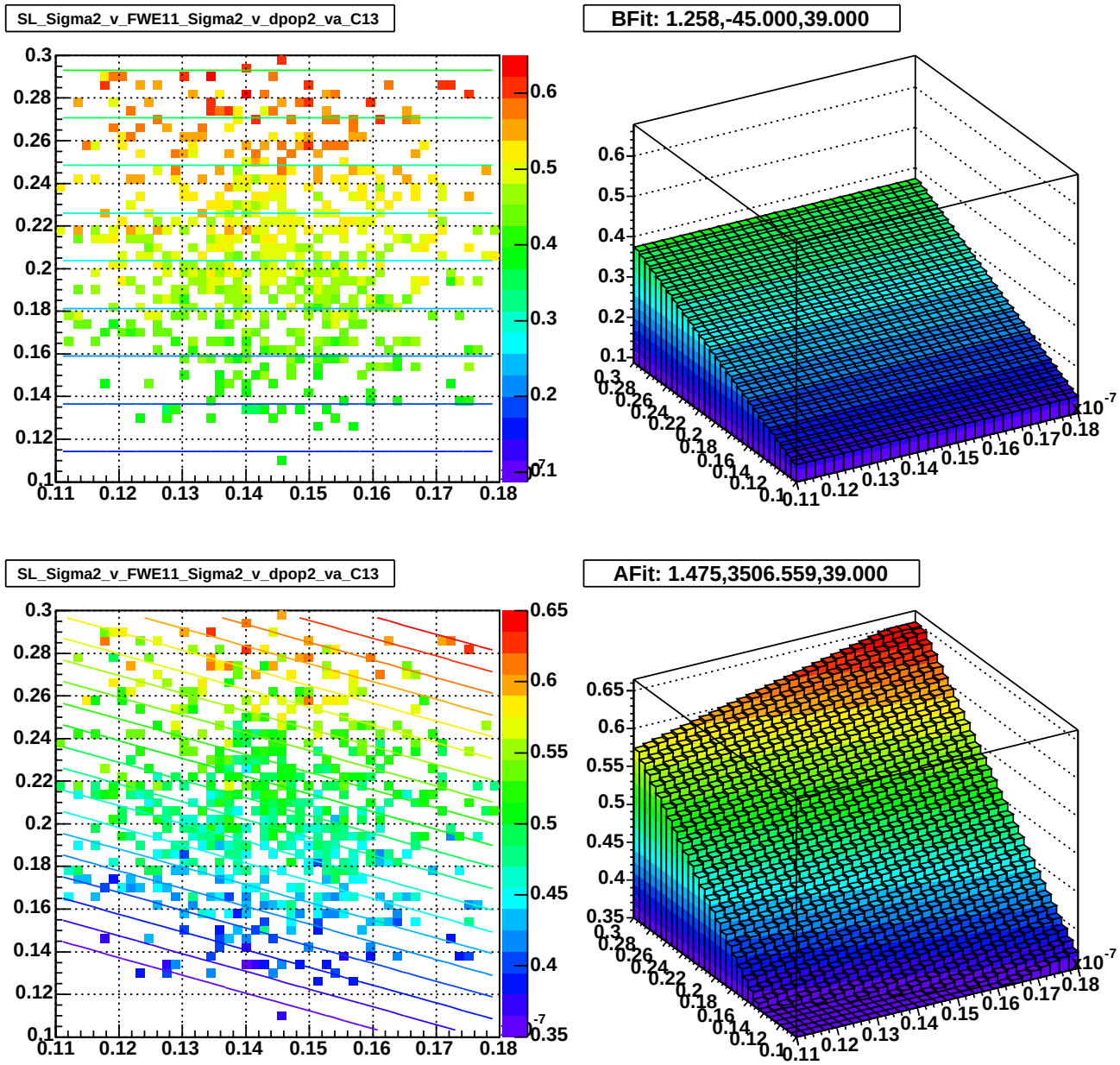

Figure 53: Antiproton beam, vertical detectors, nominal lattice: Stores 2676-2805, 980 GeV Case Remove Halo: Comparisons of Sigma squared of the bunch width distribution measurements as done by Synchrotron Light (SL) C11 Detector with predictions based on the Flying Wire (FW) E11 Detector measurement: Sigma squared of the bunch width distribution (in mm^2) as measured by the SL C11 Detector as a function of sigma squared of the bunch width distribution (in mm^2) as measured by the FW E11 Detector versus recalculated $\delta p/p$ squared (based on δt the T:SBD[A,P]WS ACNET variable) with an overlaid contour of the prediction based on the nominal lattice functions; Prediction of sigma squared of the bunch width distribution (in mm^2) for SL C11 Detector as a function of sigma squared of the bunch width distribution (in mm^2) as measured by the FW E11 Detector versus recalculated $\delta p/p$ squared based on the nominal lattice functions; two lower plots have the same data points but have contours based on the fitted lattice functions.

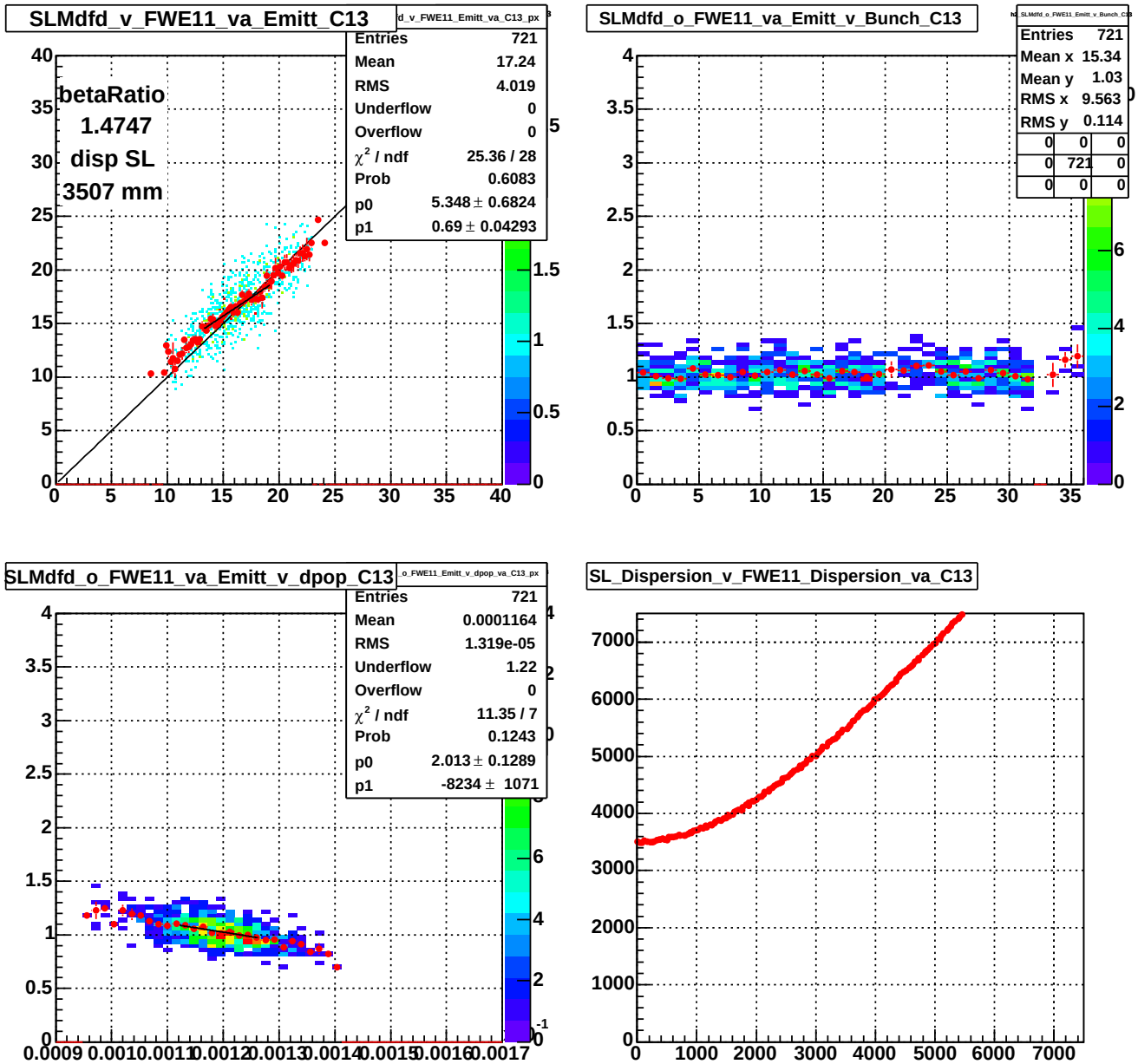

Figure 54: Antiproton beam, vertical detectors, modified lattice: Stores 2676-2805, 980 GeV Case Remove Halo: Comparisons of Emittance measurements as done by Synchrotron Light (SL) Detector at C11 and Flying Wire (FW) Detector at E11 using fitted lattice parameters and formula with dispersion term both in the horizontal and in the vertical cases: Bunch emittance (in $\pi \cdot mm \cdot mrad$) as measured by SL C11 Detector versus bunch emittance as measured by the FW E11 Detector with an overlaid horizontal profile distribution with a straight line fit and the ideal prediction; bunch emittance as measured by SL C11 Detector over bunch emittance as measured by the FW E11 Detector versus bunch number together with an overlaid horizontal profile; bunch emittance as measured by SL C11 Detector over bunch emittance as measured by the FW E11 Detector versus recalculated $\delta p/p$ (based on δt the T:SBD[A,P]WS ACNET variable) with an overlaid horizontal profile with a straight line fit; fit based C11 dispersion function as a function of the E11 dispersion function.

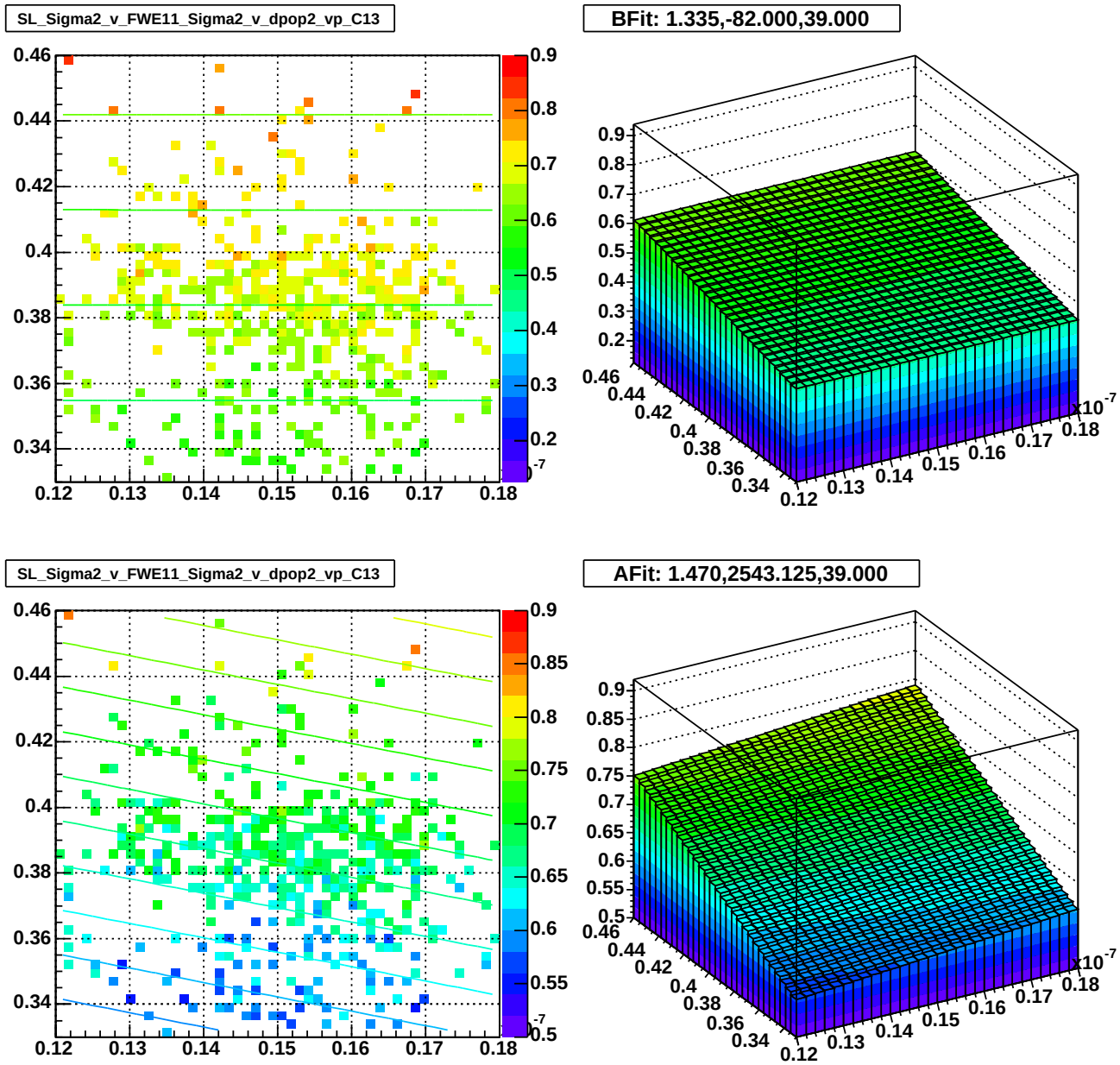

Figure 55: Proton beam, vertical detectors, nominal lattice: Stores 2676-2805, 980 GeV Case Remove Halo: Comparisons of Sigma squared of the bunch width distribution measurements as done by Synchrotron Light (SL) C11 Detector with predictions based on the Flying Wire (FW) E11 Detector measurement: Sigma squared of the bunch width distribution (in mm^2) as measured by the SL C11 Detector as a function of sigma squared of the bunch width distribution (in mm^2) as measured by the FW E11 Detector versus recalculated $\delta p/p$ squared (based on δt the T:SBD[A,P]WS ACNET variable) with an overlaid contour of the prediction based on the nominal lattice functions; Prediction of sigma squared of the bunch width distribution (in mm^2) for SL C11 Detector as a function of sigma squared of the bunch width distribution (in mm^2) as measured by the FW E11 Detector versus recalculated $\delta p/p$ squared based on the nominal lattice functions; two lower plots have the same data points but have contours based on the fitted lattice functions.

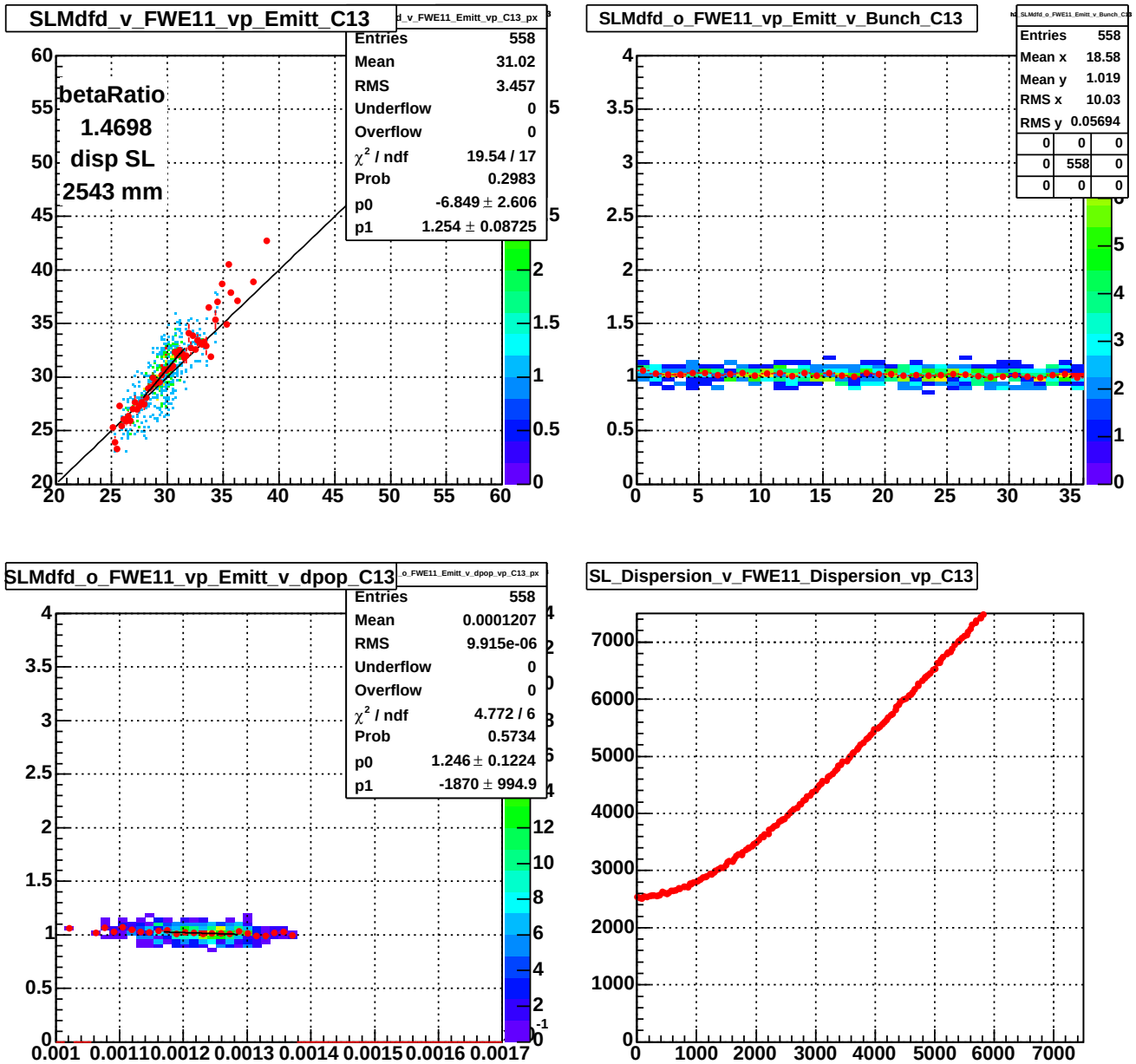

Figure 56: Proton beam, vertical detectors, modified lattice: Stores 2676-2805, 980 GeV Case Remove Halo: Comparisons of Emittance measurements as done by Synchrotron Light (SL) Detector at C11 and Flying Wire (FW) Detector at E11 using fitted lattice parameters and formula with dispersion term both in the horizontal and in the vertical cases: Bunch emittance (in $\pi \cdot mm \cdot mrad$) as measured by SL C11 Detector versus bunch emittance as measured by the FW E11 Detector with an overlaid horizontal profile distribution with a straight line fit and the ideal prediction; bunch emittance as measured by SL C11 Detector over bunch emittance as measured by the FW E11 Detector versus bunch number together with an overlaid horizontal profile; bunch emittance as measured by SL C11 Detector over bunch emittance as measured by the FW E11 Detector versus recalculated $\delta p/p$ (based on δt the T:SBD[A,P]WS ACNET variable) with an overlaid horizontal profile with a straight line fit; fit based C11 dispersion function as a function of the E11 dispersion function.

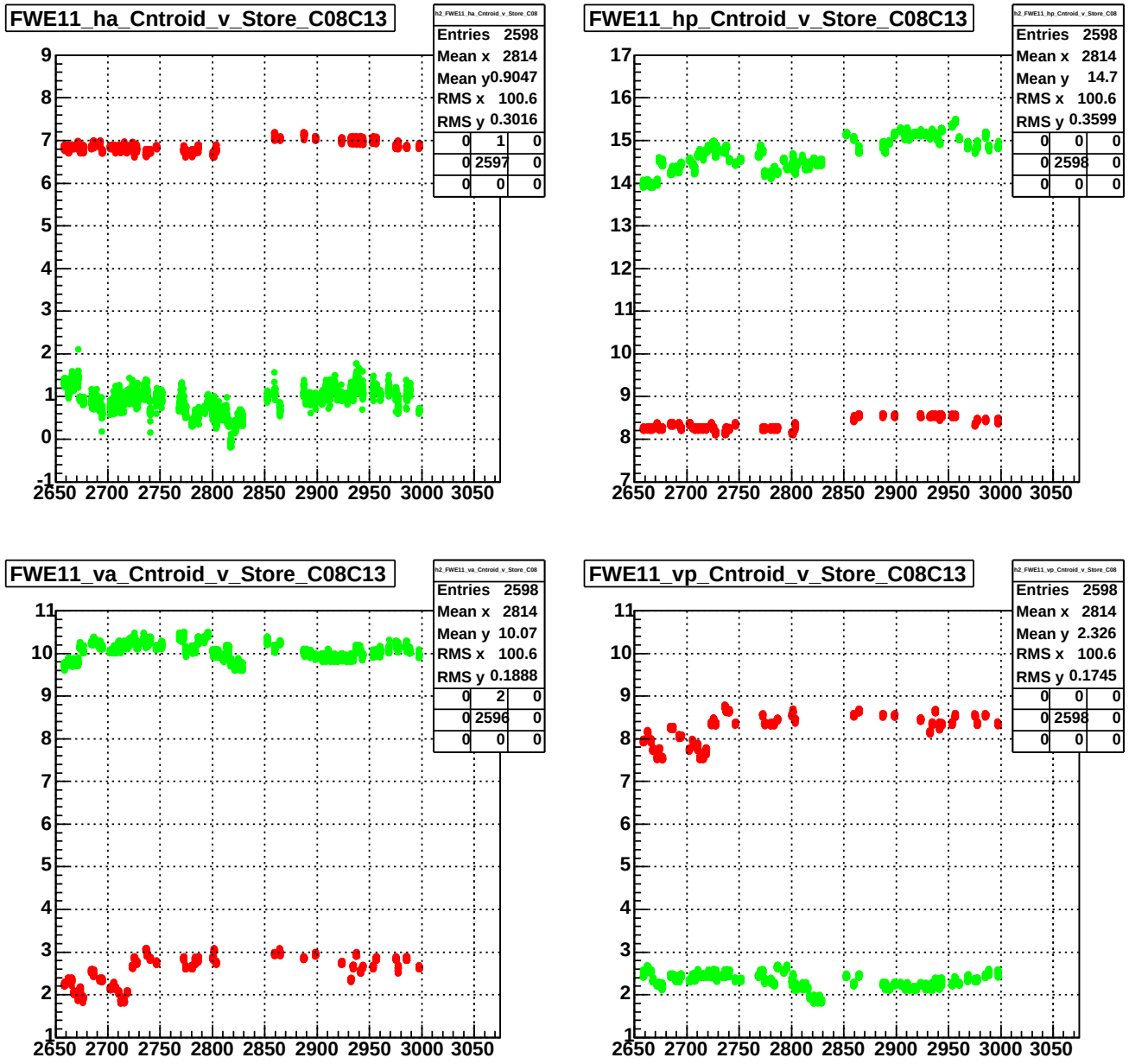

Figure 57: Stores 2650-2997, Case Before Ramp and Remove Halo: Bunch centroid position (in *mm*) (based on the T:FW[E,H,V][A,P]CE ACNET variable) versus store number for horizontal antiproton (ha) and proton (hp) as well as vertical antiproton (va) and proton (vp) FW E11 Detectors (150 GeV Before Ramp points in green, 980 GeV Remove Halo points in red).

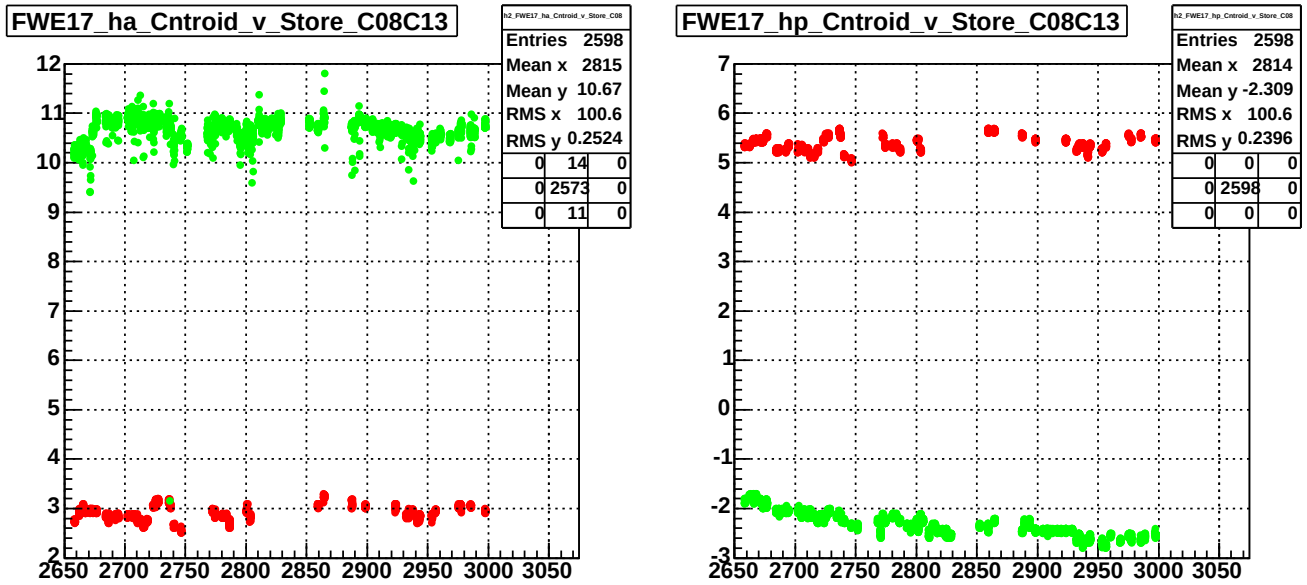

Figure 58: Stores 2650-2997, Case Before Ramp and Remove Halo: Bunch centroid position (in *mm*) (based on the T:FW[E,H,V][A,P]CE ACNET variable) versus store number for horizontal antiproton (ha) and proton (hp) as well as vertical antiproton (va) and proton (vp) FW E11 Detectors (150 GeV Before Ramp points in green, 980 GeV Remove Halo points in red).

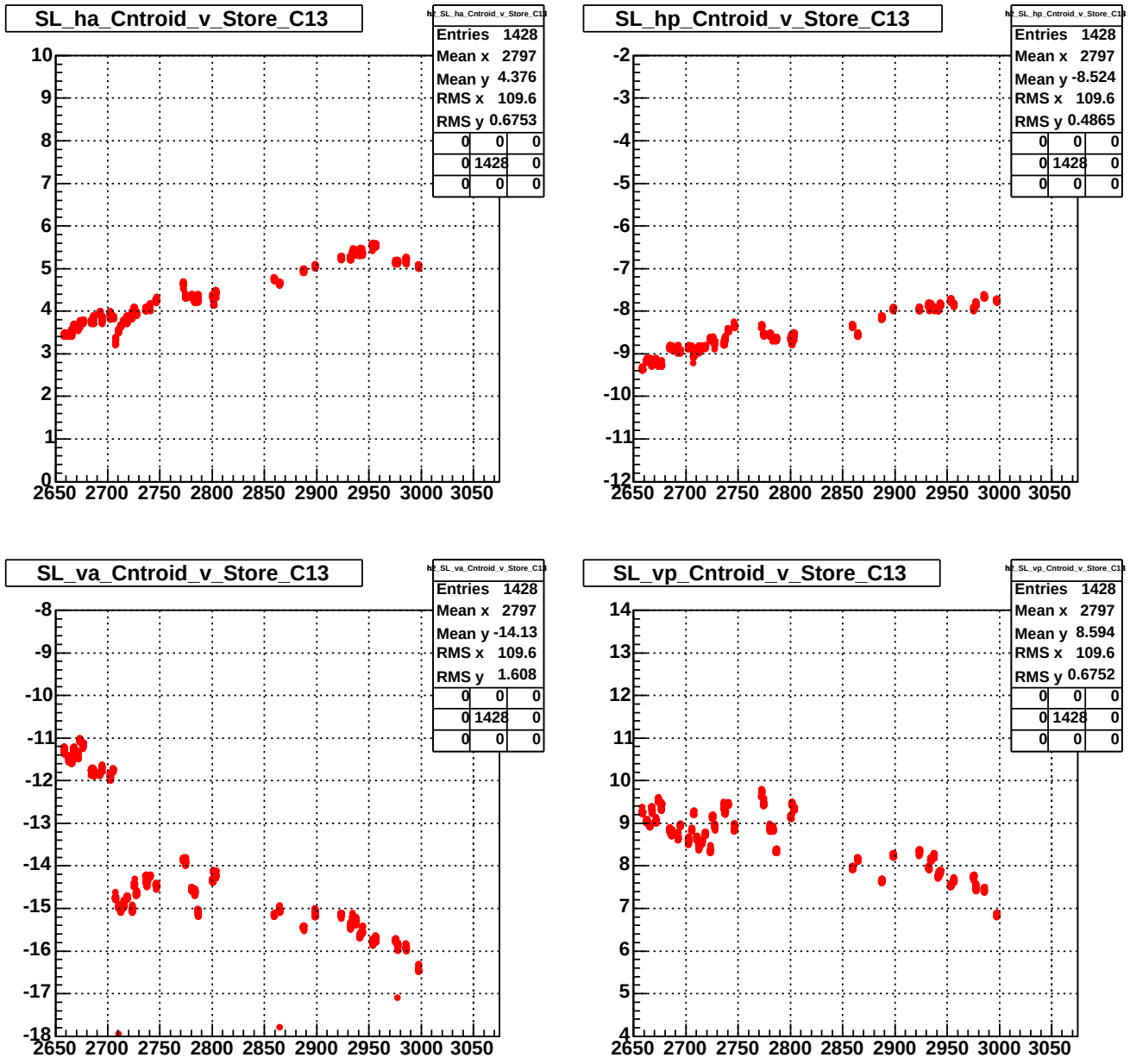

Figure 59: Stores 2650-2997, 980 GeV Case Remove Halo: Bunch centroid position (in *mm*) (based on the T:SL[A,P]C[H,V] ACNET variable) versus store number for horizontal antiproton (ha) and proton (hp) as well as vertical antiproton (va) and proton (vp) SL C11 Detectors.

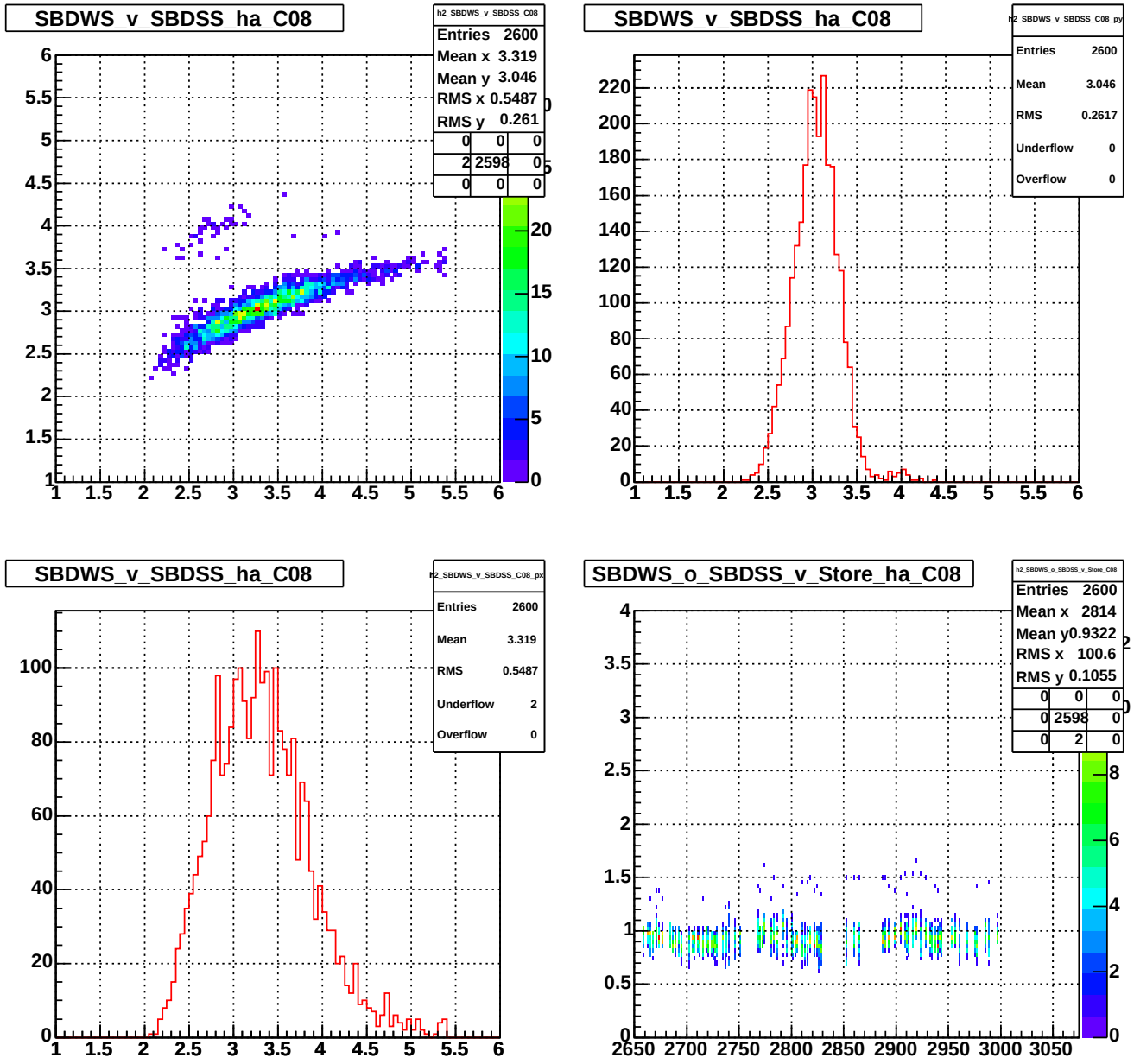

Figure 60: Antiproton beam, horizontal detectors, nominal lattice: Stores 2650-2997, 150 GeV Case Before Ramp: Comparisons of longitudinal bunch length (in *ns*) as reported by SBD according to Gaussian fit sigma and RMS (based on T:SBD[A,P]SS and T:SBD[A,P]WS ACNET variables): RMS versus sigma; RMS; sigma; ratio of RMS and sigma versus store number.

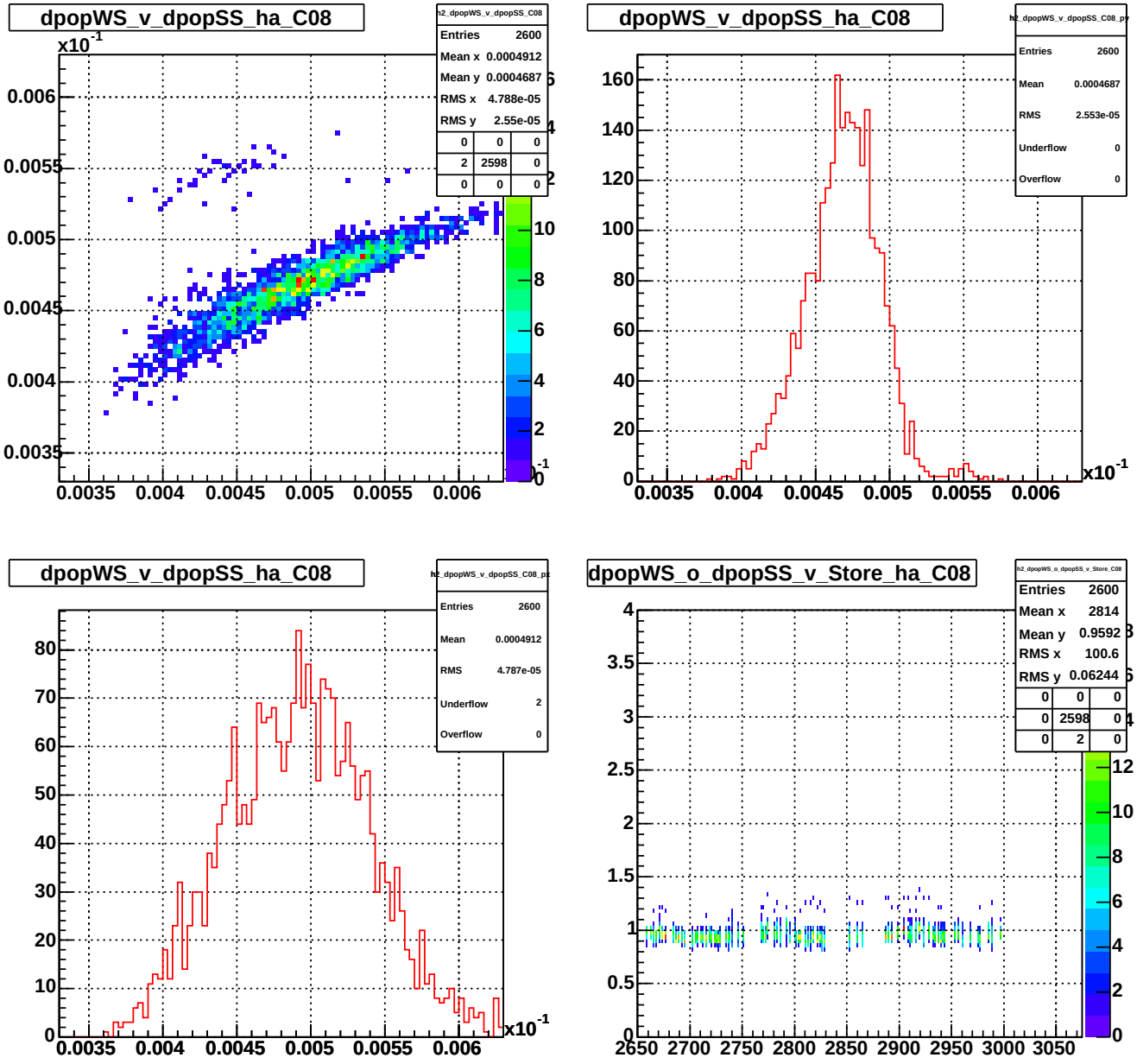

Figure 61: Antiproton beam, horizontal detectors, nominal lattice: Stores 2650-2997, 150 GeV Case Before Ramp: Comparisons of recalculated $\delta p/p$ based on T:SBD[A,P]SS (Gaussian fit sigma) and T:SBD[A,P]WS (RMS) ACNET variables: $\delta p/p$ based on RMS versus $\delta p/p$ based on sigma; $\delta p/p$ based on RMS; $\delta p/p$ based on sigma; ratio of $\delta p/p$ based on RMS and sigma versus store number.

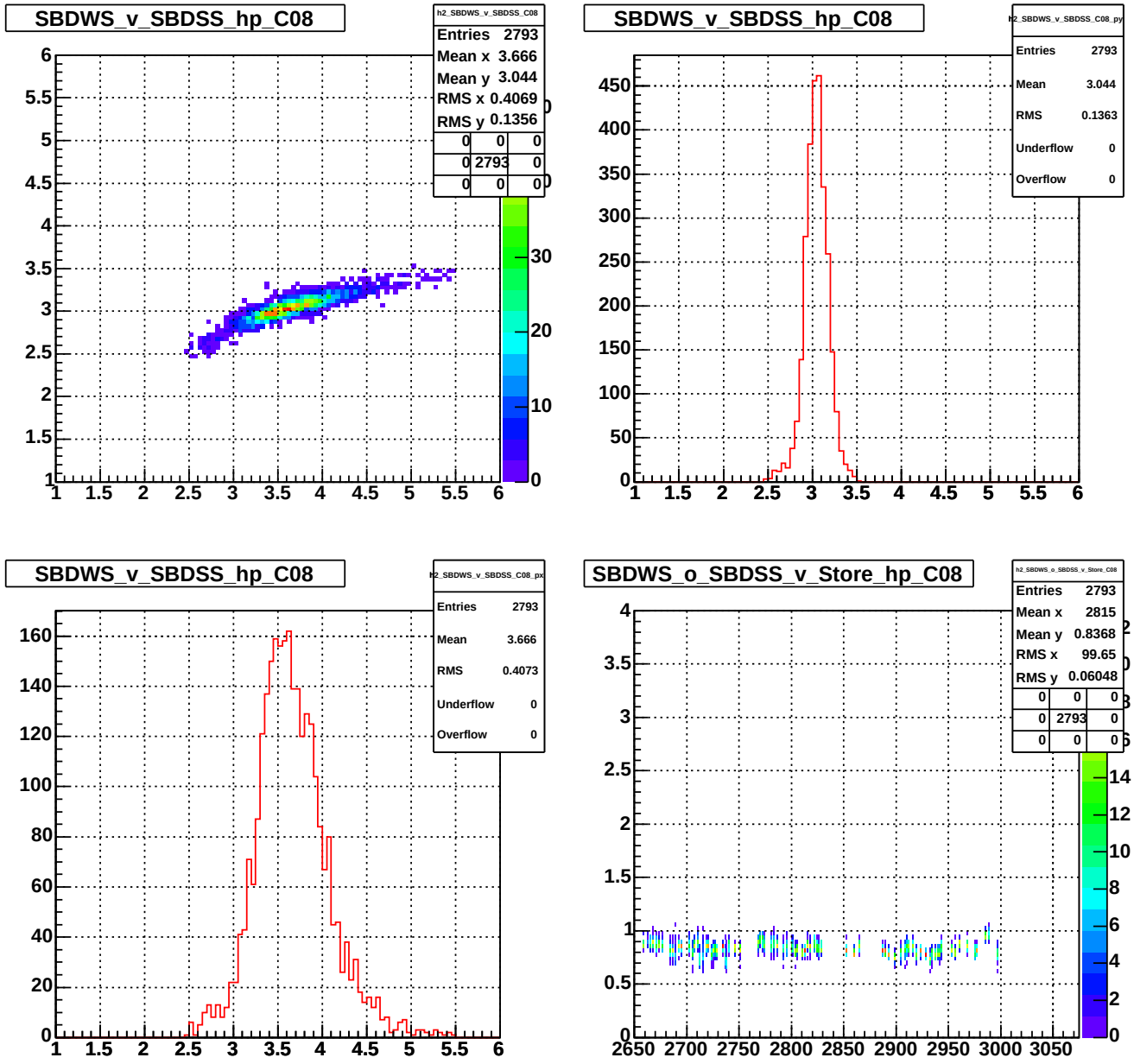

Figure 62: Proton beam, horizontal detectors, nominal lattice: Stores 2650-2997, 150 GeV Case Before Ramp: Comparisons of longitudinal bunch length (in *ns*) as reported by SBD according to Gaussian fit sigma and RMS (based on T:SBD[A,P]SS and T:SBD[A,P]WS ACNET variables): RMS versus sigma; RMS; sigma; ratio of RMS and sigma versus store number.

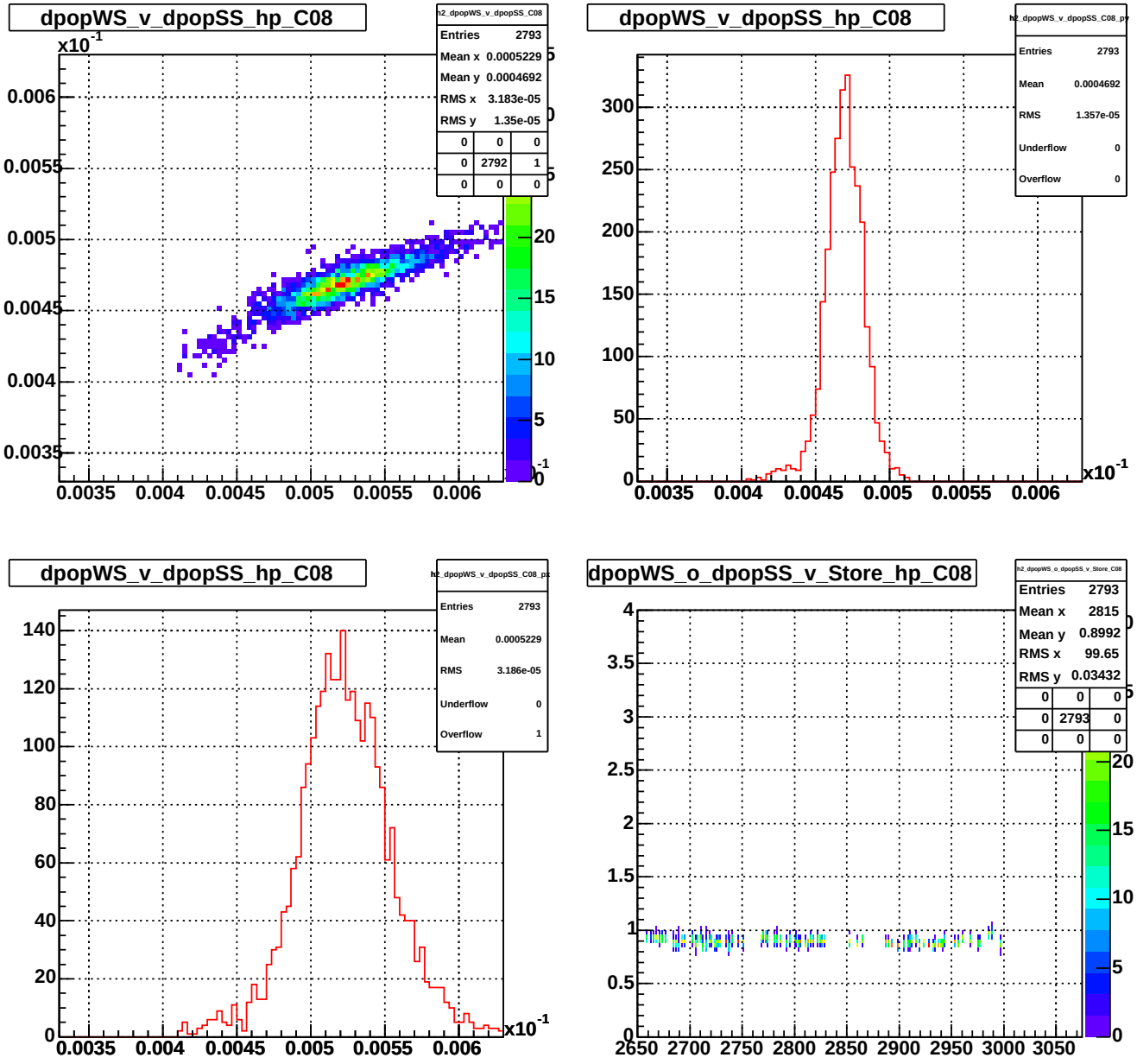

Figure 63: Proton beam, horizontal detectors, nominal lattice: Stores 2650-2997, 150 GeV Case Before Ramp: Comparisons of recalculated $\delta p/p$ based on T:SBD[A,P]SS (Gaussian fit sigma) and T:SBD[A,P]WS (RMS) ACNET variables: $\delta p/p$ based on RMS versus $\delta p/p$ based on sigma; $\delta p/p$ based on RMS; $\delta p/p$ based on sigma; ratio of $\delta p/p$ based on RMS and sigma versus store number.

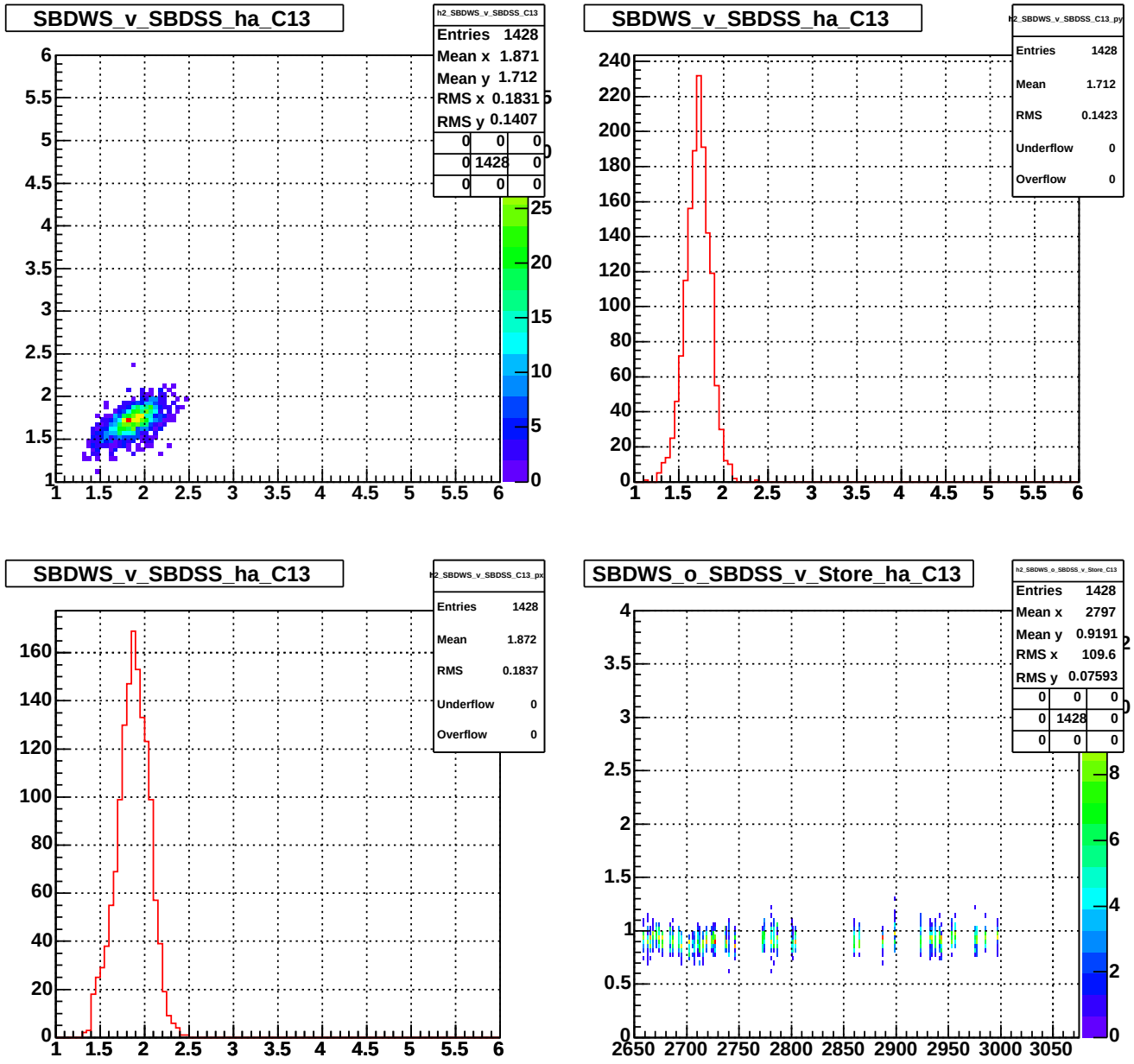

Figure 64: Antiproton beam, horizontal detectors, nominal lattice: Stores 2650-2997, 980 GeV Case Remove Halo: Comparisons of longitudinal bunch length (in *ns*) as reported by SBD according to Gaussian fit sigma and RMS (based on T:SBD[A,P]SS and T:SBD[A,P]WS ACNET variables): RMS versus sigma; RMS; sigma; ratio of RMS and sigma versus store number.

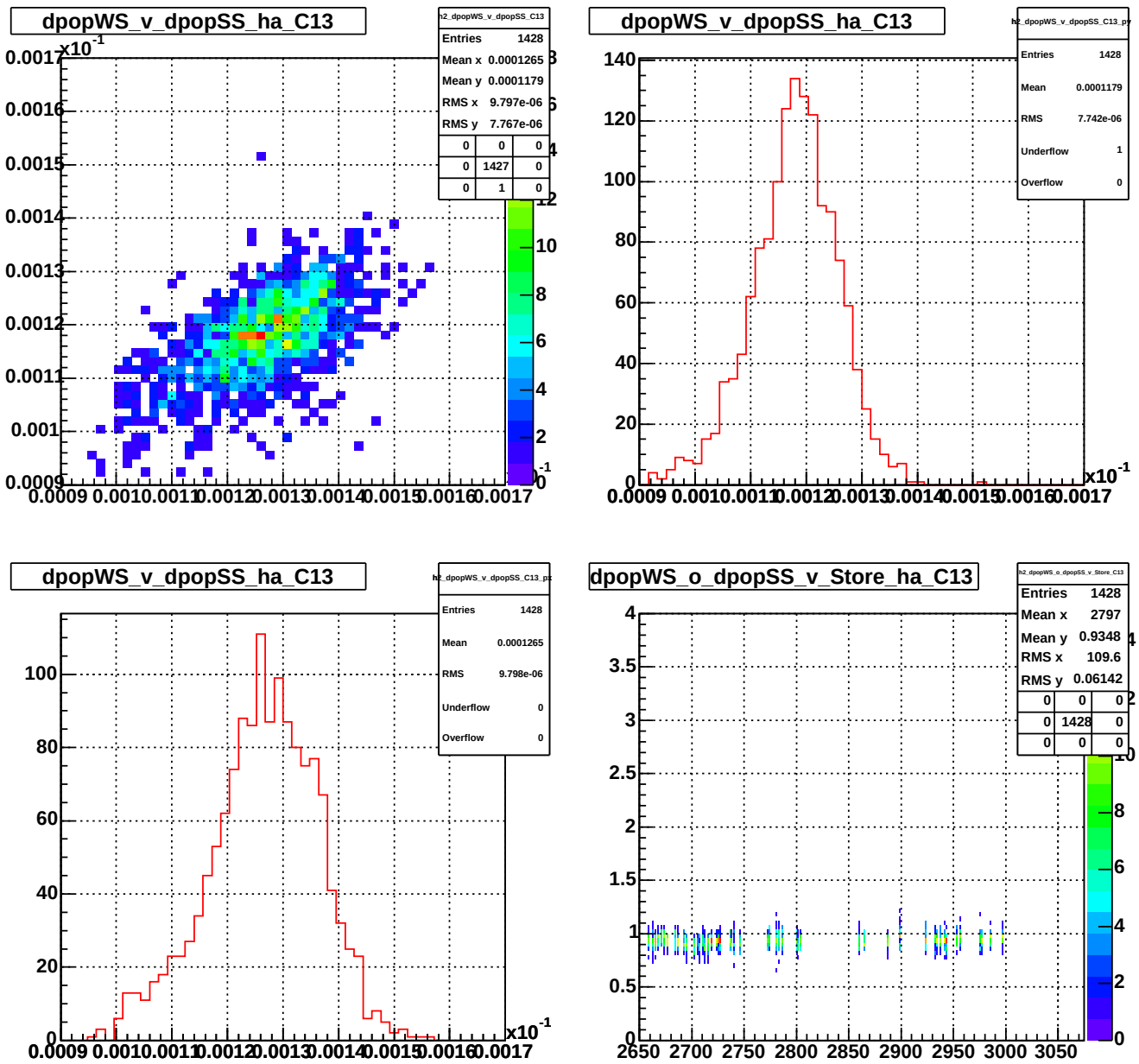

Figure 65: Antiproton beam, horizontal detectors, nominal lattice: Stores 2650-2997, 980 GeV Case Remove Halo: Comparisons of recalculated $\delta p/p$ based on T:SBD[A,P]SS (Gaussian fit sigma) and T:SBD[A,P]WS (RMS) ACNET variables: $\delta p/p$ based on RMS versus $\delta p/p$ based on sigma; $\delta p/p$ based on RMS; $\delta p/p$ based on sigma; ratio of $\delta p/p$ based on RMS and sigma versus store number.

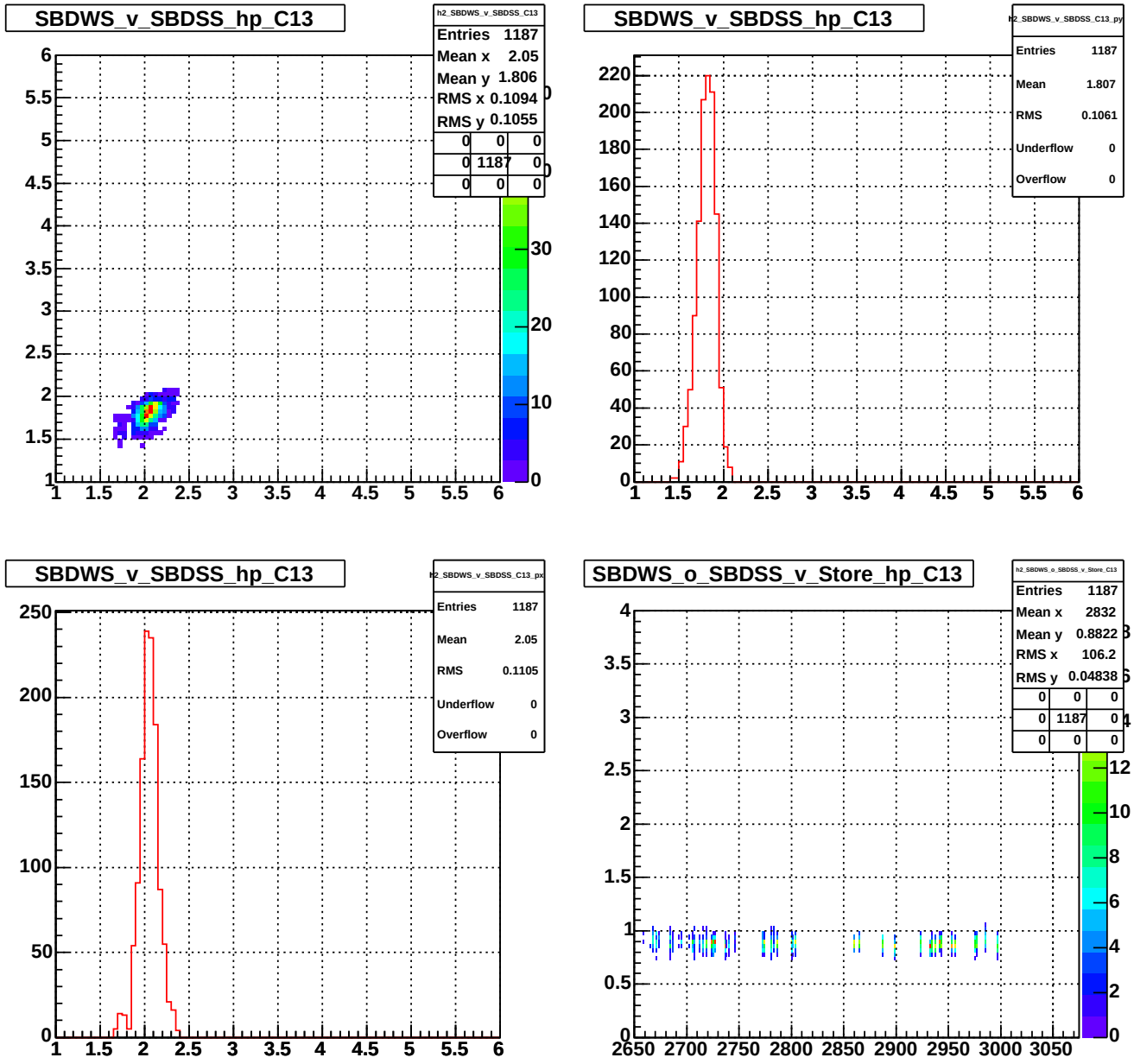

Figure 66: Proton beam, horizontal detectors, nominal lattice: Stores 2650-2997, 980 GeV Case Remove Halo: Comparisons of longitudinal bunch length (in *ns*) as reported by SBD according to Gaussian fit sigma and RMS (based on T:SBD[A,P]SS and T:SBD[A,P]WS ACNET variables): RMS versus sigma; RMS; sigma; ratio of RMS and sigma versus store number.

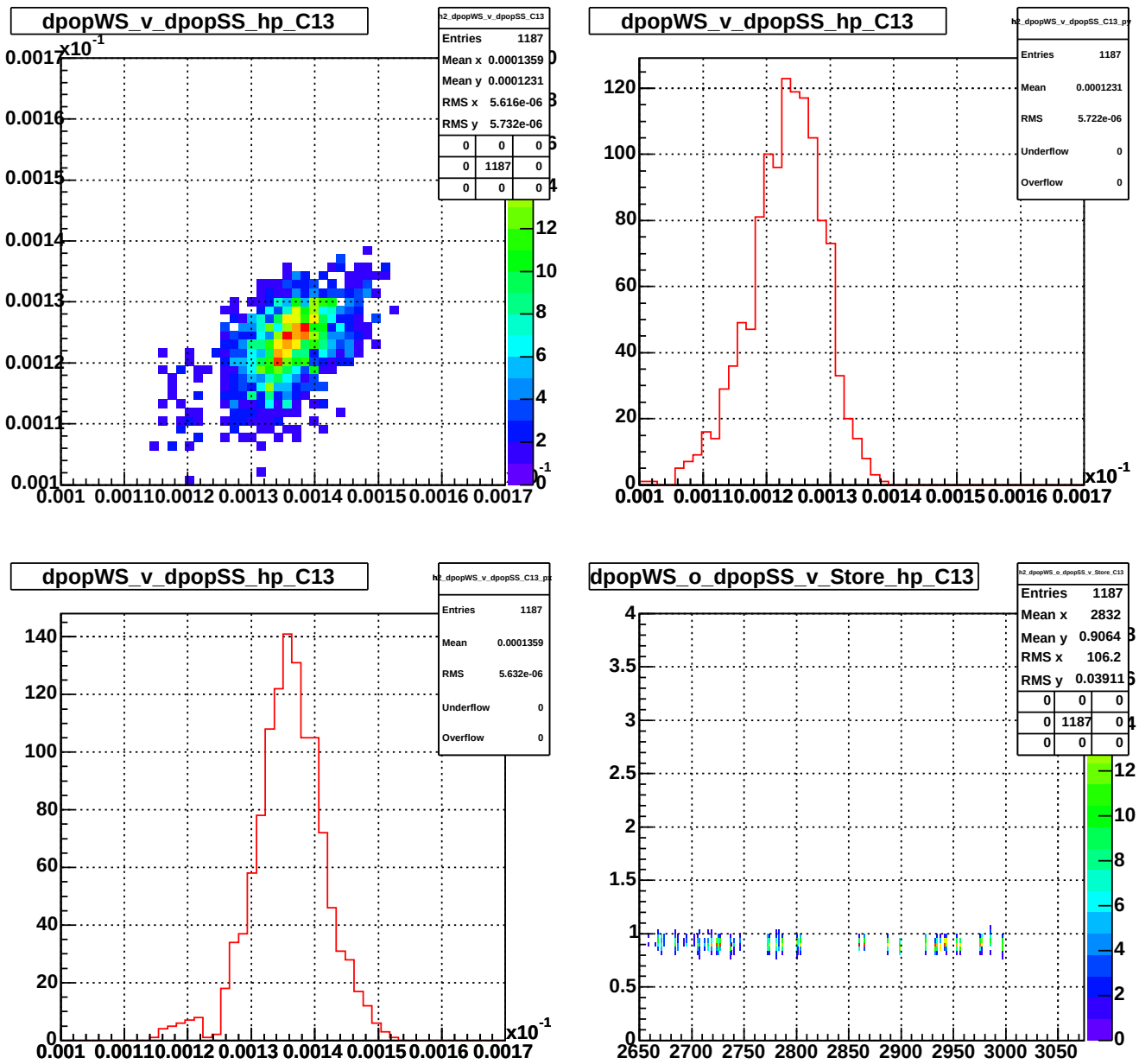

Figure 67: Proton beam, horizontal detectors, nominal lattice: Stores 2650-2997, 980 GeV Case Remove Halo: Comparisons of recalculated $\delta p/p$ based on T:SBD[A,P]SS (Gaussian fit sigma) and T:SBD[A,P]WS (RMS) ACNET variables: $\delta p/p$ based on RMS versus $\delta p/p$ based on sigma; $\delta p/p$ based on RMS; $\delta p/p$ based on sigma; ratio of $\delta p/p$ based on RMS and sigma versus store number.

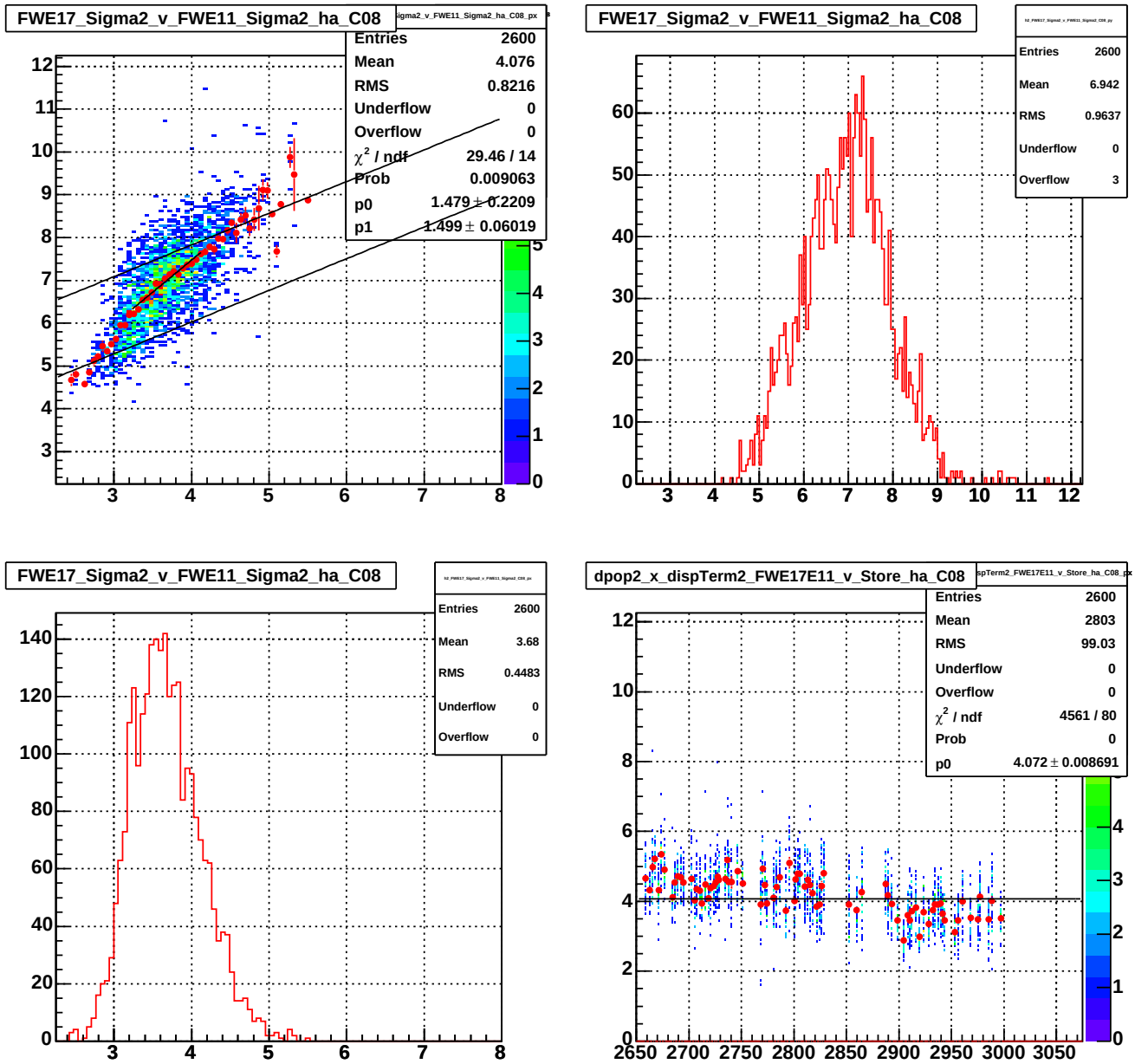

Figure 68: Antiproton beam, horizontal detectors, nominal lattice: Stores 2650-2997, 150 GeV Case Before Ramp: Comparisons of sigma squared of the bunch width distribution measurements as done by Flying Wire (FW) E17 Detector with measurements done by FW E11 Detector: Sigma squared of the bunch width distribution (in mm^2) as measured by the FW E17 Detector versus sigma squared of the bunch width distribution (in mm^2) as measured by the FW E11 Detector with an overlaid horizontal profile with a straight line fit, the two straight lines are edges of the plain resulting from the fit based prediction of E17 measurement given E11 sigma measurement and minimum and maximum of $\delta p/p$ used in the fit; Sigma squared of the bunch width distribution (in mm^2) as measured by the FW E17 Detector; Sigma squared of the bunch width distribution (in mm^2) as measured by the FW E11 Detector; Difference of sigma squared of the bunch width distribution (in mm^2) as measured by the FW E17 Detector *and* sigma squared of the bunch width distribution (in mm^2) as measured by the FW E11 Detector times ratio of nominal beta functions: $\sigma_17^2 - \sigma_{11}{}^2\beta_{17}/\beta_{11}$ versus store number with an overlaid horizontal profile with a straight line fit.

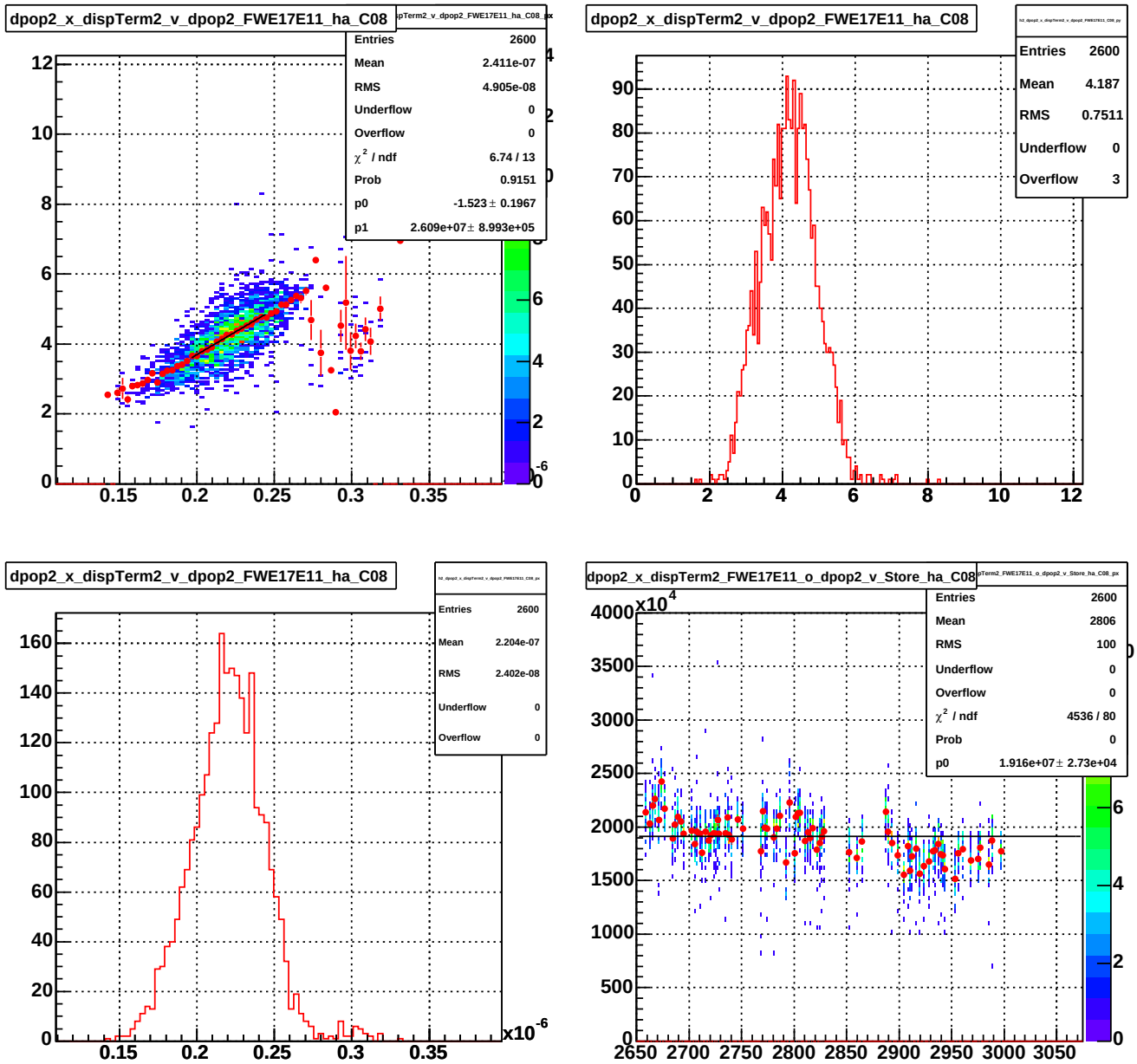

Figure 69: Antiproton beam, horizontal detectors, nominal lattice: Stores 2650-2997, 150 GeV Case Before Ramp: Comparisons of the combined sigma squared of the bunch width distribution measurements as done by Flying Wire (FW) E17 and E11 Detectors with recalculated $\delta p/p$ based on T:SBD[A,P]WS (RMS) ACNET variables: Difference of sigma squared of the bunch width distribution (in mm^2) as measured by the FW E17 Detector *and* sigma squared of the bunch width distribution (in mm^2) as measured by the FW E11 Detector times ratio of nominal beta functions: $\sigma_17^2 - \sigma_{11}{}^2\beta_{17}/\beta_{11}$ versus recalculated $\delta p/p$ squared (based on δt the T:SBD[A,P]WS ACNET variable) with an overlaid horizontal profile with a straight line fit; Difference of sigma squared of the bunch width distribution (in mm^2) as measured by the FW E17 Detector *and* sigma squared of the bunch width distribution (in mm^2) as measured by the FW E11 Detector times ratio of nominal beta functions: $\sigma_{17}{}^2 - \sigma_{11}{}^2\beta_{17}/\beta_{11}$; recalculated $\delta p/p$ squared (based on δt the T:SBD[A,P]WS ACNET variable); Difference of sigma squared of the bunch width distribution (in mm^2) as measured by the FW E17 Detector *and* sigma squared of the bunch width distribution (in mm^2) as measured by the FW E11 Detector times ratio of nominal beta functions: $\sigma_{17}{}^2 - \sigma_{11}{}^2\beta_{17}/\beta_{11}$ over recalculated $\delta p/p$ squared (based on δt the T:SBD[A,P]WS ACNET variable) versus store number with an overlaid horizontal profile with a straight line fit.

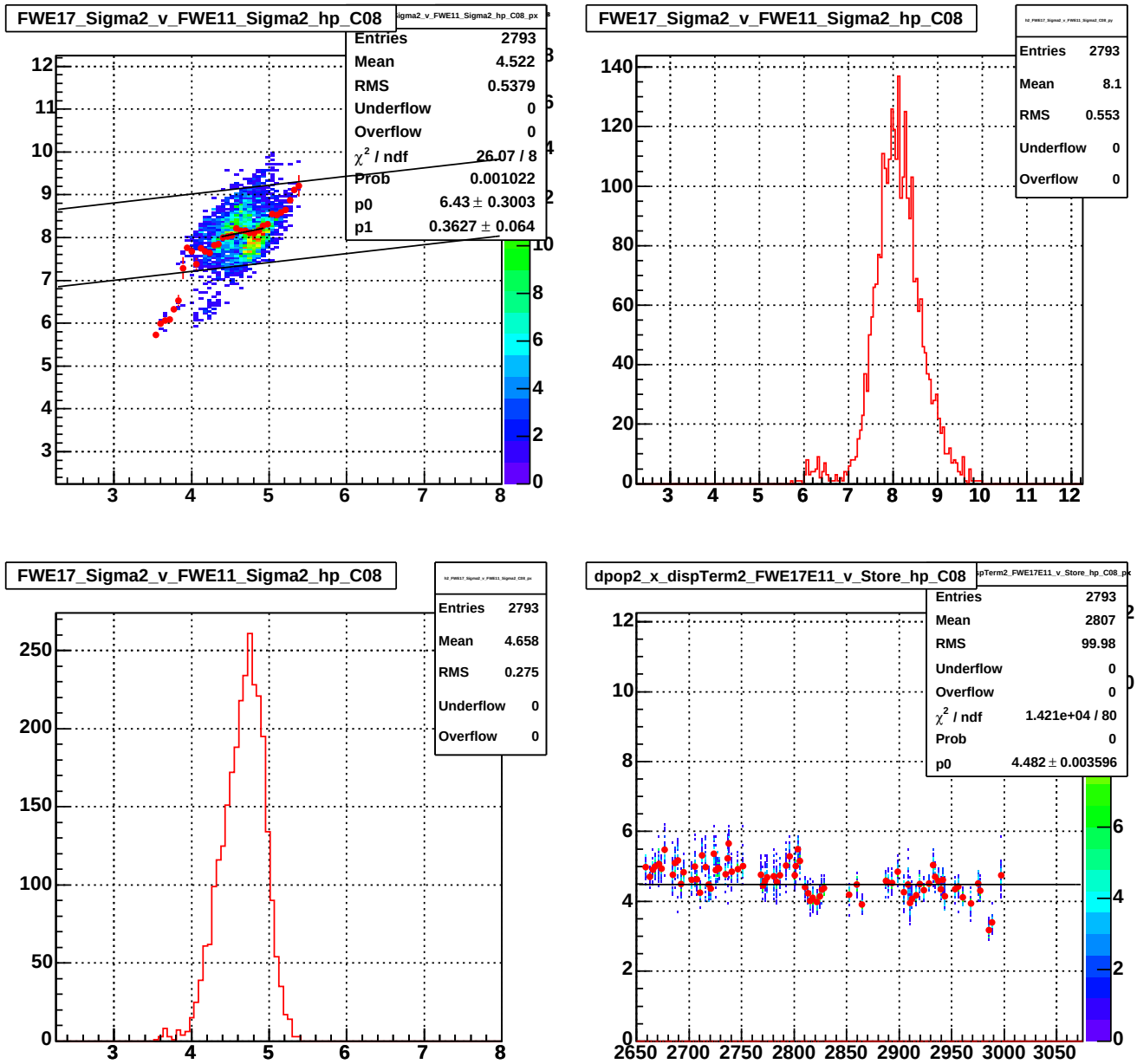

Figure 70: Proton beam, horizontal detectors, nominal lattice: Stores 2650-2997, 150 GeV Case Before Ramp: Comparisons of sigma squared of the bunch width distribution measurements as done by Flying Wire (FW) E17 Detector with measurements done by FW E11 Detector: Sigma squared of the bunch width distribution (in mm^2) as measured by the FW E17 Detector versus sigma squared of the bunch width distribution (in mm^2) as measured by the FW E11 Detector with an overlaid horizontal profile with a straight line fit, the two straight lines are edges of the plain resulting from the fit based prediction of E17 measurement given E11 sigma measurement and minimum and maximum of $\delta p/p$ used in the fit; Sigma squared of the bunch width distribution (in mm^2) as measured by the FW E17 Detector; Sigma squared of the bunch width distribution (in mm^2) as measured by the FW E11 Detector; Difference of sigma squared of the bunch width distribution (in mm^2) as measured by the FW E17 Detector *and* sigma squared of the bunch width distribution (in mm^2) as measured by the FW E11 Detector times ratio of nominal beta functions: $\sigma_17^2 - \sigma_{11}{}^2\beta_{17}/\beta_{11}$ versus store number with an overlaid horizontal profile with a straight line fit.

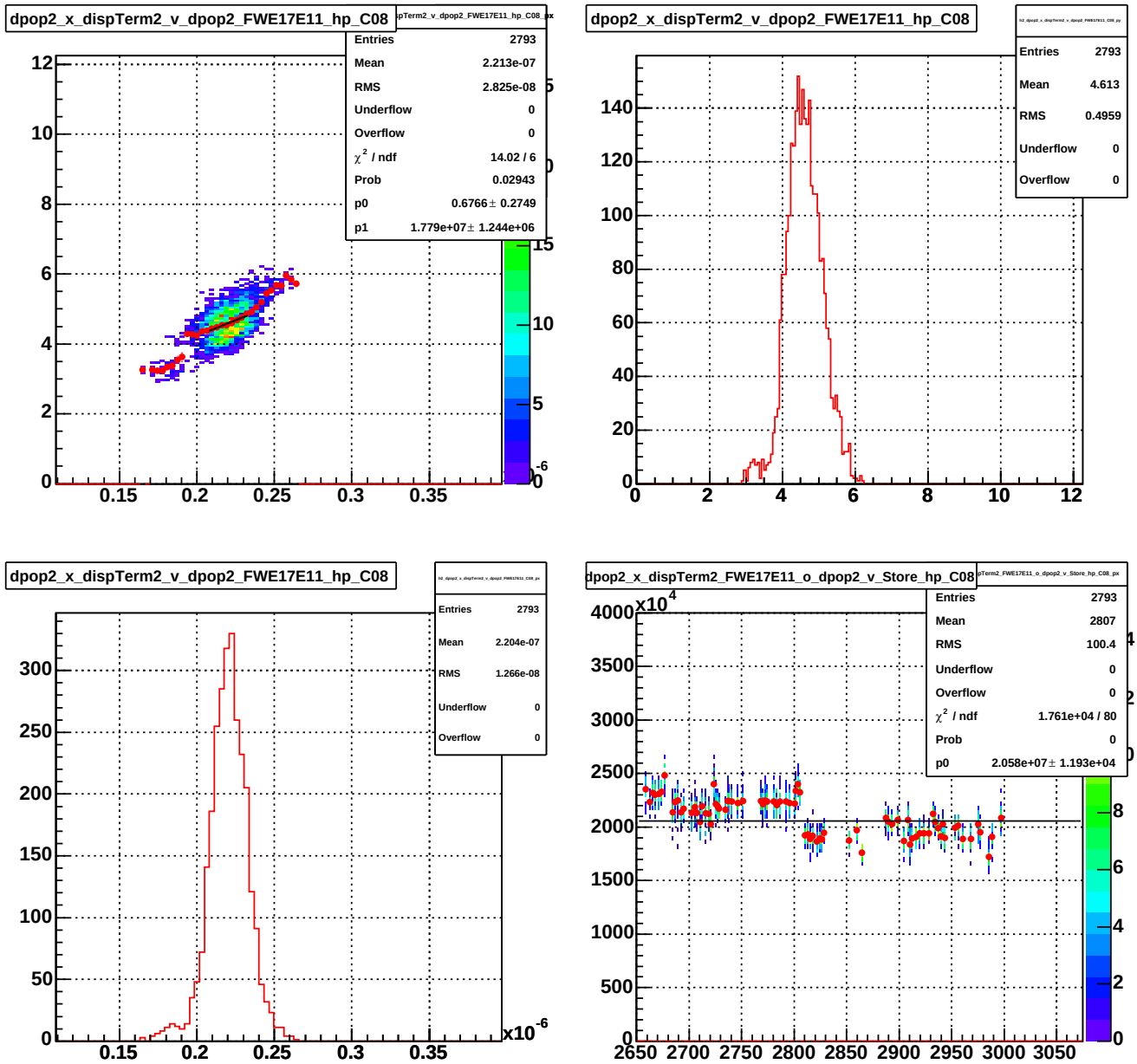

Figure 71: Proton beam, horizontal detectors, nominal lattice: Stores 2650-2997, 150 GeV Case Before Ramp: Comparisons of the combined sigma squared of the bunch width distribution measurements as done by Flying Wire (FW) E17 and E11 Detectors with recalculated $\delta p/p$ based on T:SBD[A,P]WS (RMS) ACNET variables: Difference of sigma squared of the bunch width distribution (in mm^2) as measured by the FW E17 Detector *and* sigma squared of the bunch width distribution (in mm^2) as measured by the FW E11 Detector times ratio of nominal beta functions: $\sigma_17^2 - \sigma_{11}{}^2\beta_{17}/\beta_{11}$ versus recalculated $\delta p/p$ squared (based on δt the T:SBD[A,P]WS ACNET variable) with an overlaid horizontal profile with a straight line fit; Difference of sigma squared of the bunch width distribution (in mm^2) as measured by the FW E17 Detector *and* sigma squared of the bunch width distribution (in mm^2) as measured by the FW E11 Detector times ratio of nominal beta functions: $\sigma_{17}{}^2 - \sigma_{11}{}^2\beta_{17}/\beta_{11}$; recalculated $\delta p/p$ squared (based on δt the T:SBD[A,P]WS ACNET variable); Difference of sigma squared of the bunch width distribution (in mm^2) as measured by the FW E17 Detector *and* sigma squared of the bunch width distribution (in mm^2) as measured by the FW E11 Detector times ratio of nominal beta functions: $\sigma_{17}{}^2 - \sigma_{11}{}^2\beta_{17}/\beta_{11}$ over recalculated $\delta p/p$ squared (based on δt the T:SBD[A,P]WS ACNET variable) versus store number with an overlaid horizontal profile with a straight line fit.

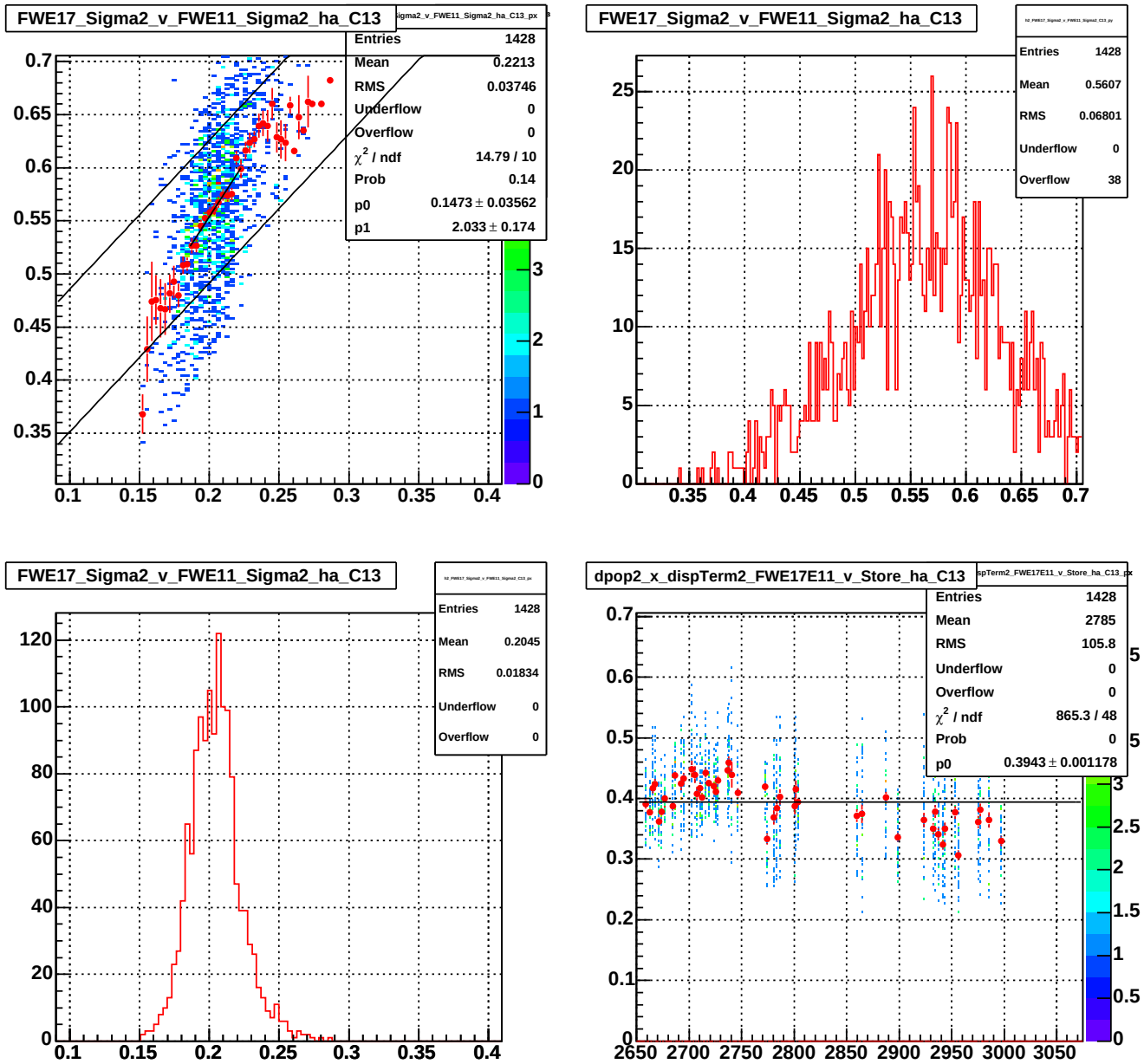

Figure 72: Antiproton beam, horizontal detectors, nominal lattice: Stores 2650-2997, 980 GeV Case Remove Halo: Comparisons of sigma squared of the bunch width distribution measurements as done by Flying Wire (FW) E17 Detector with measurements done by FW E11 Detector: Sigma squared of the bunch width distribution (in mm^2) as measured by the FW E17 Detector versus sigma squared of the bunch width distribution (in mm^2) as measured by the FW E11 Detector with an overlaid horizontal profile with a straight line fit, the two straight lines are edges of the plain resulting from the fit based prediction of E17 measurement given E11 sigma measurement and minimum and maximum of $\delta p/p$ used in the fit; Sigma squared of the bunch width distribution (in mm^2) as measured by the FW E17 Detector; Sigma squared of the bunch width distribution (in mm^2) as measured by the FW E11 Detector; Difference of sigma squared of the bunch width distribution (in mm^2) as measured by the FW E17 Detector *and* sigma squared of the bunch width distribution (in mm^2) as measured by the FW E11 Detector times ratio of nominal beta functions: $\sigma_17^2 - \sigma_{11}{}^2\beta_{17}/\beta_{11}$ versus store number with an overlaid horizontal profile with a straight line fit.

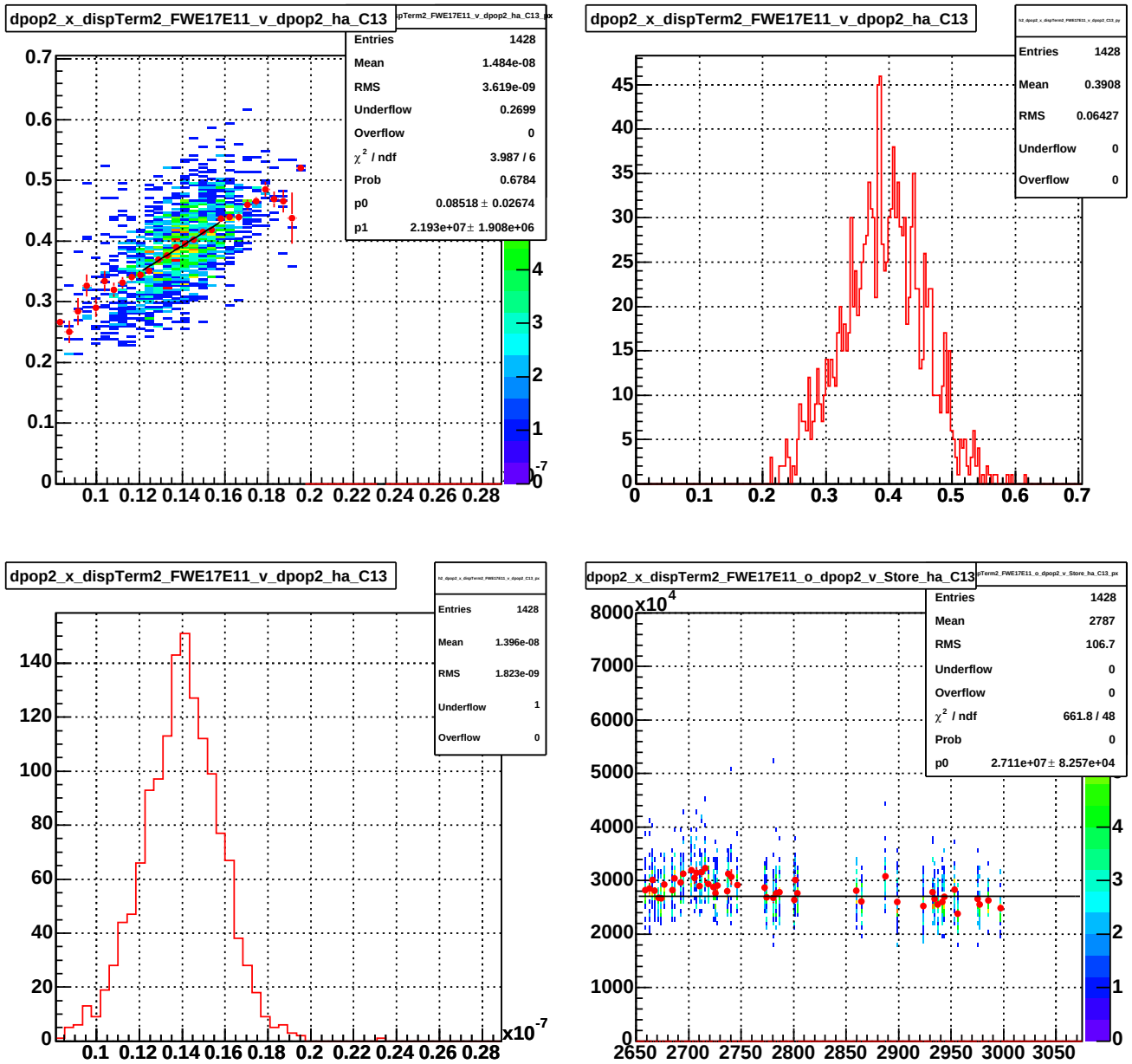

Figure 73: Antiproton beam, horizontal detectors, nominal lattice: Stores 2650-2997, 980 GeV Case Remove Halo: Comparisons of the combined sigma squared of the bunch width distribution measurements as done by Flying Wire (FW) E17 and E11 Detectors with recalculated $\delta p/p$ based on T:SBD[A,P]WS (RMS) ACNET variables: Difference of sigma squared of the bunch width distribution (in mm^2) as measured by the FW E17 Detector *and* sigma squared of the bunch width distribution (in mm^2) as measured by the FW E11 Detector times ratio of nominal beta functions: $\sigma_17^2 - \sigma_{11}{}^2\beta_{17}/\beta_{11}$ versus recalculated $\delta p/p$ squared (based on δt the T:SBD[A,P]WS ACNET variable) with an overlaid horizontal profile with a straight line fit; Difference of sigma squared of the bunch width distribution (in mm^2) as measured by the FW E17 Detector *and* sigma squared of the bunch width distribution (in mm^2) as measured by the FW E11 Detector times ratio of nominal beta functions: $\sigma_{17}{}^2 - \sigma_{11}{}^2\beta_{17}/\beta_{11}$; recalculated $\delta p/p$ squared (based on δt the T:SBD[A,P]WS ACNET variable); Difference of sigma squared of the bunch width distribution (in mm^2) as measured by the FW E17 Detector *and* sigma squared of the bunch width distribution (in mm^2) as measured by the FW E11 Detector times ratio of nominal beta functions: $\sigma_{17}{}^2 - \sigma_{11}{}^2\beta_{17}/\beta_{11}$ over recalculated $\delta p/p$ squared (based on δt the T:SBD[A,P]WS ACNET variable) versus store number with an overlaid horizontal profile with a straight line fit.

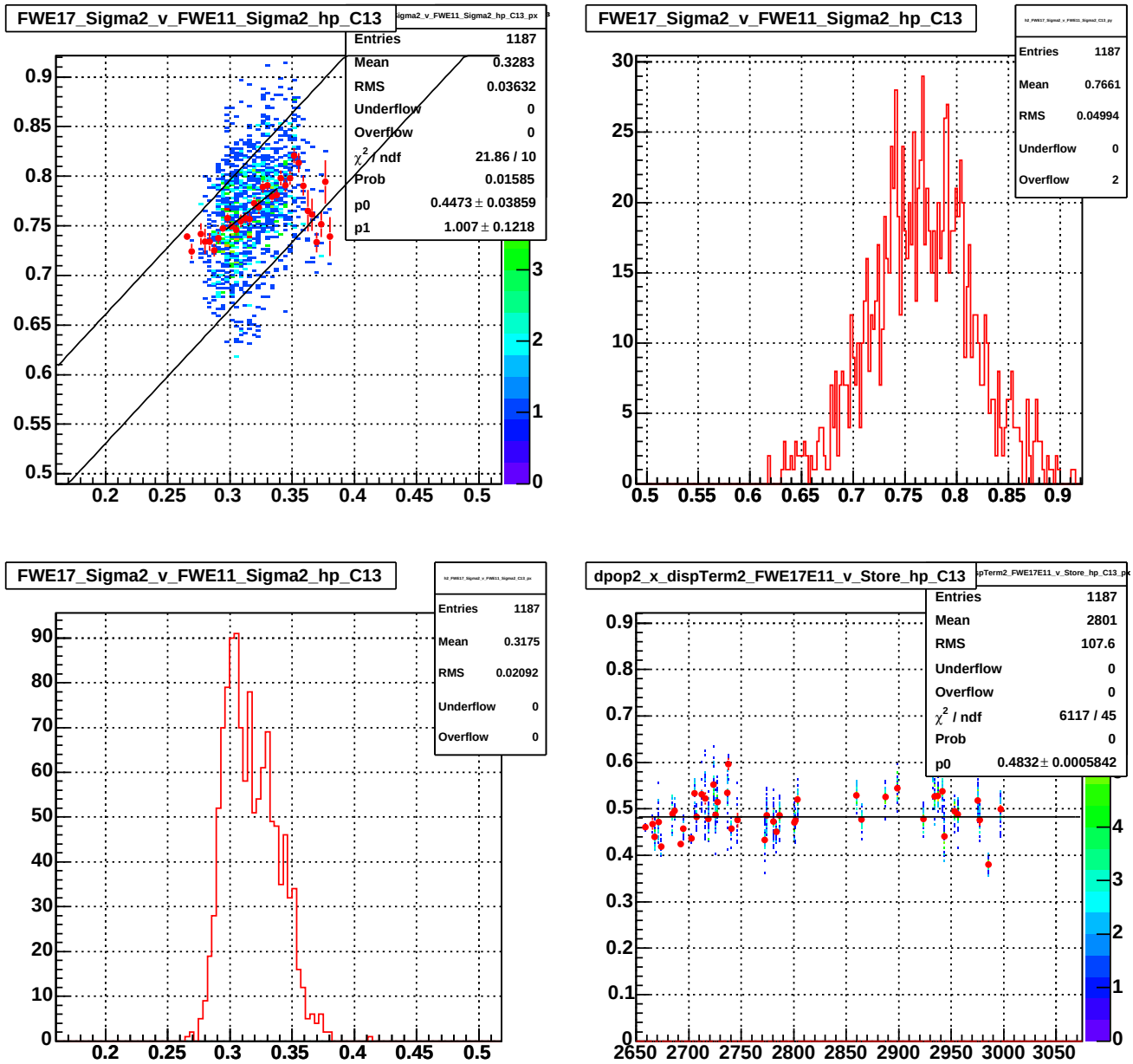

Figure 74: Proton beam, horizontal detectors, nominal lattice: Stores 2650-2997, 980 GeV Case Remove Halo: Comparisons of sigma squared of the bunch width distribution measurements as done by Flying Wire (FW) E17 Detector with measurements done by FW E11 Detector: Sigma squared of the bunch width distribution (in mm^2) as measured by the FW E17 Detector versus sigma squared of the bunch width distribution (in mm^2) as measured by the FW E11 Detector with an overlaid horizontal profile with a straight line fit, the two straight lines are edges of the plain resulting from the fit based prediction of E17 measurement given E11 sigma measurement and minimum and maximum of $\delta p/p$ used in the fit; Sigma squared of the bunch width distribution (in mm^2) as measured by the FW E17 Detector; Sigma squared of the bunch width distribution (in mm^2) as measured by the FW E11 Detector; Difference of sigma squared of the bunch width distribution (in mm^2) as measured by the FW E17 Detector *and* sigma squared of the bunch width distribution (in mm^2) as measured by the FW E11 Detector times ratio of nominal beta functions: $\sigma_17^2 - \sigma_{11}{}^2\beta_{17}/\beta_{11}$ versus store number with an overlaid horizontal profile with a straight line fit.

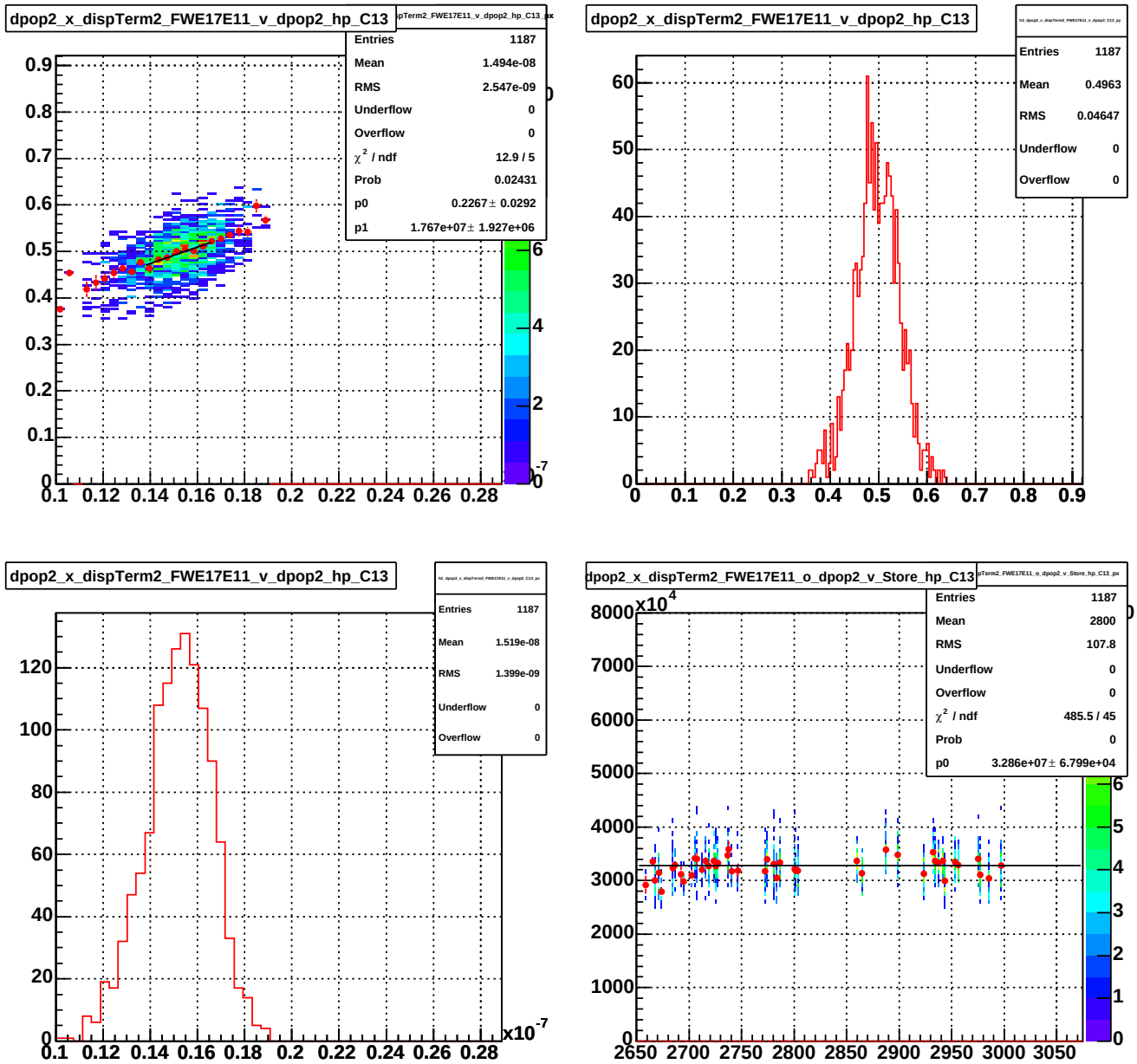

Figure 75: Proton beam, horizontal detectors, nominal lattice: Stores 2650-2997, 980 GeV Case Remove Halo: Comparisons of the combined sigma squared of the bunch width distribution measurements as done by Flying Wire (FW) E17 and E11 Detectors with recalculated $\delta p/p$ based on T:SBD[A,P]WS (RMS) ACNET variables: Difference of sigma squared of the bunch width distribution (in mm^2) as measured by the FW E17 Detector *and* sigma squared of the bunch width distribution (in mm^2) as measured by the FW E11 Detector times ratio of nominal beta functions: $\sigma_17^2 - \sigma_{11}{}^2\beta_{17}/\beta_{11}$ versus recalculated $\delta p/p$ squared (based on δt the T:SBD[A,P]WS ACNET variable) with an overlaid horizontal profile with a straight line fit; Difference of sigma squared of the bunch width distribution (in mm^2) as measured by the FW E17 Detector *and* sigma squared of the bunch width distribution (in mm^2) as measured by the FW E11 Detector times ratio of nominal beta functions: $\sigma_{17}{}^2 - \sigma_{11}{}^2\beta_{17}/\beta_{11}$; recalculated $\delta p/p$ squared (based on δt the T:SBD[A,P]WS ACNET variable); Difference of sigma squared of the bunch width distribution (in mm^2) as measured by the FW E17 Detector *and* sigma squared of the bunch width distribution (in mm^2) as measured by the FW E11 Detector times ratio of nominal beta functions: $\sigma_{17}{}^2 - \sigma_{11}{}^2\beta_{17}/\beta_{11}$ over recalculated $\delta p/p$ squared (based on δt the T:SBD[A,P]WS ACNET variable) versus store number with an overlaid horizontal profile with a straight line fit.